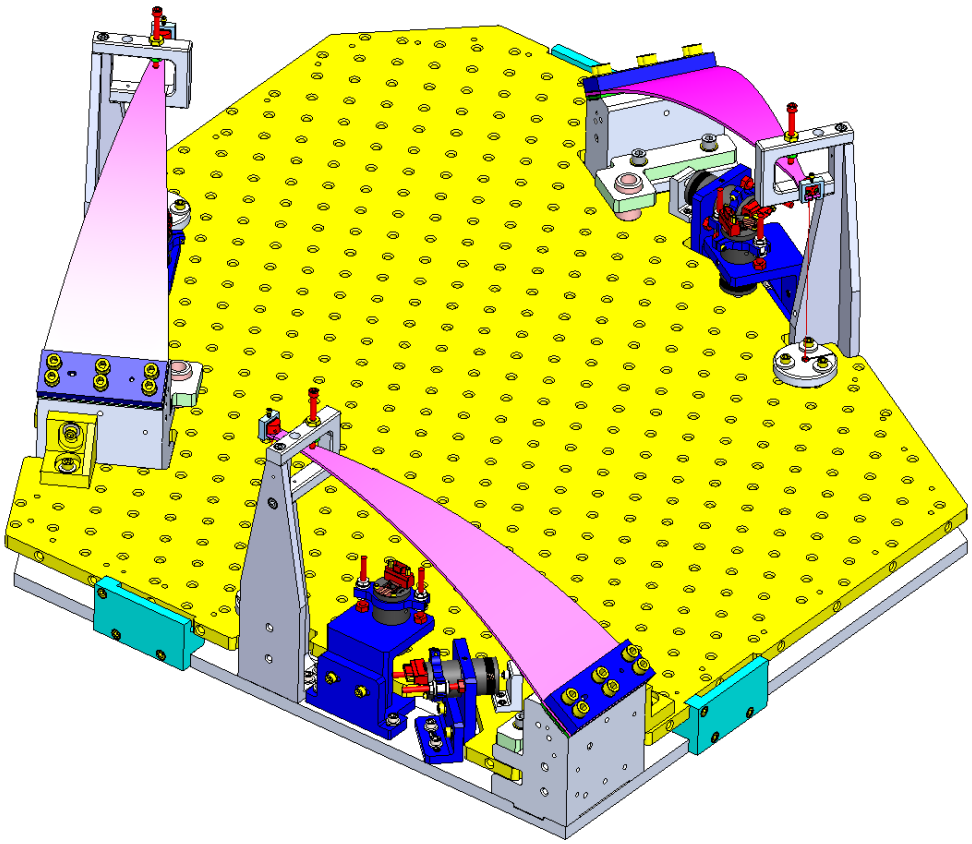

VOPO SUSPENSION DESIGN

A SINGLE STAGE SUSPENSION FOR THE SQUEEZER INSTRUMENT

Álvaro Fernandez Galiana |Fabrice Matichard, Guilhem Michon| PFE
ISAE-SUPAERO/ETSEIB-UPC | November 23, 2015

INDEX

INTRODUCTION

LIGO PROJECT, aLIGO

This project has been performed at the MIT LIGO laboratory. This Laboratory is one of the main contributors to the LSC (LIGO Scientific Collaboration) group. The Laser Interferometer Gravitational-Wave Observatory (LIGO) project is designed to directly detect gravitational waves of cosmic origin predicted by Einstein's General Relativity. To do so, LIGO has built two identical 4km arm interferometers within the United States -one in Hanford, WA and the other in Livingston, LA. Using the same principle applied by Michelson's interferometer with a Fabry-Perot cavity, as described in *(Saulson, 1998)*, these 4km arm interferometers have the capability of detecting almost imperceptible strains (up to 10-24 m/in the so called "test masses", the 40kg mirrors located at the extremes of the arms, *Figure 1*. This high sensitivity makes LIGO to be one the most sensitive metrology experiment in the world.

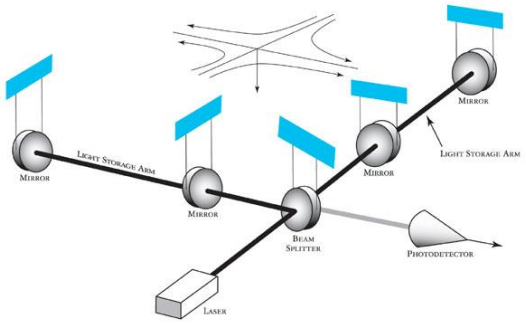

Figure 1: LIGO interferometer principle

At this point the LIGO project is running the first scientific run (O1) of the second generation of interferometer, which that started on September 2015. This second generation, known as advance LIGO (aLIGO), is an upgrade of the previous generation (iLIGO), improved seismic (ground vibration) isolation, better ways to hang our mirrors like pendula, a more powerful laser, more massive mirror, better coatings on the mirrors, and new ways to reuse laser light to increase the laser power in the arms. All of this is results in an overall enhancement in sensitivity of 10. This improvement towards its predecessor gives aLIGO the capability of observing astronomical events in a 1000 times greater volume, as shown in Figure 2.

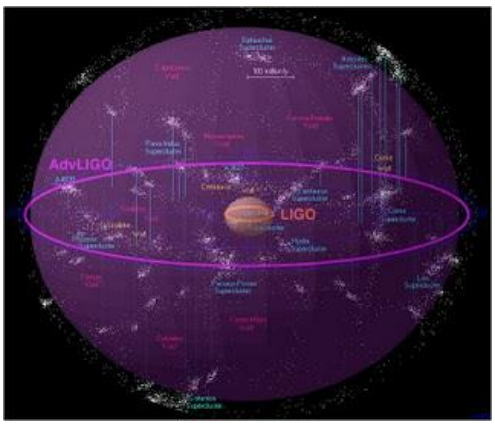

Figure 2: Sensitivity improvement in aLIGO

One of the main concerns of the LSC group, and the main limitation in sensitivity, is the noise perceived by the detector. Figure 3 shows the diverse sources of noise for aLIGO, as well as the total noise of the device, and so the derived global sensitivity is about 10-23 for some specific width band.

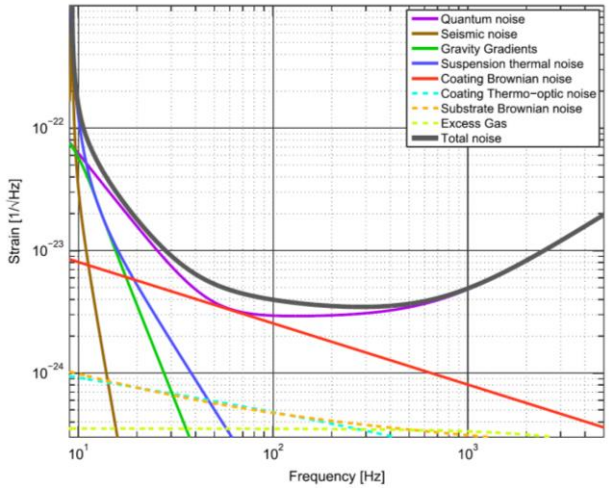

Figure 3: Expected sensitivity curve for aLIGO

In the figure, extracted from (Advanced LIGO, 2015) it can be observed that at very low frequencies the sensitivity is poor due to the "wall", mainly driven by the seismic noise and suspension thermal noise. On the other side, the quantum noise is the major contributor to the total noise in the rest of the bandwidth. Consequently, LSC group dedicates an important amount of human power in the task of reducing the quantum noise and being isolated from the group noise, and that is with is project has taken place.

SEISMIC AT LIGO

aLIGO interferometers are not only composed of the two arms shown in Figure 1, but they also have an important number of supporting systems to treat the laser beam that goes to the interferometer in order to improve the global sensitivity. At the start of this specific project, the overall layout of the aLIGO sites was the one presented in Figure 4, with 5 primary chambers titled BSCX that host the test masses and constitute the 4km arms of the interferometers and 6 surrounding chambers named HAMX where the supporting systems are allocated.

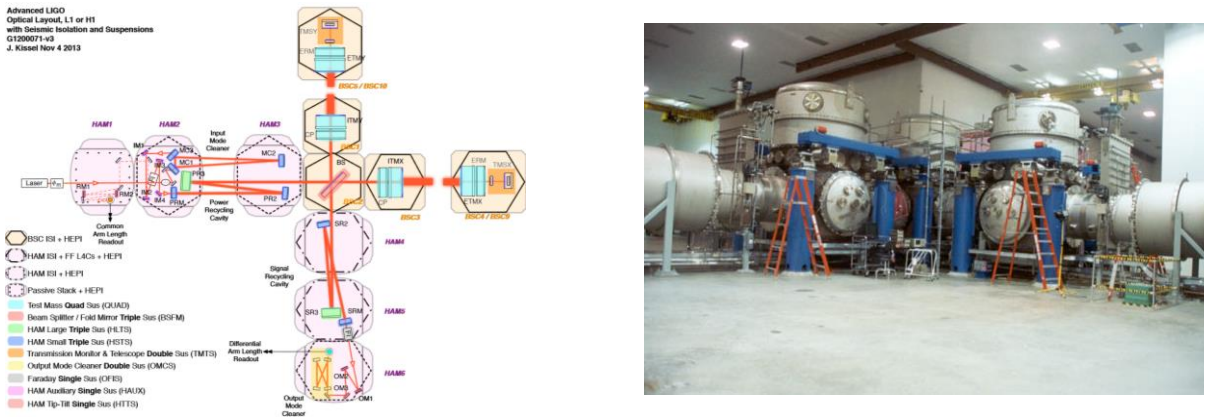

IS

Figure 4: aLIGO chambers layout

It is important to notice that is one of this chamber is provided with a Seismic isolation system on top of whom all the optical instruments are placed. This huge suspensions are called HAM-ISI or BSC-ISI and both can be seen in Figure 5, (Matichard & al., 2015). On the top of that, all the interferometer system works under high vacuum, which adds an important constraint for all the systems that are used.

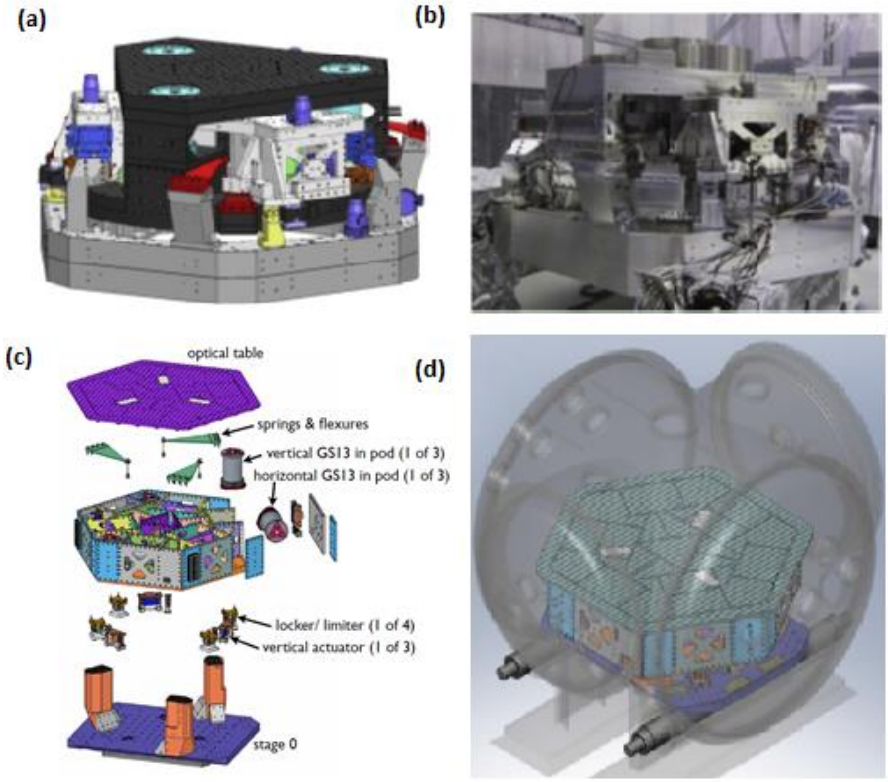

Figure 5: BSC-ISI CAD model (a) and prototype (b); HAM-ISI exploded view (c) and in chamber (d)

VOPO SQUEEZER IN aLIGO

At this time, the layout presented in Figure 4 is being used for the first run of aLIGO, but LIGO experts consider that it needs to be upgraded before the second run in order to improve sensitivity, (VOPO - Preliminary optical design, 2015). One of the upgrades that has been considered is to introduce an Optical Parameter Oscillator (OPO) to produce phase squeezed light and consequently reduce the quantum noise at high frequencies. This instrument will be located in HAM 6 chamber, which is the one presenting more available surface, as it has to interact with the Faraday instrument, located in HAM 5. In a second stage, expected for the third run (O3), a Filter Cavity will also be introduced in order to allow amplitude-phase squeezing.

NASCENT VOPO SUSPENSION DESIGN

STATE OF THE ART

This project consist of the design of the seismic isolation system for the VOPO instrument that will be used by aLIGO after the upgrade period in between O1 and O2. This isolation system, as all its previous aLIGO peers, is intended to guarantee the mechanical isolation between the optical instruments and the ground motion. Regarding its specific quantitative requirements, the isolation has to be effective so that it provides isolation comparable to the one provided by the tip-tilt suspensions, which are in the same optical path. These tip-tilts are actuated mirrors used to control the light path and their frequency is around of 1.5 Hz.

The general way used in preceding isolators to guarantee the required performance is to suspend the optical bench using a multi stage spring-mass system to guarantee the passive isolation and combine that with the use of actuators for the active damping control of the rigid body modes. However, the first considered option was to investigate the possibility of using a rubber spring-dampers and leg elements as shown in Figure 6, relying on the chamber's suspension system to reach the required behavior. This approach was particularly appealing for its simplicity, low-cost and easiness of procurement.

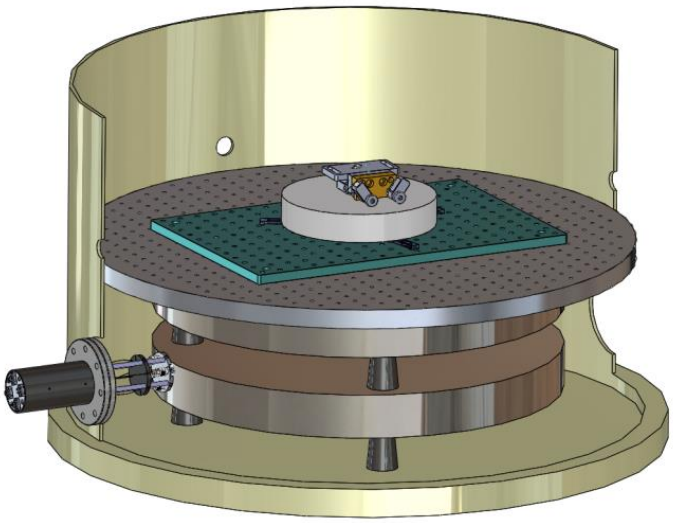

Figure 6: CAD Model of the stack assembly used in the VOPO experiment at MIT.

Notwithstanding, this option was tested using diverse values of masses, geometries of rubber (cones, pads…), and different number of layers and it resulted to be inefficient for the targeted level of isolation. Figure 7 shows transmissibility curves in the vertical directions for various configurations. The lowest corner frequency was around 10 Hz. Lower corner frequencies were obtained in the horizontal direction, but only with no more than a factor of 3 of isolation at 10 Hz. Additionally, the better results were obtained with two layers of isolation, which is difficult to fit in the vertical space available (4 inches between the top surface of the HAM-ISI, and the optical plane).

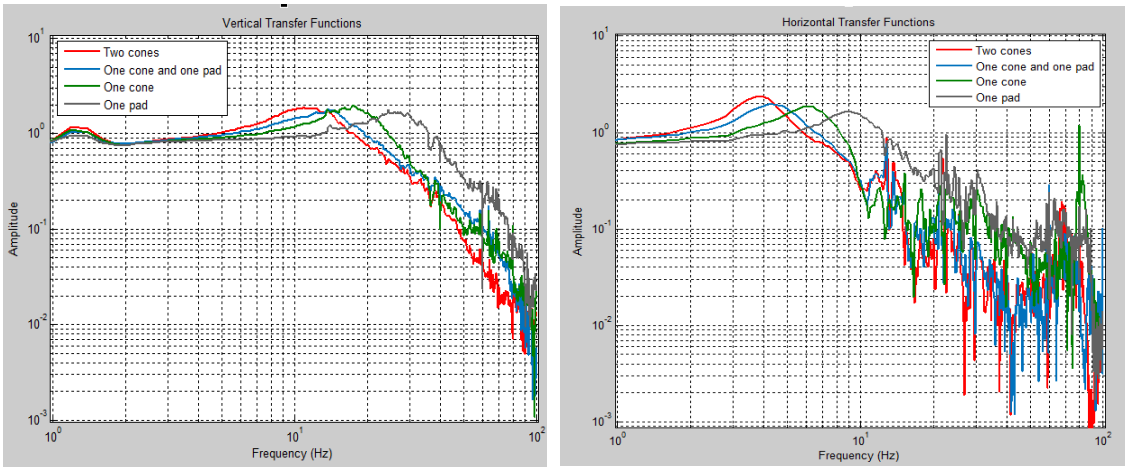

Figure 7: Horizontal (left), and vertical (right) measurements of transmissibility stack layers

EARLY VOPO SUSPENSION DESIGNS

In light of these results, LIGO group decided to move to a more "regular" suspension based on the blade springs and suspension wires system, which has been favorably developed in an important number of the existing suspensions, including the chambers suspensions as well as in the Tip-Tilt themselves. At first, it was decided to study the possibility of reusing an existing suspension, which will consequently imply a huge reduction on the design task and the cost associated to it. Indeed, this "recycling" approach has already been successfully adopted in the design of earlier isolation systems such as the Faraday Single suspension (FI in Figure 4), which uses a slightly modified version of the Output Mode Cleaner Suspension (OMCS in Figure 4). Therefore, a preliminary design for the VOPO suspension was developed trying to employ the OMCS two stage suspension, trying to make as few changes as possible. Two of the considered models for this preliminary design are presented in Figure 8.

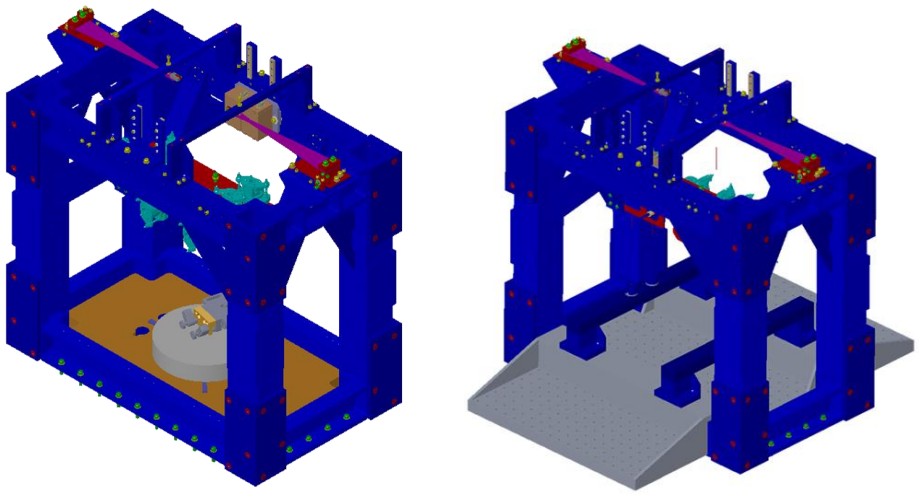

Figure 8: Early VOPO suspension concepts re-using the OMC structure and spring assemblies.

Nevertheless, this option was finally rejected as the dimensions of the VOPO optical layout (see Figure 10) are much larger than the ones of the abovementioned suspensions and therefore the main structure (blue in

Figure 8) was too narrow. Given the fact that none of the existing suspensions was a good fit for the VOPO layout, it was decided to develop a new suspension from scratch.

After a first study it was decided that given the level of isolation required a single stage suspension may be considered as an option. If feasible, this mono-stage design presents advantages when compared with multi-stage suspensions as, due to its simplicity, it is supposed to be more economical and easier to procure. The final design that will be presented in this report, which is a mono-stage suspension, is the result of an important number of iterations that have left behind a considerable amount of "almost" final designs. Two examples of these designs are presented in Figure 9.

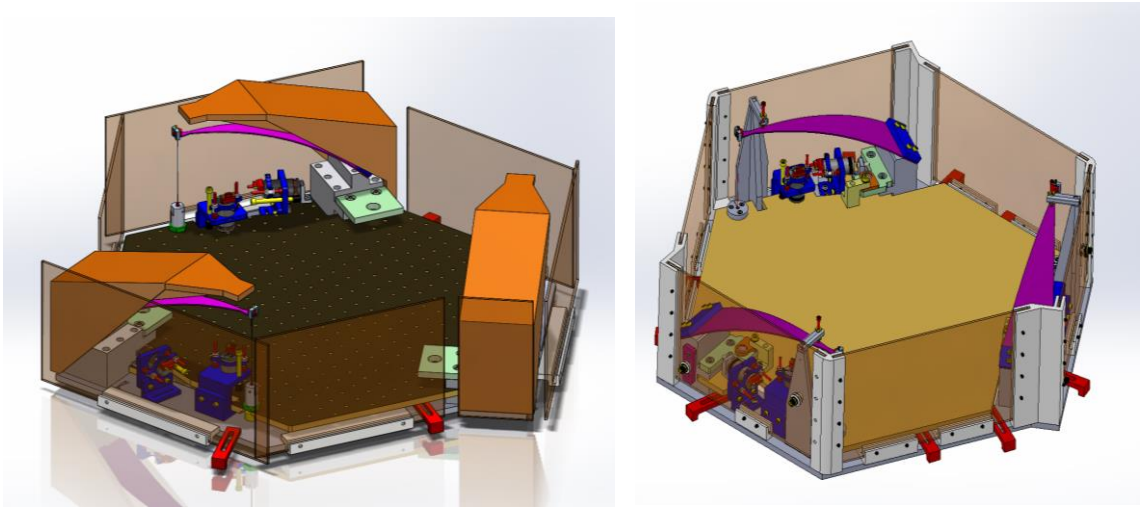

Figure 9: Concepts using a hexagonal table suspended with three spring assemblies

At this point, I would take the liberty of quoting an outstanding figure of the history, Thomas A. Edison, when he said his famous "I have not failed. I've just found 10,000 ways that won't work". However, one of the goals of this report is the prevent future suspension designers to fail as many times as we have by giving what we consider is the right approach when trying to design suspension for LIGO from scratch.

However, starting from scratch gives us the opportunity of orienting this project not only as a suspension design but as the chance to test new strategies that have not been applied before in LIGO. The three main "breakthroughs" of these instrument's design are schematized below.

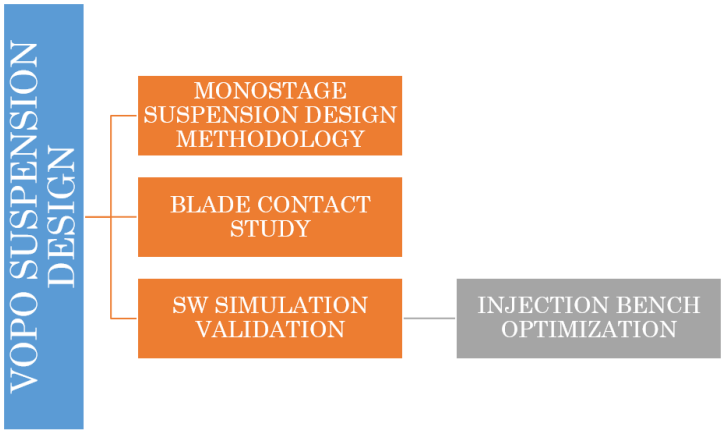

MONOSTAGE SUSPENSION DESIGN METHODOLOGY

CONSTRAINTS AND REQUIREMENTS

When designing a suspension for a particular optical instrument you are usually given a set of constraints that is extremely important to keep in mind during the whole design process. For the VOPO suspension, these constraints were of four different nature. The first constraint, already mentioned above, is to keep the natural frequency of the suspension around 1.5Hz. Secondly, the suspension has to hold a number of optics and instruments. This is an important constraint as it related with two of the main drivers in any suspension design: the mass that is going to be suspended and the area required to have an appropriate optical layout. Then, we are also given the desired height between the optical bench of the chamber and the beam path. For the VOPO suspension, the beam path has to be at 4" from the optical bench, which is the distance that will be between the base of the suspension and the midplane of the optics. Finally, there is a fourth constraint that is also associated with the space management that is the available space or, to put it another way, where do you want the suspension to be located. As it has already been said, for the VOPO cavity, HAM6 chamber has been established as the best fit due to the proximity to HAM5, where the Faraday instrument is situated, and its free space.

Coming back to the second constraint, it is crucial to understand that during the design and test development of the isolation system there might be changes in the optical layout design. The solution against this is to take into account some contingency to prevent the design from being obsolete by the time it has to be installed. It is also important to notice that, for the type of suspensions that we are considering, there might be a correlation between the size and the weight of optics as, in general, larger layouts usually use more mirrors, which increases the total weight of the optics.

As it can be inferred from the designs presented in Figure 9, one of the main ideas of this new suspension is to have a "useful" area as large as possible, what means that we try to avoid the use of huge structures to suspend small benches and we rather would like a ratio of one between the total surface of the suspension and the surface of the injection bench. Actually, this kind of suspension might be seen as a "mini ISI", as it maximizes the available area for optics vis-à-vis the occupied area. Additionally, we tried to keep the optics in the top of the suspension instead of bolt them from underneath, as it makes the suspension more accessible.

INSTRUMENT'S OPTICAL LAYOUT

If we focus now on the VOPO layout, we can find in Figure 10 the preliminary arrangement for the optics for O2 and O3, (aLIGO VOPO Optical Layout, 2015).

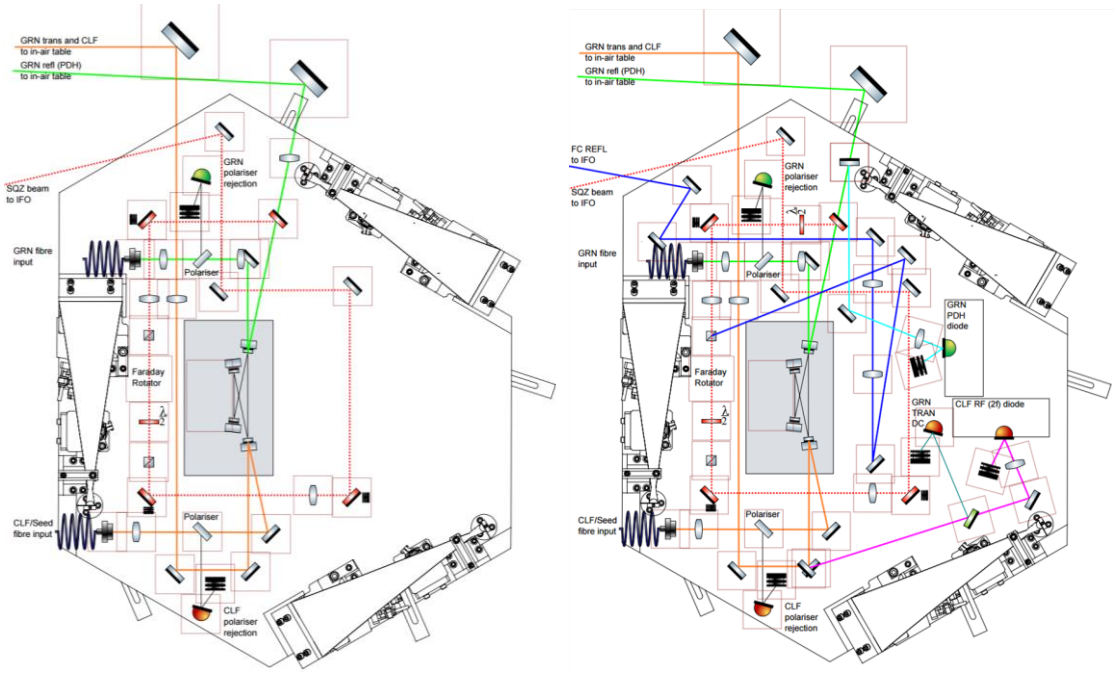

Figure 10: VOPO optical layout for O2 (left) and O3 (right)

The most important part of both layouts is the VOPO cavity, marked in gray color in Figure 10. That is the key point of the VOPO and when the squeezed light is produced. We are not going to explain the particular as it is not the main goal of this document, but in this cavity, so called because it "captures" the light in between its four mirrors and forces it to go through the non-linear PPKTP crystal. This crystal is the key element of the cavity as it is where each photon of 532nm light is converted into two 1064nm photons that are consequently in phase and the same wave length used in the interferometer. Figure 11 present the design of the VOPO cavity and the MIT prototype that is being tested at the moment.

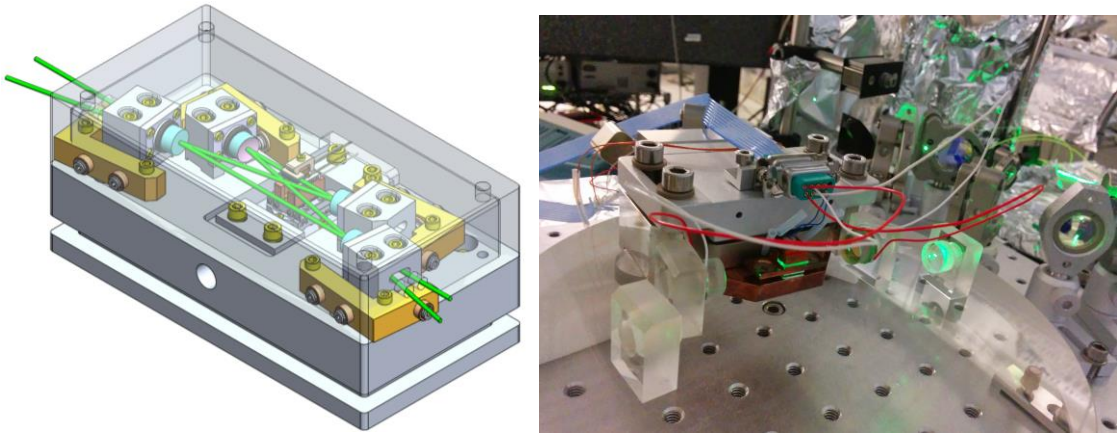

Figure 11: CAD model (left) and prototype built at MIT (right) of the VOPO Cavity

In order to work as expected, this cavity has to be pumped with a light income. Going back to the O2 configuration presented in Figure 10, both fiber in can be observed in the left edge of the layout, pumping the cavity with the beams represented in green and orange. There is a critical parameter in the design of the layout that is the distances between the fiber in, the lenses and the mirrors of the cavity. These distances are carefully calculated to match the pump beam with the cavity and therefore avoid losses on it. It can also be

observed that there are also two output beams coming out from the cavity. The orange output is then reflected by some mirrors and leaves the suspension. With the green beam something similar happens, but with an important difference. This output is split into two different beams, the green and the red, being this last beam the most important one as it is the actual squeezed light. This squeezed light goes then through lenses, polarizers, a wave plate and the Faraday rotator, being its final target the Faraday suspension placed in HAM5. Again, the position of the lenses is critical in order to match this beam with the target. Additionally, one of the constraints regarding the chambers layout is that in between the VOPO and the Faraday, the beam has to be reflected in two Tip-tilt mirrors in order to allow LIGO people to actuate from the outside. Concerning the green and orange outputs, their target is, for O2, the detectors that will be placed in air next to the chamber.

If we move to the O3 layout in Figure 10, the same base arrangement can be observed but with some differences. The main one is the blue beam, which will replace the red one as the one that is injected into the interferometer. This is because in O3 the squeezed beam goes to a filter cavity (presumably a 16m single cavity between HAM4 and HAM5) and comes back to the VOPO, where a polarizer separates it from the squeezed light going out of the cavity; separation that is represented in Figure 10 with the blue beam. The other main difference, which may be applied or not, is the introduction of in Vacuum RFPD detectors. As it has been stated above, these detectors are originally (O2) on a table next to HAM6, and the beams reach them by going through the View Ports (the "windows" of the chambers). Having them in Vacuum will represent an advantage as the value of the detected data will be higher, even if it bring some technical challenges.

STEP 1: SITUATION IN THE CHAMBER

After all the general requirements have been defined and, even if it may be counterintuitive, the first thing that has to be defined is what will be the overall shape of the suspension. To define it, both the available area and the minimum required space for the optics have to be considered. In the case of the VOPO suspension, a 2 x 1.5 ft^2 suspension was needed. Comparing this preliminary estimation with the HAM6 layout, presented in Figure 12, it was decided that the best place to allocate the new suspension is in the highlighted area of Figure 13, as all the red rectangles are just balancing mass that can easily be removed and that was intended to host the upcoming instruments.

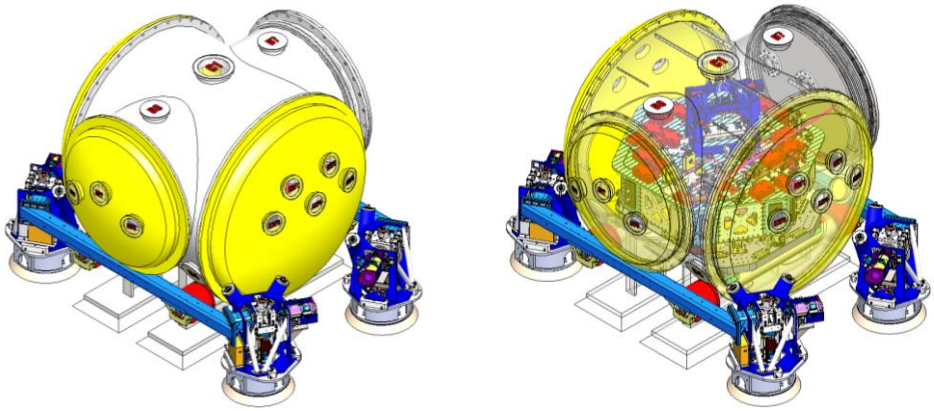

Figure 12: HAM6 chamber Layout prior to the installation of the Squeezer

In general, it might be recommended to define symmetric shapes, but in our situation, and as we do not wanted to move any of the existing equipment, the shape is a heptagon. As shown in Figure 13, in the definition of the suspension's shape different needs have been considerate. Firstly, the availability of holes around the structure is important if we want to use dog clamps to attach it to the optical bench. Also, a free

area has to be left for the Tip-Tilts that will be used to address the squeezed beam to the next chamber. In addition, we need to anticipate the need of a "shooting area" in the suspension, which is an area where no other parts of the suspension will interact with the beams leaving it.

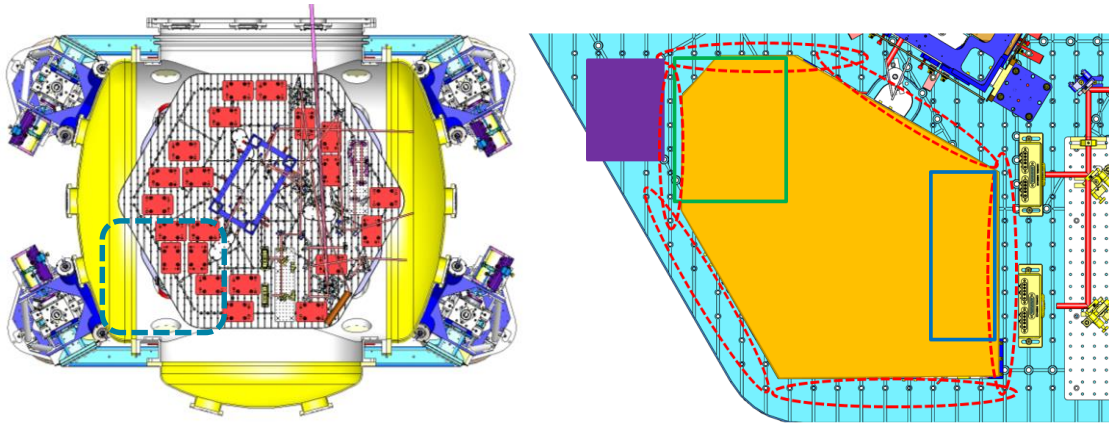

Figure 13: HAM5 chamber selected location for the squeezer

STEP 2: MASS BUDGET ESTIMATION

Once the shape of the suspension was defined, we worked on the preliminary mass budget. What we basically were looking for is to know the total weight that will conform the first stage, i.e. the suspended. This weight may be broken down into three: the optics weight, the injection bench weight and the balancing mass weight. This last mass is important because, as it has been shown in previous suspensions, it is important to have a way to do the final adjustment in order to have a well-balanced suspension.

Consequently, the first important thing to do is to estimate the total weight of the optics that are going to be on the suspension. To do so, the people in charge of the design and development of the VOPO instrument made a preliminary design and estimated that this weight will be around 12kg. Given that number, we considered that the total suspended weight, without the injection bench, must be considered to be 18kg. This six extra kilograms are seen as both the balancing mass and the contingency for the optics weight. Finally, the weight of the injection bench has also to be estimated. The injection bench has to be stiff enough to hold all the optics' mass and keep its resonance frequency as high as possible. As it will further discussed, the minimum acceptable frequency will be related with the bandwidth of the actuators. Finally, 18kg where considered a good guess for the required weight of the bench. All in all, the total weight considered for the first stage is 36kg, distributed as it follows:

$$\begin{aligned} Optics: &\quad 12\ kg \\ Injection\ Bench: &\quad 18kg \\ Balancing\ mass + contingency: &\quad 6kg \end{aligned}$$

STEP 3: BLADES PRELIMINARY DESIGN

With this first estimate the blades' dimensions can be calculated. To do so, we use the procedure described in Subassemblies, Blade Assembly, Blade and that we have implemented as a Matlab document *BladeDesign.m*. This procedure is applied in the definition of a "bent when loaded blade". That means that the blades are going to be flat when machined and they will be bent once they are in service. This approach is contrasting with other suspensions, like the OMCS, where the blades where subjected to a forming and heat treatment process to be curved when unloaded. The problem with this type of blades is that the

procurement time and the price are both much higher than for the ones that have been considered, which is one of the main reasons for this election.

In the VOPO design one of the main restrictions is the available space, and we want to keep the "useful" area as large as possible. Basically, there are three parameters that have to be defined in the global blade design process, which are the number of blades, the material of those and the degree of freedom in the blade's dimensions (length, wide or thickness). This might be an iterative process in which a compromise has to be found in order to avoid having too much low-loaded blades or too fee high-loaded ones. For the VOPO suspension, the number of blades has been set at 3, which means that each blade will have to support 12kg.

Given this load, the selection of the material is one of the key points in the blade design. In LIGO, the majority of the blades are designed using Maraging steel (C250, for example), as they present superior strength and toughness without losing malleability compared to other steels. However, again both the cost and the uneasiness in the procurement made us analyze other potential options. The two studied options were 17-4 SSTL and 440C SSTL, being the second the one that was finally chose. This material, as a Martensitic steel, is a high carbon steel, which attains the highest hardness, wear resistance and strength of all stainless steel grades after heat treatment. Additionally, grade 440C is more readily available than the other standard grades in the 440 series.

On the top of that, this steel has a corrosion resistance lower than that of other austenitic grades and it is Ultra High Vacuum compatible. Actually, the main drawbacks of this kind of steel are its loss of strength caused by over-tempering at high temperatures, and its loss of ductility at temperatures below zero, two problems that should not perturb us. The properties for the considered material can be found highlighted in Table 1. It can be observed that the Tempering Temperature to attain the desired strength and hardness is 204°C. Even if the Yield Strength after this thermal treatment is expected to be 1900MPa, a Yield strength of 1800MPa has been considered in all the calculations. Regarding the Young's Modulus, for the 440C the value is 210GPa.

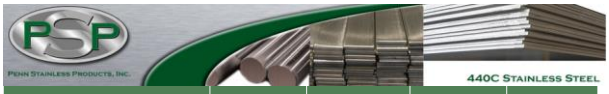

Tempering Temperature (°C)	Tensile Strength (MPa)	Yield Strength 0.2% Proof (MPa)	Elongation (% in 50mm)	Hardness Rockwell (HR C)	Impact Charpy V (J)
Annealed*	758	448	14	269HB max#	-
204	2030	1900	4	59	9
260	1960	1830	4	57	9
316	1860	1740	4	56	9
371	1790	1660	4	56	9

* Annealed properties are typical for Condition A of ASTM A276# Brinell Hardness is ASTM A276 specified maximum for annealed 440A, B and C.

Table 1: Mechanical properties of 440C SSTL; highlighted the heat treatment selected

Finally, regarding the definition of one of the three main dimensions of the blade, its length has been set at 280mm, value that is consider to fit adequately given the overall size of the suspension. With all this values, and considering a factor of safety (FoS) of at least 3.5, the dimensions of the blade are presented in Figure 14.

$$\begin{aligned} Length\ (l): &\quad 280mm \\ Width\ (b): &\quad 85mm \\ Thickness\ (h): &\quad 2.1mm \end{aligned}$$

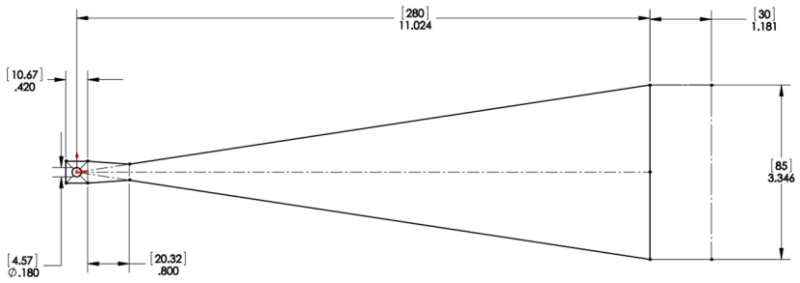

Figure 14: VOPO blade preliminary dimensions

The importance about this first calculation of the blade parameters is to see if with the combination of the material selection and the defined length the global dimensions of the blade are reasonable. In this case, a width of 85mm is totally acceptable considering the instrument dimensions. Regarding the detailed shape of the blade (tip, hole, etc.), it depends on the type of clamp that it is going to be used to attach de wire and the blade. As it will be discussed further on, this shape in particular has been defined to fit a clamp analogous to the one used in the Faraday instrument.

On the other hand, there are two important datum that are extracted from this first analysis: the vertical stiffness of the blades –and hence the vertical frequency– and the Factor of Safety, both presented below:

$$K_{zz} = 1255.1\, {}^{N}/_{m}$$

$$f_{ZZ} = 1.6277\ Hz$$

$$FoS = 3.4117$$

The frequency is slightly larger than the requirement of 1.5Hz that was set at first. However, the main advantage of these solution, and the reason why this increase in frequency is allowed, is that the blade will be working with a stress lower that the 30% of its Yield strength.

STEP 4: FLEXURE DESIGN

After the pre-definition of the blade, another important element that has a crucial task in the suspension is the flexure. This element is the equivalent of the blade for the horizontal motion, as it defines the horizontal frequency of the suspension in both X and Y directions. After the calculation detailed in (Subassemblies, Blade Assembly, Flexure), the flexures of the VOPO cavity are going to be steel music wires with a diameter of 0.024". This kind of flexures has already been used in the aLIGO project, adding confidence to that choice. The results extracted from that study show that the horizontal frequency attains acceptable values for a length of 130mm, a reasonable value given the global dimensions of the suspension. The frequency, stiffness and Zero Moment Point (ZMP), which are going to be used through all the design, are presented below.

$$K_{zz} = 955.62\, {}^{N}/_{m}$$

$$f_{ZZ} = 1.4203\ Hz$$

$$ZMP = 3.4066\ mm$$

STEP 5: LOCATION OF THE BLADES

After the definition of the dimensions of the flexure and the blade, which will be checked using Finite Element Analysis (FEA) in upcoming steps, it is important to decide where to locate them in our suspension. This is

important because the tips of the blades will define a geometric figure in whose centroid the gravity center of the suspended stage will have to be located in order to have a balanced instrument. That means that arrangements where the centroid of the blade's geometry is distant to the "center" of the suspension should not be considered as it will make the balancing process hard. An exception to that may be the case in which it is known beforehand that the optical layout will not be centered in the bench. For the VOPO suspension an equilateral triangle distribution was finally selected, as shown in Figure 15, where the green dot represent the point where the center of mass of the suspended stage will have to be. Due to all the work that had been done before, in the case of this suspension we had already defined other positions, as may be observed in the mentioned figure. However, the main goal of this step is to define the available space for optics, as the next step will be to define the optical layout. Thus, what it is needed at this point is to define the "forbidden" areas for optics, as shown in Figure 15.

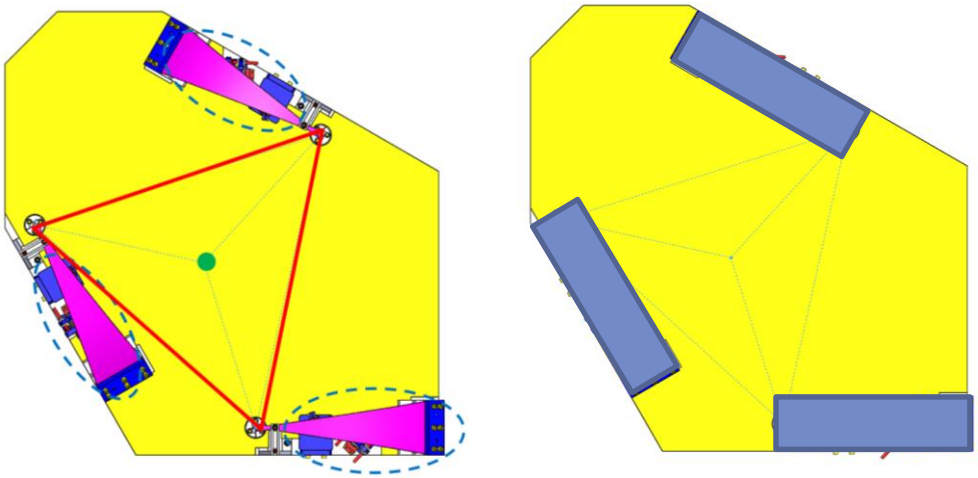

Figure 15: Location of the blades in the VOPO suspension (left) and "forbidden" area (right)

STEP 6: CAD MODEL OF THE OPTICAL LAYOUT

Knowing the estimated free area for optics, it is time to check if this area is adapted to the real requirements. It may seem that it is too soon the work on the detailed layout as the suspension is barely defined, but it is important to do so at this point in order to avoid having to redefine everything in the end.

In the definition of the layout both the mass the volume of each optical instrument must be taken into account. To do so, SolidWorks models from existing designs were adapted to match our design. The aim was not to change the optics but to adapt their height because, with the predesign of the VOPO cavity that was used to define the physical arrangement, the level of the optics and the injection bench are constraint, as presented in Figure 16.

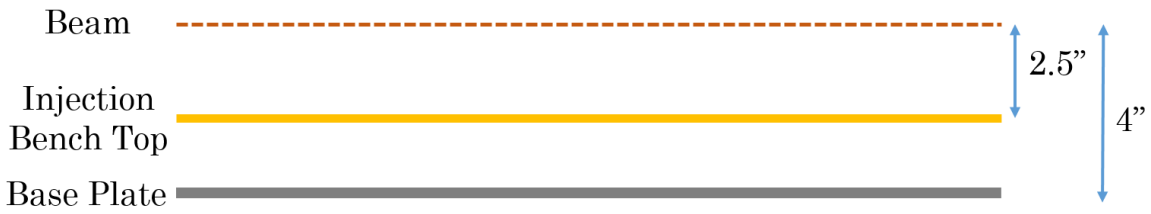

Figure 16: Height of the beam and injection bench

Typically, the optics used by LIGO are 4" height, so they had to be all adapted to 2.5" high to match the requirements. On the other side, not all the optical parts had been properly defined and, for example, mirror mounts have been used to represent both polarizers and fiber inputs. We know that this may not be 100% accurate but it was considerate as a good estimate, especially considering the high level of contingency that was selected. Detailed information about these models and their weight may be found in additional documentation (VOPO Suspension, E1500446-v).

Using these models and after a few iterations the presented layouts for O2 (Figure 17) and O3 (Figure 18) are considered to be acceptable and fulfill all the requirements. Again, a detailed overview of both layouts may be found in (VOPO Suspension, E1500446-v).

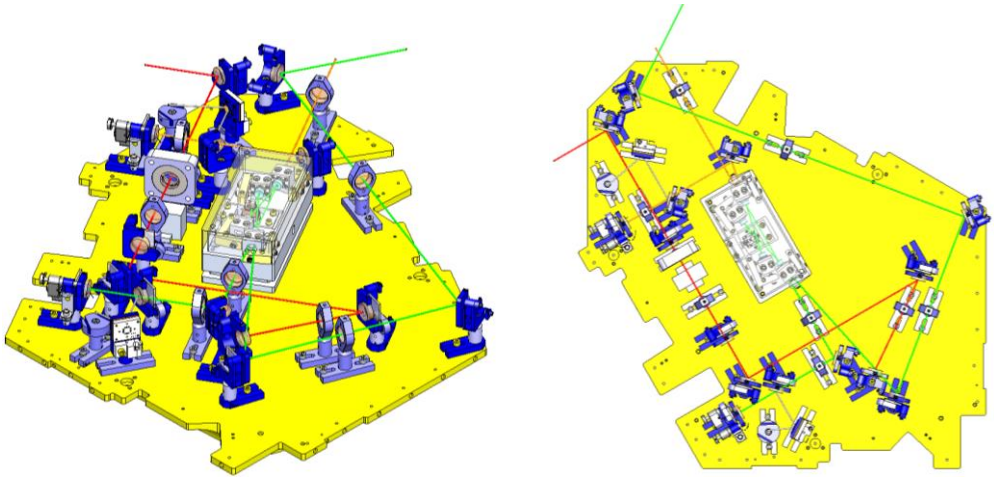

Figure 17: CAD model of the O2 configuration layout

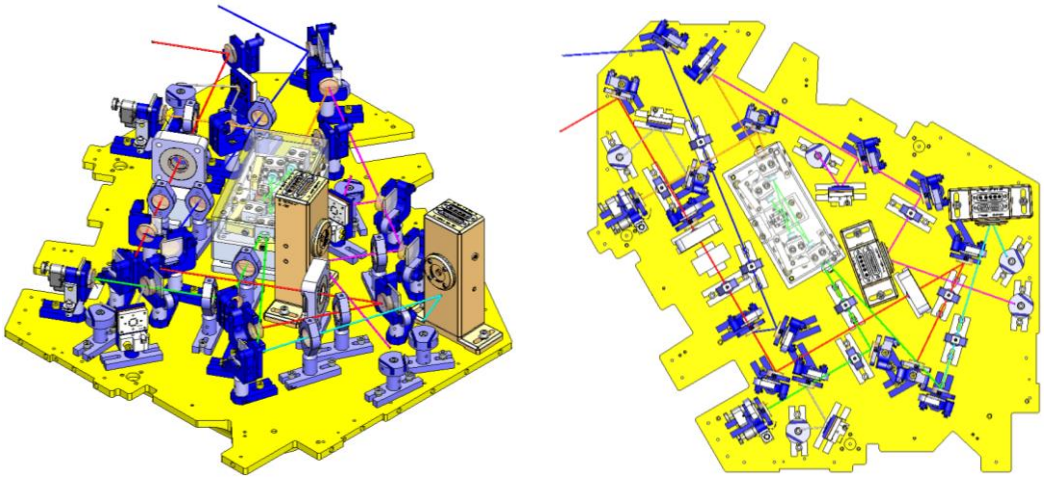

Figure 18: CAD model of the O3 configuration layout

For the VOPO suspension it seemed to us that the optical layout matched the available space without being excessively constraint or having too much free space. If that is the case in any other suspension, it is necessary to come back to the first step and reconsider the location and/or the area used by the instrument.

STEP 7: CHAMBERS' LAYOUT

An important aspect to keep in mind while trying to find an adequate layout is to think about the whole chamber layout to check if the directions of the beams leaving the suspension can match the overall layout requirements. To do so, a full HAM5 and HAM6 model was developed and it shown that, even if some small changes may be done by the time of the implementation, the layout was correct. This full model is detailed in (VOPO Suspension, E1500446-v).

STEP 8: *REAL* MASS BUDGET

One of the main results that must be obtained after the layout definition is the *real* weight of the optics, *real* being in italic as probably it will not be the final weight, but it is a better estimate. Table 2 shows the results of the mass budget for the VOPO cavity at both O2 and O3 configurations.

MASS BUDGET

ELEMENT TYPE	Name	Description	Unit Weight (g)	Quantity O3	Total mass O3 (g)	Quantity O2	Total mass O2 (g)	Mass Checked?
OPTICS	MIRROR	With Beam Dump	205.87	4	823.48	2	411.74	YES
OPTICS	MIRROR	With Beam Dump 2	207.55	4	830.20	1	207.55	YES
OPTICS	MIRROR	Without Beam Dump	192.90	4	771.60	6	1157.40	YES
OPTICS	MIRROR II	1in Lens Mount	121.38	0	0.00	0	0.00	YES
OPTICS	MIRROR III	Lens Sigle Base	97.07	0	0.00	0	0.00	YES
OPTICS	LENS	Desc 2	121.38	9	1092.38	8	971.00	YES
OPTICS	BEAM DUMP	Without One Black Glass	156.83	5	784.15	2	313.66	YES
OPTICS	QPD	QPD	142.98	3	428.94	2	285.96	YES
OPTICS	POLARIZER	Polarizer (Mirror Mount)	203.05	4	812.19	4	812.19	YES
OPTICS	WAVE PLATE	Wave Plate	299.69	2	599.38	1	299.69	YES
OPTICS	RFPD in Vacuum	4" RFPD	270.41	2	540.82	0	0.00	YES
OPTICS	FIBER IN	Mirror Mount	252.01	2	504.02	2	504.02	YES
OPTICS	FARADAY ROTATOR	Aluminum Base	170.43	1	170.43	1	170.43	YES
OPTICS	VOPO CAVITY	D1500296	3289.00	1	3289.00	1	3289.00	YES
SUSPENSION	INJECTION BENCH	Injection Bench	18000.00	1	18000.00	1	18000	NO
SUSPENSION	LIMITERS & CLAMPS	Magnet, motion limiter...	0.00	1	0.00	1	0	NO
MASS	BALANCE MASS 1	Lateral	1857.36	0	0.00	0	0.00	NO
MASS	BALANCE MASS 2	Lateral Removable	1391.65	0	0.00	0	0.00	NO
MASS	BALANCE MASS 3	On Bench	2631.72	0	0.00	0	0.00	NO
MASS	SCREWS	On Bench	174.88	0	0.00	0	0.00	NO
OPTICS					**10.647 kg**		**8.423 kg**	
SUSPENSION					**18.000 kg**		**18.000 kg**	
MASS					**0.000 kg**		**0.000 kg**	
TOTAL WEIGHT					**28.647 kg**		**26.423 kg**	
Mass to 36 kg					**7.35 kg**		**9.58 kg**	

Table 2: Mass budget for both O2 and O3 configuration

It can been observed that the first estimate we considered was a little bit too low, being the new expected mass for the optics to be 10.647 kg. Of course, for O2 this mass is going to be lower, but the weight that drives the suspension is the "worst" case, i.e. O3. With that new distribution, the expected dummy mass weight is 7.35kg, which can be seen as too much. However, given the level of uncertainty in the weight of the elements –we have used mirrors instead of fibers, for example- it has been stated that this is a quite balanced design. On the other side, we will have to deal later on with the stiffness of the suspension and maybe we need more than 18kg to reach the desired level, so this high level of contingency is somehow justified. Additionally, the dummy mass by itself plays a crucial role in the balancing process.

Summarizing all, we have reached the point where the main design of the suspension and it is time to move on into more detailed design and to think about sub-assemblies. However, before to do so it should be considerate which will be the thickness of the base plate, the part that is going to connect the stage 0 and the optical bench of the ISI. In this suspension it has been stated that 0.4" are expected to guarantee a good contact and allow the use of previously designed dog clamps, Figure 19, to secure it on the chamber's table.

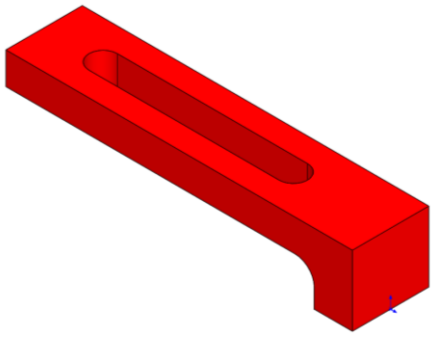

Figure 19: Dog clamps used to lock the base plate on the optical bench of HAM6

STEP 9: ACTUATORS

The next think to think about is the active damping control of the instrument. Almost all the LIGO suspensions possess active control systems in order to damp the rigid modes of the instrument. Among all these systems we have considered the so-called OSEM, a LIGO designed magnetic actuator. There are two different versions for these actuators, the AOSEM and the BOSEM, being the second one bigger and with more actuation capacity. Both actuators are base in a fixed coil free magnet system. Usually, the magnets, which can also act as flag, are attached to the suspended stage while the coil is attached to the ground. Their mechanism is roughly explained in Figure 20. The OSEM use a LED-photodiode pair to know the position of the magnet and its movement. In addition, the position of this magnet may be controlled via the injection of current through the coil (LIGO-T1200468).

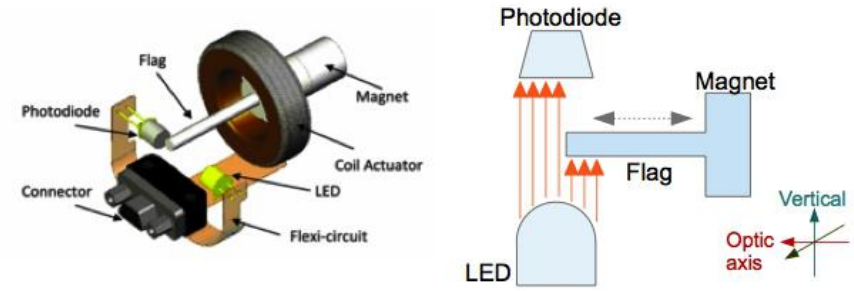

Figure 20: A schematic of OSEM shadow sensor operation

At first, the BOSEM were selected but we realized that we were oversizing our system as with a 36kg suspended mass and the needs in terms of damping, the AOSEMs satisfy all the requirements. Additionally, LIGO has some spare AOSEM that may be used for the VOPO suspension what will result in an important cost and procurement time reduction. Thus, AOSEM were finally selected to actuate the VOPO suspension, guaranteeing good performance as they have already been successfully used in precedent LIGO suspensions, such as the HSTS.

Specifically, the suspended bench is actively damped by six AOSEM actuators, being half of them used for the vertical control and the other for the horizontal one. About its disposition, the actuators will be placed

under the blade in order to use as less space as possible. In addition, the horizontal actuators are placed tangentially to the bench radius to ease the control, as shown in Figure 21. The detailed about the AOSEM alignment system and its FE study is in (Subassemblies, AOSEM and Magnets), where it can also be found the description of the magnet holders.

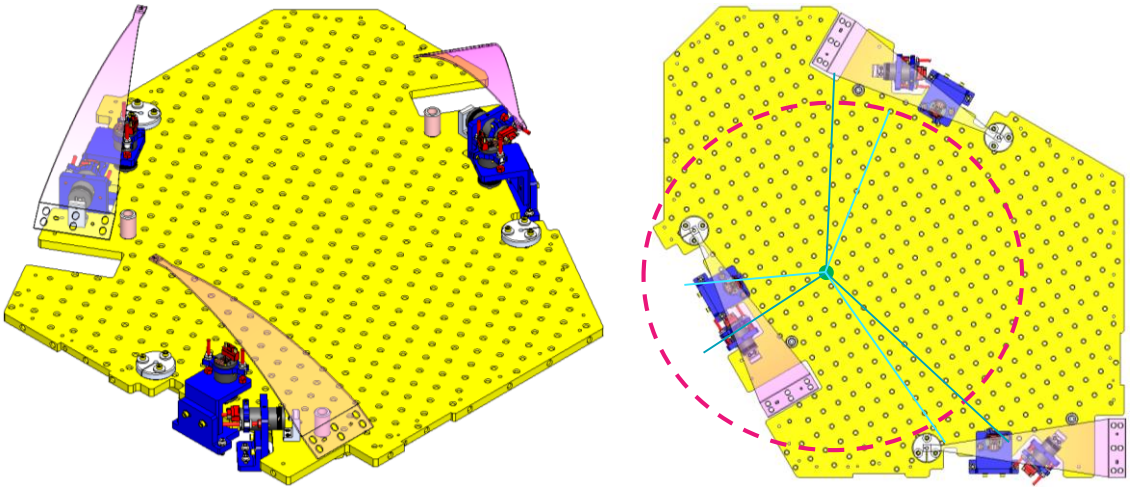

Figure 21: Position of the AOSEM under the blades; horizontal AOSEM tangently located

The selection of AOSEM as actuators has an important implication as it defines the minimum resonance frequency for all the elements of the instrument. The bandwidth of the AOSEM is approximately to 30-40Hz, which means that the frequencies of the elements should be as far away from those as possible. Approximately, a minimum frequency of 150Hz will be stablished for the design.

In parallel with the AOSEM alignment system, a system to hold the magnet on the first stage has to be designed. The design of this system, whose principle is to hold magnetically the magnet, is detailed in (Subassemblies, AOSEM and Magnets). It is important to check that by the end of this process the preliminary layout is still feasible and that none of its space has been used.

After the AOSEM selection we do have a criteria to select whether the elements are stiff enough or not. This criteria is going to be used in the injection bench design, using a cyclic process.

STEP 10: INJECTION BENCH DESIGN & BALANCING

In order to optimize the design of the injection bench it is necessary to link this design with the expected optical layout. By this time, we already have the position and mass of the optics defined so the only elements that are missing are the balancing masses. This masses have to be movable as it is likely that during the assembly some discrepancies in weight will appear and part of the dummy mass will have to be added or removed. Another important aspect about this masses that must not be forgotten is that they should never interfere with the optics or its tenability. Consequently, it was decided that in the VOPO suspension a fair portion of the added weight will be attached to the edge of the suspension as a cantilever, as shown in Figure 23.

That being said, the abovementioned cyclic process consists in optimizing the shape of the injection bench and trying to position the masses in order to keep the center of mass in the right position (green point in Figure 15). Of course, the position of this center of gravity depends on the shape of the injection bench, but also the position of the different masses depends on the best shape for the optical bench as Figure 22 exposes.

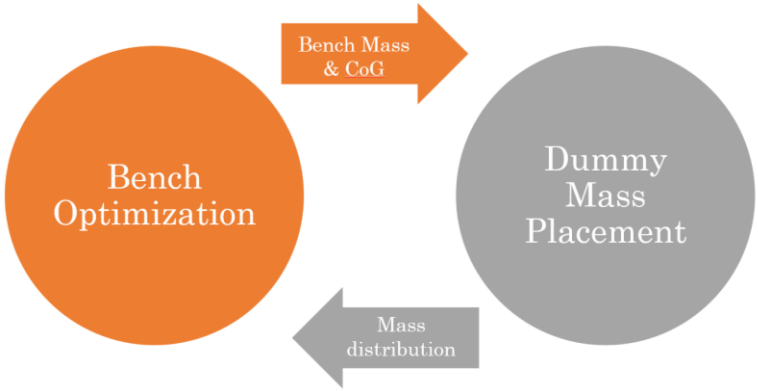

Figure 22: Schematic of the iterative process of optimization on the injection bench

At this point, we know that in O3 approximately 6.76kg will have to be added as "dummy" mass to reach the 36kg. The idea is to place half of this mass in the lateral edges of the injection bench. However, the proximity to surrounding instruments in HAM 6 –see Figure 13– causes that only certain edges of the suspension are suitable to hold these cantilevered masses.

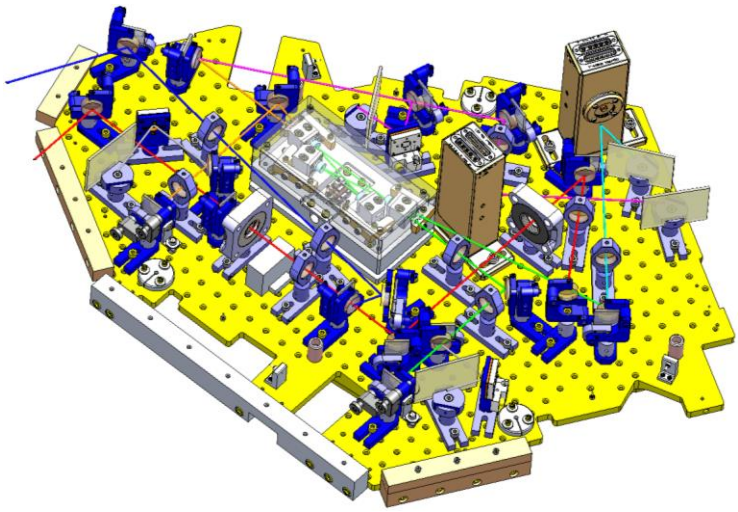

Figure 23: Lateral masses distribution in O3 configuration (same for O2)

Figure 23 shows the distribution of the lateral masses, which have a total weight of 3643g, screws included. It can be observed that this mass is completely tunable and it can be easily removed. The materials and specifications of each element can be found in (E1500446-v). This arrangement is going to be set for O2 configuration as well, in which lateral masses will also help to balance the suspended stage. Therefore, all the difference in mass between O2 and O3 will be added on the top of the table and, as the number of components is substantially inferior, fitting problems are not expected.

Thus, with the lateral mass already added, it is time to start the cyclic process of placing the dummy mass –with a total weight of 3.11kg– and optimizing the injection bench's shape. Actually, what we are trying to optimize is the underneath shape of the injection bench, as well as the thickness of each area of the component. The details of this cyclic process are explained in (Subassemblies, Injection Bench), but the resultant shape of the bench, weighting 18.373 g, is presented in Figure 24.

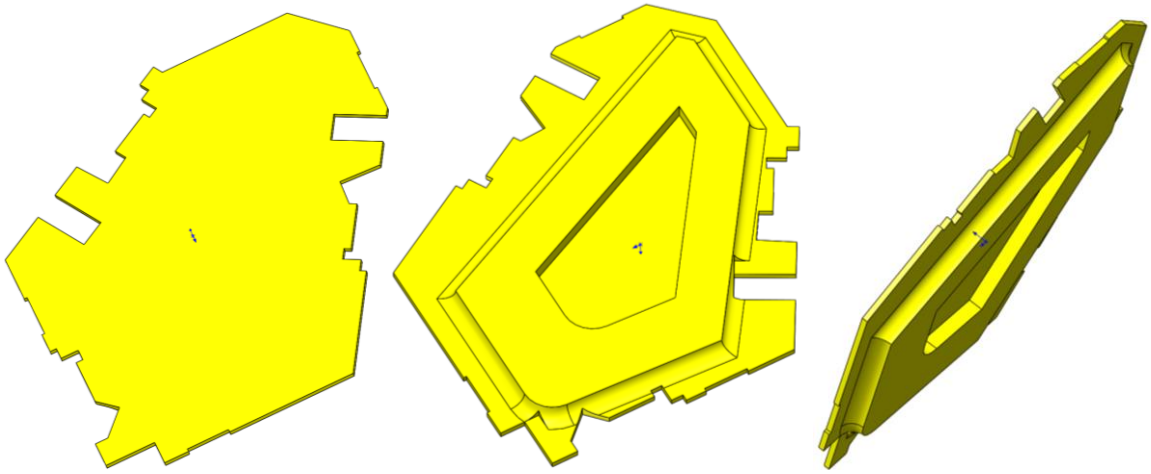

Figure 24: Injection bench design showing the stiffener underneath

Additionally, the process described in Figure 22 also gives the distribution of all the optics and the dummy masses in order to have a balanced stage. Obviously, some changes are expected to be done as the layout does not represent with 100% of accuracy the elements. However, these adjustments are anticipated to be minor and do not invalidate all the calculation made.

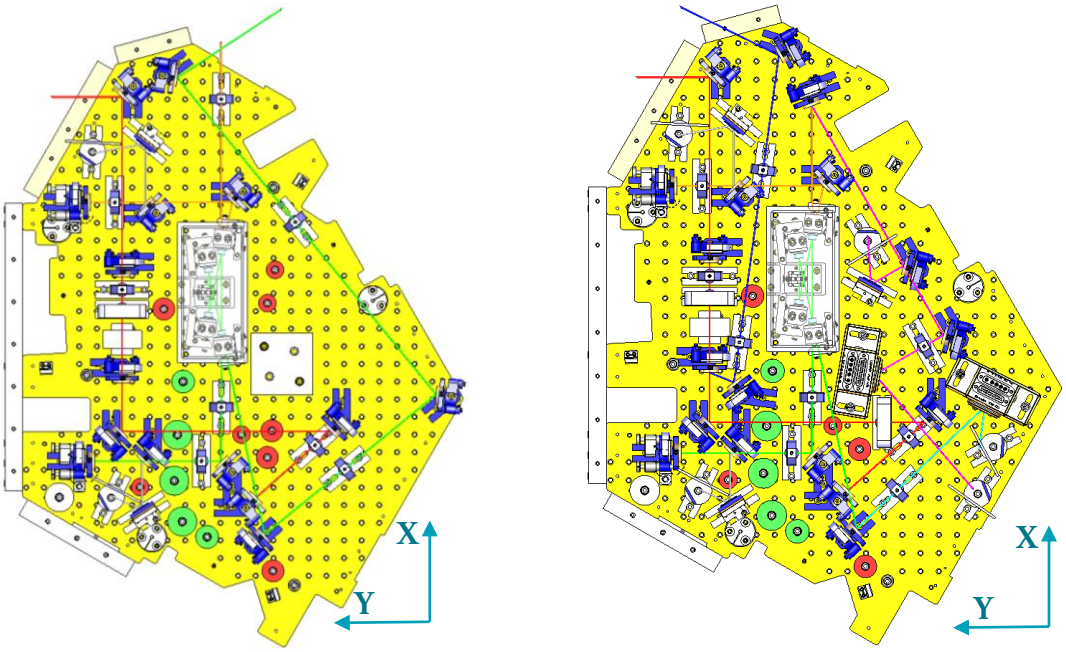

Figure 25: Balanced layout for O2 (left) and O3 (right) configurations

The Figure above presents the balanced layout for both O2 and O3 configurations for a total weight of 36kg. The detailed mass budged can be found in Table 4, as well as the moments of inertia for both arrangements.

Using the information extracted from the calculation of the blade and the flexure all the frequencies of the suspension may now be calculated. For the VOPO suspension this frequencies have been double checked – see (E1500446-v)– and the results, presented below, confirm that both the blades and the flexures are adapted to the requirements.

	FREQ. (Hz)
X	1.4175
Y	1.4190
Z	1.6277
Roll	2.0666
Pitch	1.6222
Yaw	1.6114

Table 3: Translational and rotational frequencies of the VOPO suspension

Notice that the roll frequency is slightly higher than the reference frequency. However, it has been considered that 2.07Hz is still acceptable and so the design is considerate appropriate. If that was not the case and one the frequencies was unacceptably high, the blade and/or flexure design should be revised.

STEP 11: BASE PLATE

The next step is to design the Base Plate. As stated in (Subassemblies, Base Plate), this element is the link between the suspension and the optical bench of the chamber. So, it has to be designed in order to both guarantee a good contact between the suspension and the optical bench and be stiff enough to resist the transport phase.

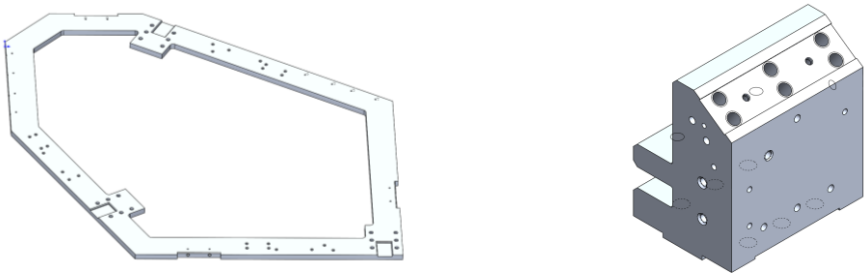

Figure 26: Base plate of the VOPO suspension (left) and Blade platform (right)

STEP 12: BLADE PLATFORM

The design of the suspension reaches at this point the acceptance level. To summarize, all the passive isolation systems seem to be adequately designed. However, there are other important parts of the suspension that need to be checked and designed. One of these parts is the blade post, a key element in the suspension design. This post has two key parameters: height and top angle. It is critical that these parameters are defined properly as the position of the blade depends on them and hence the position of the whole suspension. The post design, as well as the contact study on the blade to determine the exact deformation of it, are accurately defined in further sections.

STEP 13: MOTION LIMITERS, LOCKERS & ASSEMBLY BRACKETS

Another important point that may appear as secondary but that it is also crucial is the motion limiters and the lockers. The function of the first of them is to causing any damage to the AOSEM actuators avoid as a consequence of an excessive displacement of the suspended bench during the lifetime of the instrument. So, the maximum motion of the first stage has to be limited and the design of this limiters should take into account the ease of use of them. Differently, the function of the locker is to block completely the motion of the suspended stage by locking it into the base, assuaging the transportation and assembly of the suspension, as well as any commissioning task on it. Of course, this is completely useless during operation as all the

isolation is suppressed so the locker should never be used during runs or testing periods, and this is why it is important to design a system both easy to inspect and manipulate. The details of this elements can be found in Subassemblies section.

STEP 14: ASSEMBLY PROCEDURE & FINAL MASS BUDGET

The last step of detail is to define an assembly procedure to check that everything has been properly designed and that the building is feasible. One key element in this procedure is to set all the elements in the right position with respect to the others because, in a precision instrument like the VOPO suspension, it is extremely important to avoid misalignments that will lead to poor performances. Particularly, this suspended instruments require a precise alignment of the flexure as otherwise it may produce an important displacement of all the first stage when released. With this aim, the position of the first stage with respect to the base and the position blade's platform with respect to both the injection bench and the base plate have to be accurately controlled. To do so, it was first considered to use pin-hole systems, an approach that has been successfully implemented in LIGO before. However, do to the difficulties in the assembly procedure this pin-hole systems were substituted by tight tolerance surface contact, as may be seen in (Appendix, Drawings). Additionally, Figure 27 presents the final design of the VOPO suspension with the O2 optical layout.

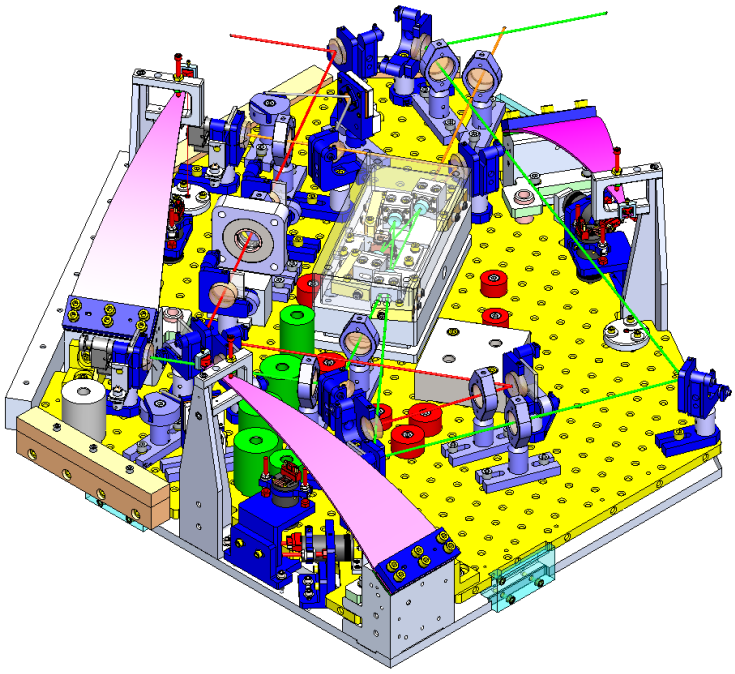

Figure 27: final design of the VOPO suspension with the O2 optical layout

FINAL DESIGN

Ultimately, the suspension is fully defined and so the first stage of the project is accomplished. Nevertheless, there is one important part that has not be treated yet and that will play a huge role in the suspension's performance and that it is the actuators control design. Figure 28 summarizes the design procedure that has been followed for the VOPO instrument and that may be used in future similar suspension designs. In addition, Table 4 presents the final Mass budget for both O2 and O3 configurations and the FEA models.

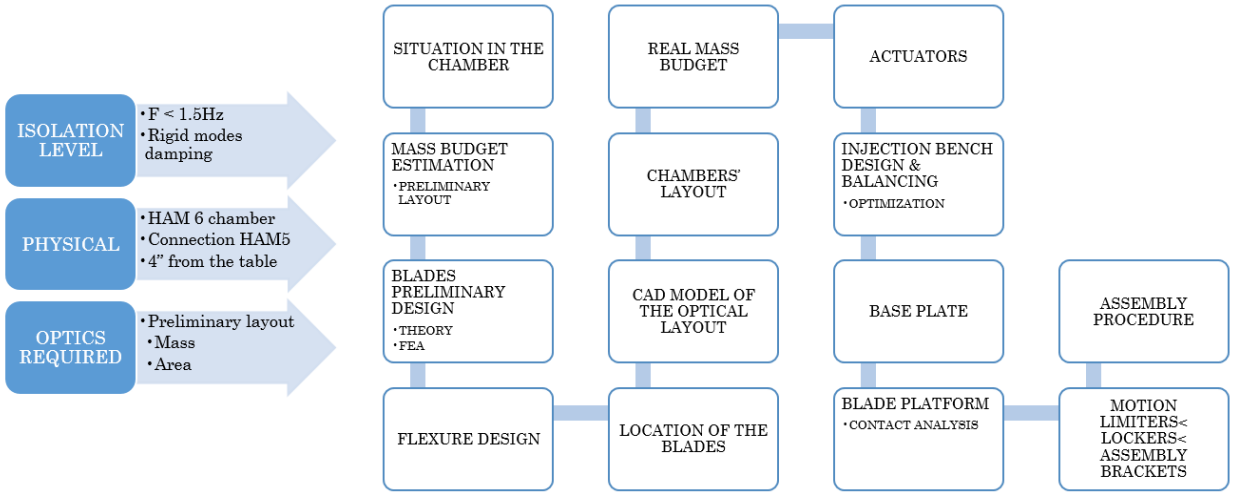

Figure 28: Monostage suspension design methodology schematics

MASS BUDGET

Highlight Items to reorder?

ELEMENT TYPE	Name	Description	Unit Weight (g)	Quantity O3	Total mass O3 (g)	Quantity O2	Total mass O2 (g)	Mass Checked?	Mass FEA (g)	Total Mass FEA
OPTICS	MIRROR	With Beam Dump	205.87	4	823.48	2	411.74	YES	202.7	810.8
OPTICS	MIRROR	With Beam Dump 2	207.55	4	830.20	1	207.55	NO	202.7	810.8
OPTICS	MIRROR	Without Beam Dump	192.90	4	771.60	6	1157.40	NO	202.7	810.8
OPTICS	MIRROR II	1in Lens Mount	121.38	0	0.00	0	0.00	NO	202.7	0
OPTICS	MIRROR III	Lens Sigle Base	97.07	0	0.00	0	0.00	NO	202.7	0
OPTICS	LENS	Lens	121.38	9	1092.38	8	971.00	NO	120.02	1080.18
OPTICS	BEAM DUMP	Without One Black Glass	156.83	5	784.15	2	313.66	NO	162.6	813
OPTICS	QPD	QPD	142.98	3	428.94	2	285.96	NO	143.35	430.05
OPTICS	POLARIZER	Polarizer (Mirror Mount)	203.05	4	812.19	4	812.19	NO	202.7	810.8
OPTICS	WAVE PLATE	Wave Plate	299.69	2	599.38	1	299.69	NO	298.65	597.3
OPTICS	RFPD in Vacuum	4" RFPD	270.41	2	540.82	0	0.00	NO	278.74	557.48
OPTICS	FIBER IN	Mirror Mount	252.01	2	504.02	2	504.02	NO	191.14	382.28
OPTICS	FARADAY ROTATOR	Aluminum Base	170.43	1	170.43	1	170.43	NO	170.43	170.43
OPTICS	VOPO CAVITY	D1500296	3289.00	1	3289.00	1	3289.00	NO	3289.34	3289.34
SUSPENSION	INJECTION BENCH	Injection Bench	18373.39	1	18373.39	1	18373.39	NO	18536.16	18536.16
SUSPENSION	LIMITERS & CLAMPS	Magnet, motion limiter...	219.57	1	219.57	1	219.57	NO	126.4	126.4
MASS	BALANCE MASS 1	Lateral	2939.60	1	2939.60	1	2939.60	NO	3666.9	3666.9
MASS	BALANCE MASS 2	Lateral Removable	543.67	1	543.67	1	543.67	NO	0	0
MASS	BALANCE MASS 3	507g + Screw	515.19	4	2060.76	4	2060.76	NO	516.2	2064.8
MASS	BALANCE MASS 4	302g + Screw	310.25	2	620.50	2	620.50	NO	306.5	613
MASS	BALANCE MASS 5	100g + Screw	107.47	3	322.41	4	429.88	NO	107.3	321.9
MASS	BALANCE MASS 6	50g + Screw	57.59	2	115.18	4	230.36	NO	55.2	110.4
MASS	BALANCE MASS 7	2kg + Screws	1995.66	0	0.00	1	1995.66	NO	0	0
MASS	LATERAL SCREWS	Lateral screws	159.25	1	159.25	1	159.25	NO	0	0
OPTICS					10.647	kg	8.423	kg		10.563
SUSPENSION					18.593	kg	18.593	kg		18.663
MASS					6.761	kg	8.980	kg		6.777
TOTAL WEIGHT					36.001	kg	35.995	kg		36.003
Mass to 36 kg					0.00	kg	0.00	kg		0.00

Table 4: Final mass budget for O2, O3 and the FEA models

Finally, a prototype of the VOPO suspension has to be built in order the check all the calculations before installing the new instrument into the LIGO sites. In (Appendix, Drawings) all the drawings of the designed parts, which have been sent to the manufacturers, are presented.

SUBASSEMBLIES

This section is intended to give a detailed view of the design process of each one of the subassemblies that conform the squeezer suspension. First off, Figure 29 presents the overview of the squeezer suspension and shows the different subassemblies.

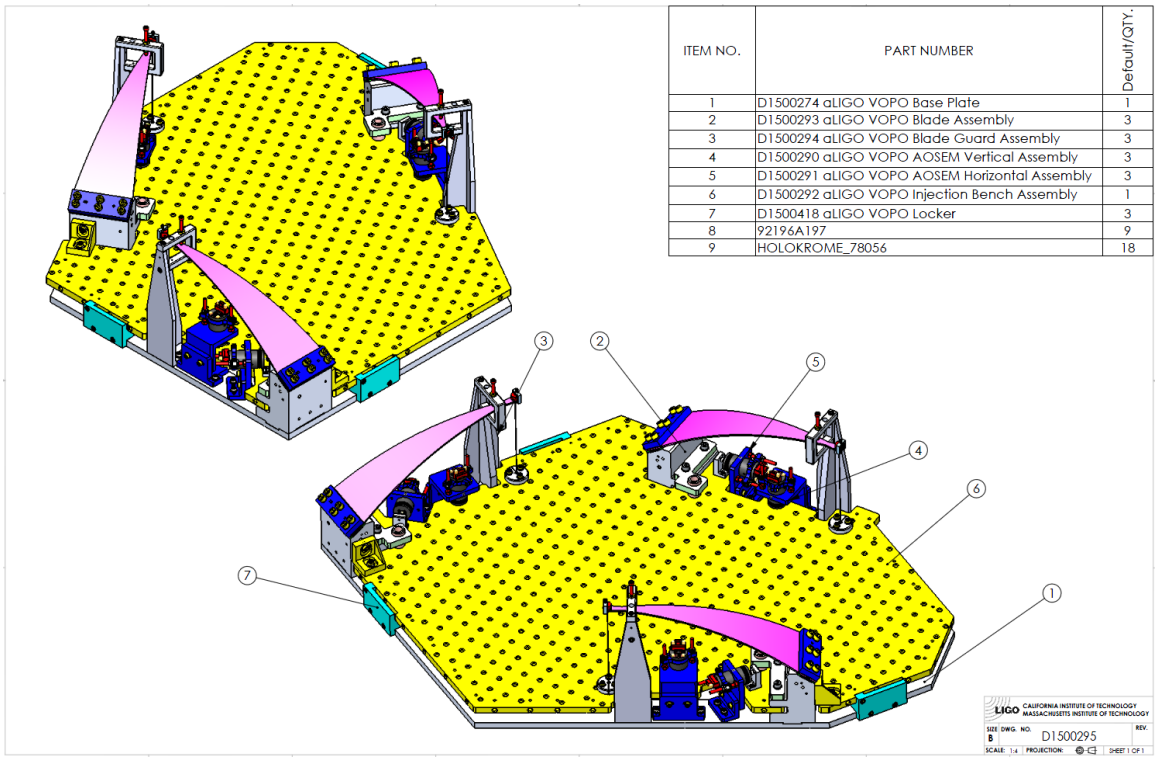

Figure 29: Overview of the subassemblies of the VOPO Suspension

AOSEM AND MAGNETS

The AOSEM actuator is based in a coil cylinder that may be controlled from outside and that acts over a magnet, as it has been explained before in this document. Nevertheless, these actuators have to be supported by an alignment system whose aim is double. First, it is intended to hold the AOSEM that that I can be at the right height and orientation with respect to the magnet. The other important feature is that this assembly has to keep all the translations tunable in order to allow the positioning of the AOSEM vis-à-vis these magnets. For the VOPO, this system has been made using a two part system specially designed for the VOPO suspension that are presented in Figure 30. As this Figure shows, all the translations are tunable thanks to the slots and the nut-shaft system.

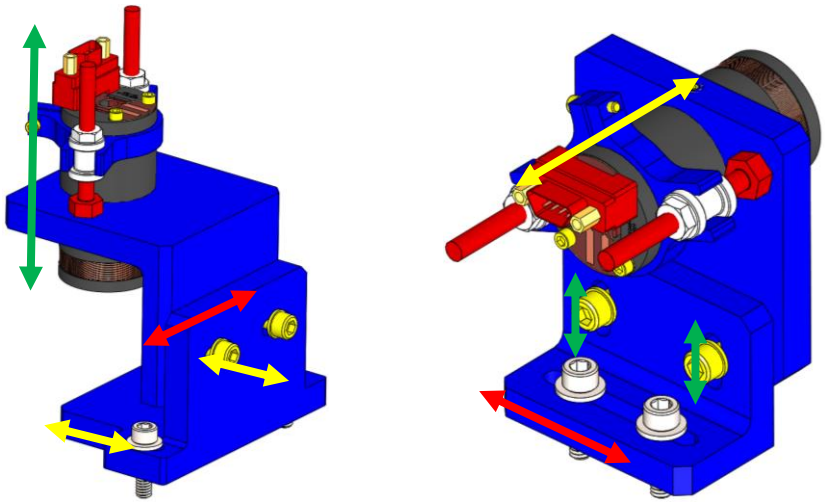

Figure 30: AOSEM vertical (left) and horizontal (right) assemblies and their motion

Similarly to other parts of the VOPO suspension, a simplified model of the AOSEM assemblies has been studied using FEA in order to guarantee that the resonance frequency are distant enough from the bandwidth of the actuator. The results of this FEA analysis, presented in Figure 31 and Figure 32, show that, with a minimum resonance frequency of 646.35Hz, the design satisfies the specifications.

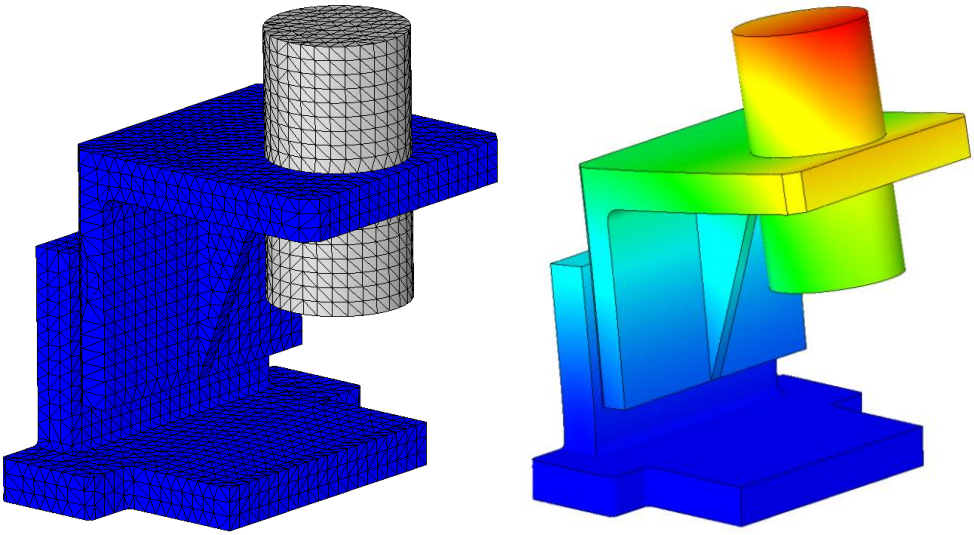

Figure 31: FEA (SW Simulation) for Vertical AOSEM Assembly. First frequency: 646.35Hz

The FEA has been performed using simplified versions of the parts of the assembly and using a bonded contact with compatible mesh. This may not give the more accurate results but it has been considered to have an acceptable accuracy, especially because, for the part that is being considered, the first resonance frequency far exceeds the requirements. If that was not the case, a new design should be developed and a refined FEA should be performed. Regarding the boundary conditions, all the base was set as fixed geometry.

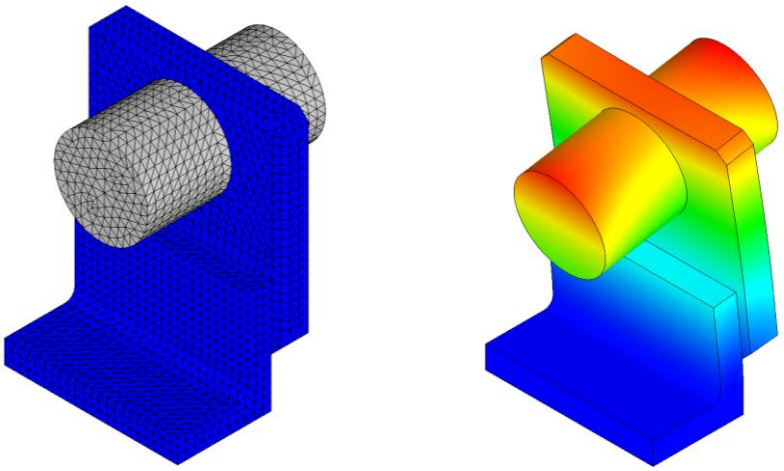

Figure 32: FEA (SW Simulation) for Horizontal AOSEM Assembly. First frequency: 873.05Hz

The magnets play also an important role in the damping control system. In the VOPO suspension, these magnets are attached to the suspended stage and they have both the magnet and the flag function. LIGO group has worked with different kinds and sizes of magnets in the previous designs so the idea for this instrument was to reuse existing magnets models. At last, 2 x 6mm cylindrical magnets were selected as there was a considerable number of them in spare so the procurement should be easy.

One of the delicate parts of these magnets is the way they are attached to the suspension. In earlier aLIGO designs, the magnets were glued to the suspended stage either directly or using a post as interface. In both cases, the UHV compatible glue had to be used and that uneased the assembly. Consequently, the idea of getting rid of this glue assembly and using the magnetic property of the magnet instead was studied. The result is a threaded part made of 440B stainless steel that holds the magnet at the right height from the top of the injection bench and guarantees an initial penetration of the magnet in the AOSEM of 0.073". With this penetration, the tip of the magnet is located in the median plane of the LED-Photodetector system, as shown in Figure 33.

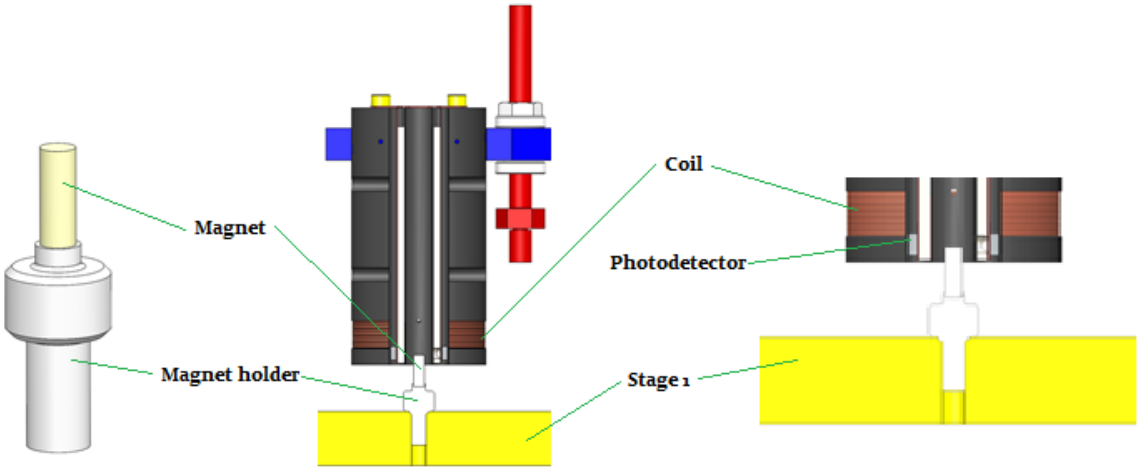

Figure 33: Overview of the magnet holder and the photodetector

Figure 34 gives an overview of the whole bracket assembly and the magnet in its position. As it can be seen, the magnet will be held in its position by being magnetically attracted by the holder, which is then screwed into the bench.

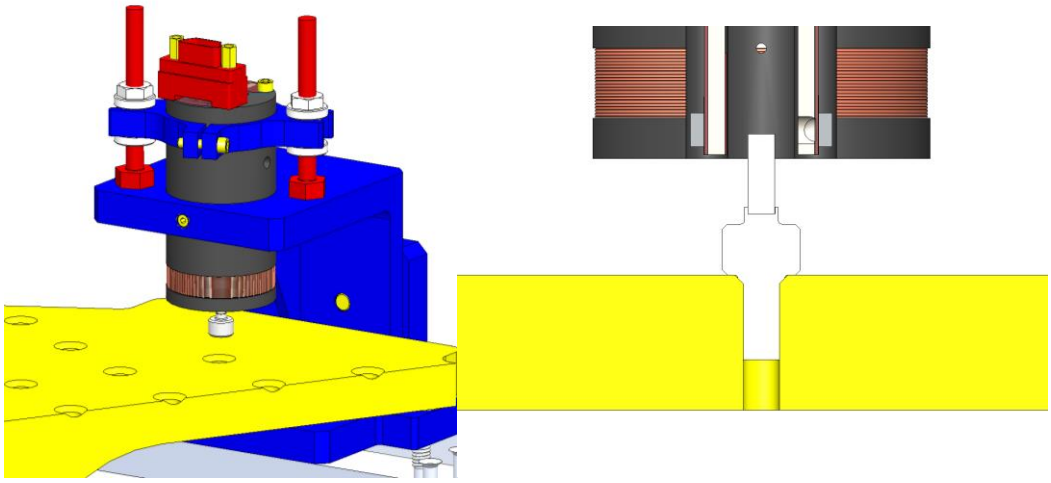

Figure 34: Position of the magnet in the AOSEM

However, for the horizontal AOSEM it is not possible, or at least not favorable, to screw the holder directly to the bench. So an intermediate part had to be designed in order to raise the magnet up and hold it horizontally. This component is presented in Figure 35 and it consists in an L shaped part that is screwed on the bench and into which the magnet holder is then screwed.

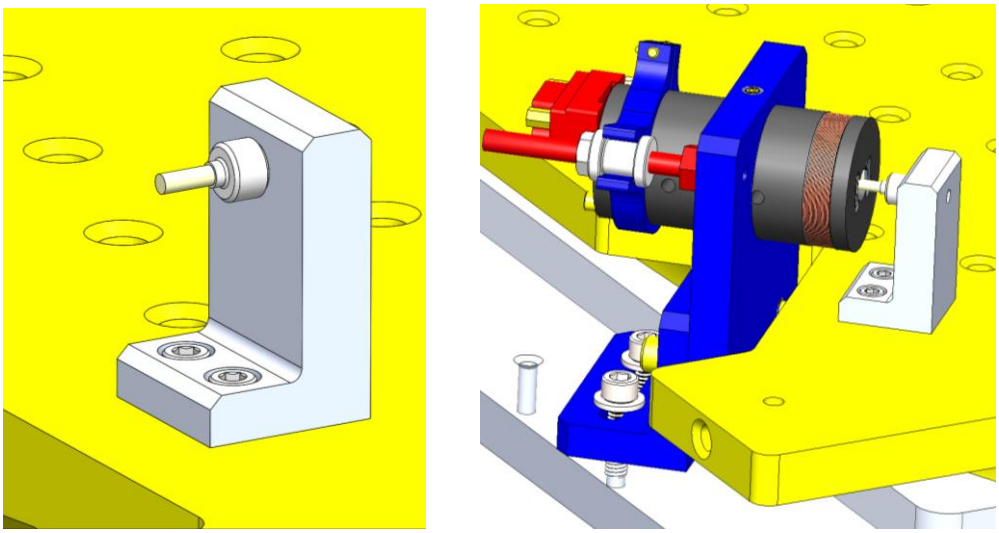

Figure 35: Magnet riser for the horizontal AOSEM assembly

This part should also be checked using FEA even if at first it seems that no resonance problems should appear. Figure 36 shows the results of these study that confirms the anticipated results, being the first resonance frequency 6892.6Hz.

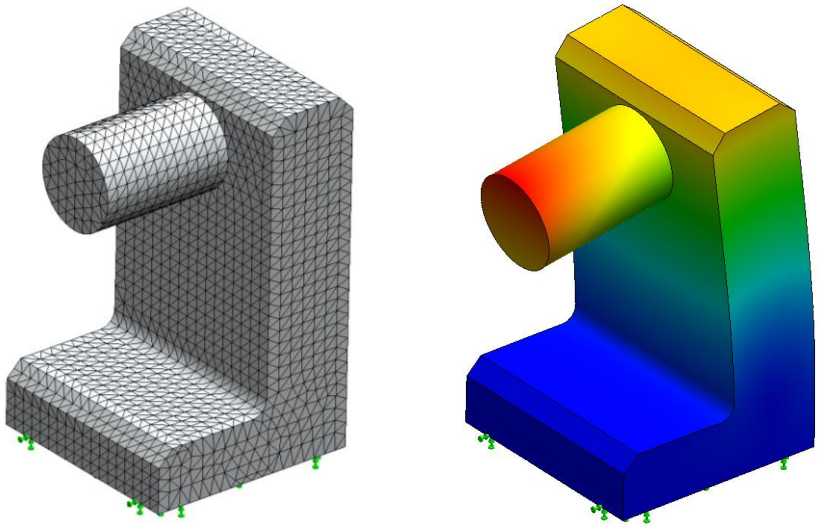

Figure 36: FEA (SW Simulation) for Magnet Holder. First frequency: 6892.6Hz

ASSEMBLY BRACKETS

During the assembly phase, the suspended stage and the base plate have to be perfectly positioned and therefore avoid misalignment issues. Their function is indeed very similar to the one of the lockers, but the last ones cannot be used from the beginning of the assembly as they are attached to the blade platform. In addition to that, the lockers are designed to have large play so they are not selectable as positioning systems. All in all, the system presented in Figure 37 guarantees the good positioning as its tolerances are well controlled. In the assembly procedure (E1500446-v) the surfaces that need to be in contact are detailed.

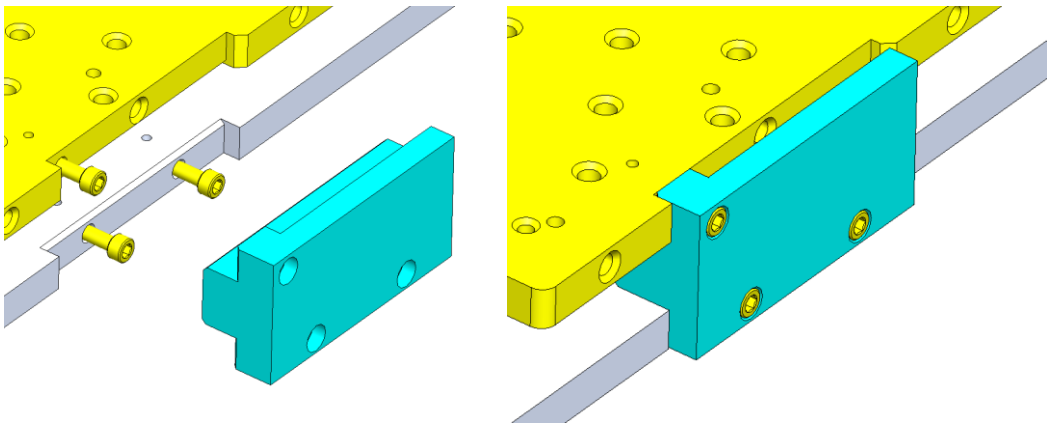

Figure 37: Assembly brackets overview

BASE PLATE

The Base Plate acts as intermediary between the VOPO suspension and the HAM6 optical bench. Its main goal is to guarantee the proper attachment of the whole suspension to the optical bench and to do so a bunch

of dog clamps are to be used, similarly to what has been done for the OMC suspension. The exact number of dog clamps is defined according to the available threads in the optical bench and this is why in the first steps of the design of the suspension we expressed the importance of consider the number of available holes as a crucial point.

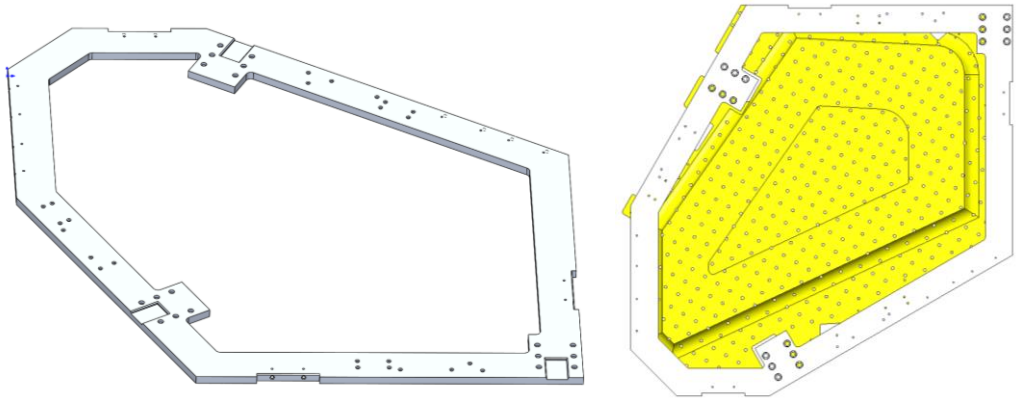

Figure 38: VOPO Base Plate (Left) and the distance to the injection bench

Figure 38 shows the final design of the base plate, which is a heptagonal 0.4" inch thick 6061-T6 Aluminum piece that weights 6.426lb (2.91 kg). The interior shape of the base plate has been designed taking into account the shape of the injection bench in order to have some margin between this two elements, as it can be observed in the above-mentioned figure. On the other side, it is relevant to mention that except from the blade platforms, all the elements are going to be clamped from the top, as shown in Figure 39.

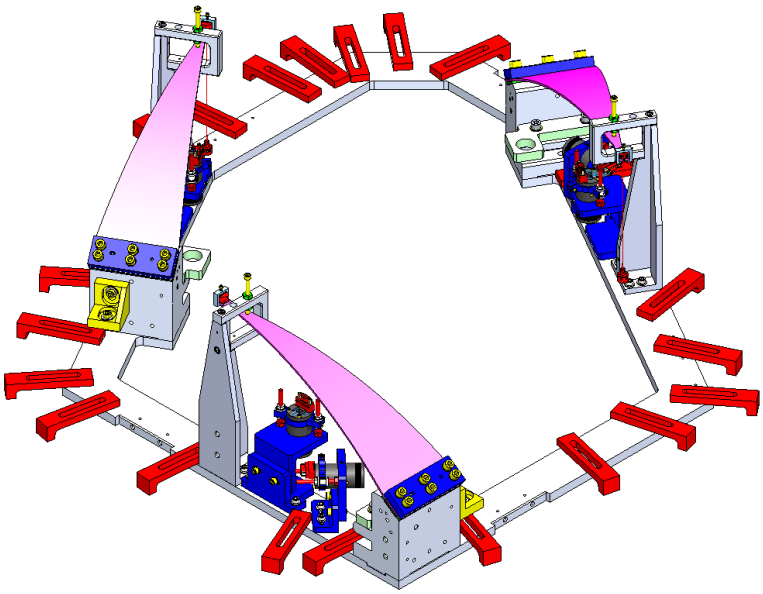

Figure 39: Elements bolt to the base plate and dog clamps

Additionally, the FEA of the transport test has been performed to check if the stiffness of the base plate is adapted to the requirements. As it can be noticed in Figure 38, the internal shape of the plate could be easily increased and therefore its stiffness. Nevertheless, one of the main concerns is to ensure a good contact between the base and the optical bench in the chamber. One option that has been considered is to clamp directly the base to the optical bench, but the main drawback of it will be that the position of the whole

suspension will be set and unmodifiable. On the other side, the use of dog clamps does not guarantee such a good contact especially if the base has a large contact surface with the optical bench. Thus, a compromise has to be found between a larger plate, which will ensure stiffness, and a shorter one, which will ensure good contact. In order to find this compromise two FEA could be performed: the static study with contact conditions between base, dog clamps and optical bench when the structure is charged and the static study of the transport. The results of this transport study can be found in (E1500446-v).

BLADE ASSEMBLY

To guarantee the passive isolation of the Injection Bench a blade and wires based suspension has been designed. The design is based on the BSC-ISI isolation concept but reduced in size and with one single stage. In this concept the blades provide the vertical damping while the wires provide horizontal isolation. These blades are positioned forming an equilateral triangle in order to have better tilt damping and to ease the balance of the bench while ensuring that all the blades take the same part of the net weight of the suspended stage. On the other side, the driving constraint in the blade assembly design has been to keep the first natural frequency below 1.5Hz.

BLADE

As stated before, the VOPO blades are designed in 440C SSTL, which is also a way to test this material, easier to procure that the Maraging steel C250 widely used in LIGO. Moreover, another important choice made in the blades design is that for VOPO they are designed to be flat when uncharged and then bent in the assembled position, see Figure 40.

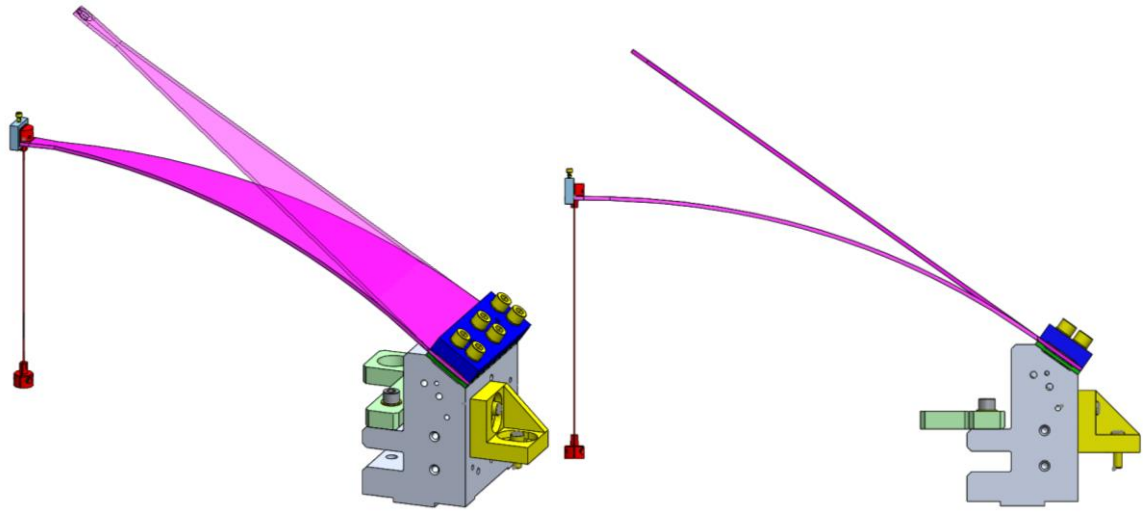

Figure 40: VOPO blade assembly; comparison between the flat unloaded position and the bent position

Blades have been first designed using Bernoulli's beam theory for a triangular shape beam (Greenhalgh, LIGO-T030285-01-K). For this kind of shape we can play with three design parameters: the width at the base (a), the length (l) and the thickness (h) of the blade. The formulas considered in that process are presented below:

$$K_{zz} = \frac{Eah^3}{4l^3}$$

$$f = \frac{1}{2\pi}\sqrt{\frac{K_{zz}}{m}}$$

$$\sigma_{max} = \frac{6Pl}{ah^2} = \frac{\sigma^Y}{FoS}$$

Where K_{ZZ} is the spring constant of the blade in N/m, f is the first natural frequency of the blade in Hz, m is the total suspended mass, σ_{max} is the maximum stress in the blade, P is the force applied at each blade's tip, σ^Y is the Yield stress of the blade's material and FoS is the used Factor of Safety. As those three equations can be reduced to a two equations system and the number of design parameters is three, it can be concluded that in this preliminary design one degree of freedom is allowed. In the VOPO blade design, this DOF has been assigned to the length of the blade, which has been fixed as 280mm. This choice was made because the global dimension of the injection bench had been previously defined.

Considering that the estimated suspended mass (m) is 36 kg, which includes 18kg for the injection bench, 12kg for the optics and 6 kg of dummy mass, which will be used to balance and position the bench, the force P is therefore 117.72N. Thus, Figure 41 is the gives different height and width combinations depending on the desired FoS.

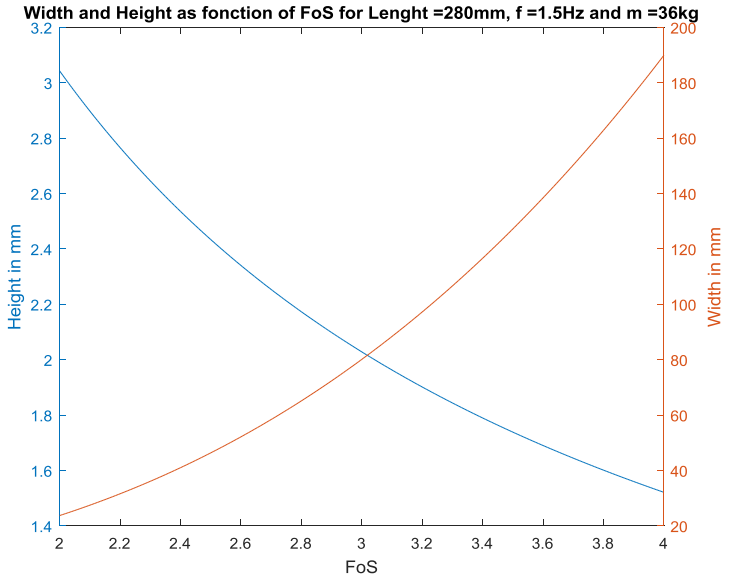

Figure 41: Width and Height as function of FoS for l=280mm, f=1.5Hz and m=36kg

However, it must not be forgotten that the blade design in constrained by the size of the suspension and that it has to be keep as compacted as possible. On this wise, whereas the height of the blade is not subjected to any constraint, its width has to be carefully selected not to interact with the optics. In view of the results plotted in Figure 41, a compromise has to be found between the FoS and the breath of the spring. However, none of the combinations fits the requirements as more than 90mm width will clearly interfere with the optics and, at the same time, a level of safety inferior to the 30% of the Yield strength -i.e. FoS>3.33- will be too risky considering that this is the theoretical calculation and that the material considered has never been used before for LIGO blades.

Consequently, the possibility of allowing higher frequencies has been studied and the results are an ample reduction of the width, as presented in Figure 42.

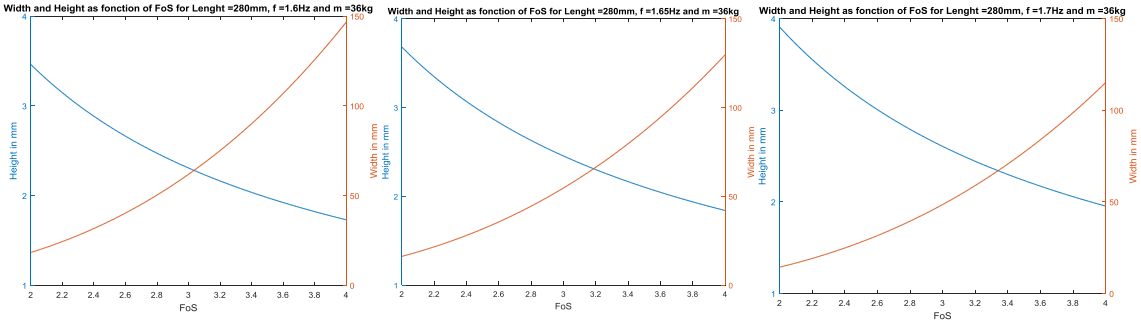

Figure 42: Width and Height as function of FoS for l=280mm and m=36kg for f=1.6, 1.65 and 1.7Hz

After taking into account several options, the selected dimensions, which fit adequately almost all the needs, are presented below.

$$l = 280 \text{ mm} \qquad a = 85 \text{ mm} \qquad h = 2.1 \text{ mm}$$

$$f = 1.6277\ Hz \qquad Kzz = 888.26 \text{ N/m} \qquad FoS = 3.4117$$

The next step in the design of the blade is to verify by running a static FE analysis that the calculated dimensions give the expected FoS. For that purpose, two different analyses have been launched using SolidWorks Simulation Add-in and ANSYS. The main goal of the double analysis is to double-check the results of the analyses and make sure that the solution obtained is reliable, but also, as mentioned before, to "validate" the SW Simulation add-in for future analysis. That first analysis is run using a fixed support for the blade and charging it with 117.72N at the point where the upper wire clamp will be supported. The results of these analysis are presented below, including the comparison between the solvers. The linear assumption cannot be made in that situation as the deflection at the tip of the blade is important and therefore the large displacement solution has to be calculated.

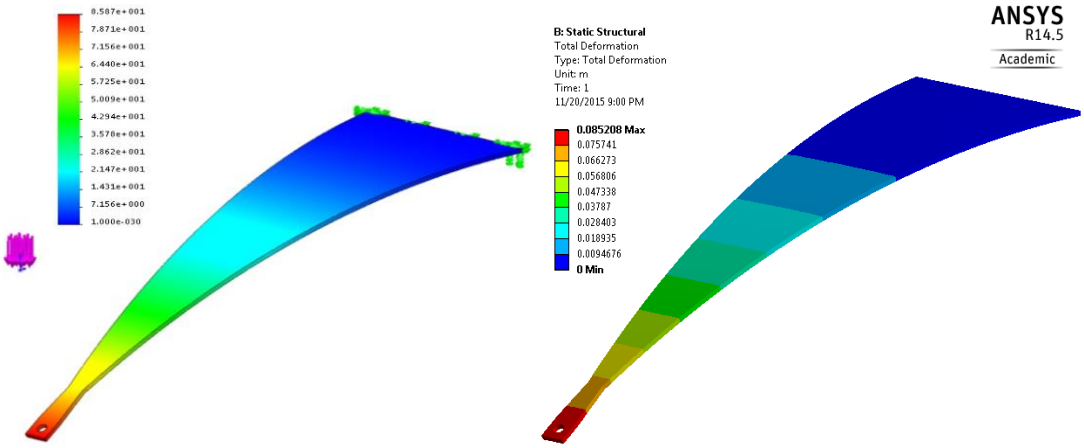

Figure 43: FEA results run in SW (left) and ANSYS (right): Blade deformation

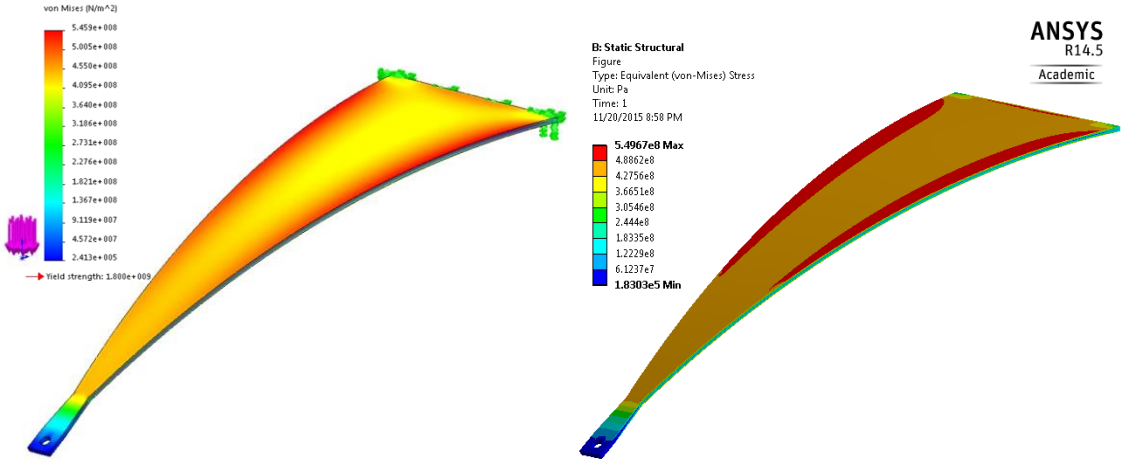

Figure 44: FEA results run in SW (left) and ANSYS (right): Blade stress

FEA BLADE					
	SW	ANSYS	Difference %	THEORY	Error
Stress (MPa)	545.9	549.67	0.686	527.60	4.016
Displacement (mm)	85.87	85.21	0.775		
FoS	3.30	3.27		3.41	

Figure 45: Comparison of the results for ANSYS, SW and Bernoulli's theory

The presented results confirm that for this problem both ANSYS and SW Simulation show similar solutions, with less than a 1% difference. Regarding the theoretical analysis compared with the results of the FEA, the error made by estimating the stress with Bernoulli's formula and considering linearized model is just a 4%. Therefore, the theoretical approach has been proven to be accurate enough to the design of the blades, especially when high FoS are selected for the design.

Another key point of the FE analysis is to define the deformed shape of the blade in order to be able to define the angle of the blade's base to have the blade's tip parallel to the injection bench plane. Figure 46 presents the bent shape of the blade, with an angle α between the base and the tip of 33.16°. This angle is crucial for the post's design as in order to keep the tip of the blade parallel to the injection bench it is necessary to identify it.

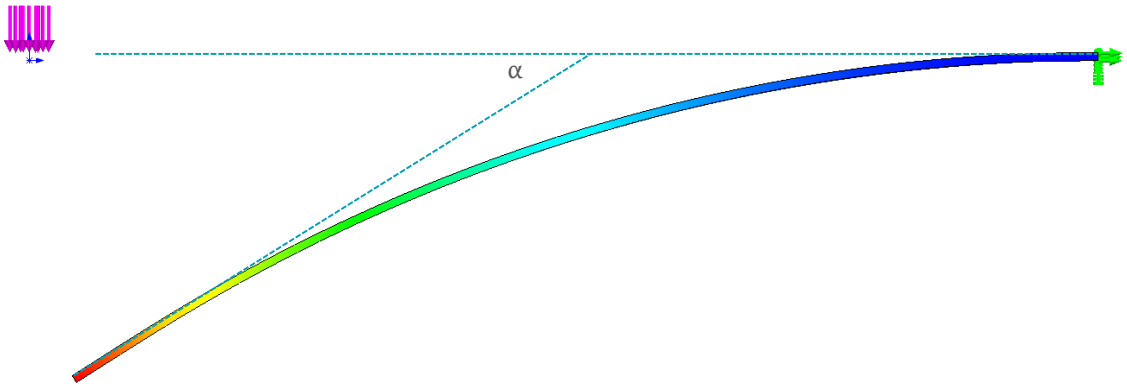

Figure 46: Angle α between the tip and the base of the bent blade

In practice, the angle α is likely to deviate from the theoretical value due to imperfect contact between the blade, platform and clamp, as we know from the experience of previous aLIGO suspensions. Therefore, a detailed FE analysis of the bolted contact in the blade base has been run to try to predict the behavior of the assembly.

CLAMP

In the first design of the blade assembly two pairs of ¼-20 bolts have been considered enough to hold the blade in the desired position. This estimation has been made firstly using a rough momentum calculation to define the required axial load of each bolt. Figure 47 presents the basic geometry parameters used for that calculation, which has been implemented using *ClampDesign.m* (E1500446-v).

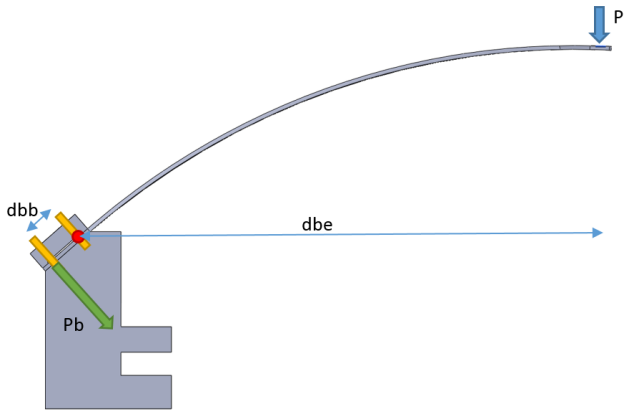

Figure 47: Simplified model used to determine the number of bolts required

According to this simple model the required axial load per bolt for the left set of bolts has been calculated as follows:

$$P_{B_{NEED}} = \frac{P}{\#\ bolts}\frac{dbe}{dbb}$$

Additionally, the maximum load per screw is calculated using the equations below, obtained from (Machinery's Handbook) :

$$d_p = d - \frac{1.299038}{n}$$

$$d_n = d - \frac{0.649519}{n}$$

$$A_s = \frac{\pi}{4}\left(\frac{d_m + d_p}{2}\right)^2$$

$$P_{B_{MAX}} = \frac{\sigma_{YIELD}}{FoS} A_s$$

The results of this calculation are presented in Table 5 and show that for a minimum FoS of 3, at least two bolts per row have to be used.

min FoS	2	3
$P_{B_{NEED}}$	2460.5 N	2460.5 N
$P_{B_{MAX}}$	3436.1 N	2290.7 N
# bolts	1	2

Table 5: Results of the simplified bolt calculation

During the assembly the control of pre-load of these bolts is done by applying the right torque to them. This applied torque can be calculated as follows:

$$T = P_B\left(\frac{0.159}{n} + 1.156\,\mu\,d\right)$$

For the VOPO blade, being the considerate material for this screws is 316 SSTL, whose Yield Strength is 334.37MPa, the real FoS is 5.5859 and the torque to be applied to the screws is 8.8702.

FLEXURE

To guarantee the horizontal isolation, the key parameter in the design is the length and the section of the music wires that hold the suspended stage. For the VOPO instrument, Music Wire Steel (E = 154-201 GPa, σ_Y = 1600-2000 MPa) has been considerate to be a good match given the requirements, and the fact that these wires have already been used and largely tested in precedent aLIGO projects reinforces this idea. This tests have proved that the wire's Yield strength is dependent on its diameter as shown in the tables below. This results have been obtained by testing the UTS of wires with different diameters.

Instron 5500R: Tensile Strength Testing, Coiled Wires					
untreated wires			cryotreated wires		
diameter (mm)	max stress (Pa)	Young's Modulus (Pa)	diameter (mm)	max stress (Pa)	Young's Modulus (Pa)
0.635	2.16E+09	1.54E+11	0.635	2.16E+09	-
0.457	2.52E+09	2.01E+11	0.457	2.51E+09	2.11E+11
0.203	2.23E+09	1.99E+11	0.2	2.24E+09	4.32E+11

Table 6: Tensile Strength Testing (T1500539)

D (in)	Min Tensile (ksi)	D (mm)	Min Tensile (MPa)
0.0047	360	0.1194	2482.11
0.0060	350	0.1524	2413.17
0.0079	340	0.2007	2344.22
0.0098	330	0.2489	2275.27
0.0106	330	0.2692	2275.27
0.0134	320	0.3404	2206.32
0.0140	320	0.3556	2206.32
0.0160	310	0.4064	2137.38
0.0180	310	0.4572	2137.38
0.0240	290	0.6096	1999.48
0.0250	290	0.6350	1999.48
0.0280	290	0.7112	1999.48
0.0433	290	1.0998	1999.48

Table 7: Minimum Tensile Strength (E1100187)

The precedent information has been extracted from the documents (LIGO-T1400539-v2) and (LIGO-E1100187 -v4). The first one of those shows an average relation between σ_Y and UTS of 84.6%. Therefore, in further calculations σ_Y is calculated as 80% of the Minimum Tensile Strength, which is indeed a way to increase the

safety of the design. Considering the previous information, Table 8 has been taken as a reference for all the further calculations.

D (mm)	0.1194	0.1524	0.2007	0.2489	0.2692	0.3404	0.3556	0.4064	0.4572	0.6096	0.6350	0.7112	1.0998
Considerated Yield Strength (Mpa)	1986	1931	1875	1820	1820	1765	1765	1710	1710	1600	1600	1600	1600
Average Porportional Yield Strength (Mpa)				1930	1840	1780	1770		1930	2190		1620	2170

Table 8: Estimated Yield strength for the Music Wires

Using this data, and considering that, again, the requirement for the lateral motion is that its first frequency has to be kept lower than 1.5Hz, the flexure parameters can be calculated. This calculation is intended to define two parameter of the wire, which are the diameter d and the physical length l. In this specific project, and after some iterations, the parameters that have been defined as they give acceptable performance are presented below.

$$l = 130\ mm$$

$$d = 0.61\ mm$$

To define this values, the script *FlexureDesign.m* (E1500446-v) has been implemented using all the equations presented further on in this section; equations that have been extracted from the document 20007235-D. The first set of equations is used to calculate the Zero Moment Point (ZMP) of the flexure and determine the effective length of the wire. The ZMP defines the length of wire that does not contribute to the pendulum motion as it is so close to the attachment point that the wire is indeed bent. Moreover, the effective length is the actual length of the wire that participates in the pendulum motion. The way to calculate them is by using the following formulas:

$$I = \pi \frac{d^4}{64}$$

$$K = \sqrt{\frac{P}{E\ I}}$$

$$ZMP = \frac{1}{K} \tanh\left(K \frac{l}{2}\right)$$

$$l_Z = l - 2\ ZMP$$

Being I the Inertia of the wire's section, K a parameter used in the calculation, l the physical length of the wire and l_z the effective length. For the VOPO suspension, given the above-mentioned parameter, the result is:

$$ZMP = 3.4066\ mm$$

$$l_Z = 123.1869\ mm$$

Notice that this results expose that even if the wire is 130mm long, the isolation has to be computed as being 123.2mm long when using the pendulum equations. Using those parameters the lateral frequency of the system may be found using the pendulum equations as shown below:

$$K_{XX} = K_{YY} = \frac{m\ g}{3\ l_Z} = 955.6213\ N/m$$

$$f_{XX} = \frac{1}{2\pi}\sqrt{\frac{3\,K_{XX}}{m}} = 1.4203\ Hz$$

The last equations extracted from the document are used to calculate the stress on the wire and to compare it with the Yield Stress of the material. Basically, the flexure is subject to two different stresses: the shear stress and the axial stress. The axial stress is caused by two factors: the normal load and the momentum. Those stresses are calculated by setting the maximal lateral displacement δ to be 1mm and using the following formulas.

$$Section = \frac{\pi\,D^2}{4}$$

$$\sigma_{norm} = \frac{P}{Section} = 402.81\ MPa$$

$$\sigma_{bend\ max} = \frac{P\ ZMP\ \frac{D}{2}\delta}{I\ l_Z} = 146.09\ MPa$$

$$\tau_{max} = \frac{P\delta}{Section\ l_Z} = 3.2699\ MPa$$

Notice that once the equivalent stress is calculated using the von-Mises formula, presented below, the contribution of the shear stress is negligible compared to the axial stress, and that the main contributor to this last one is the normal stress. Finally, using this equivalent stress, and given that the Yield Stress of the wire is 2GPa, the resulting factor of safety for the wires is 2.9148.

$$\sigma_{eq} = \sqrt{\sigma_{norm}^2 + \sigma_{bend}^2 + 3\,\tau_{max}^2} = 548.93\ MPa$$

$$FoS = \frac{\sigma_Y}{\sigma_{eq}} = 2.9148$$

Finally, Figure 48 approximates, by extrapolating the inertia and the strength, the evolution of the FoS with the diameter of the wire. In the light of these relationship, increasing the diameter would be an effective way to increase the factor of safety if the obtained is considered too low for the design. Another option, with less impact as it is not linked to the normal stress, would be to increase the wire's length, what will also decrease the value of the frequency. However, we need to keep in mind that increasing this value is equivalent to increasing the height of the post of the blade. On the other hand, there will also be the possibility of changing the material to one with higher Yield Stress, but this option is not considered.

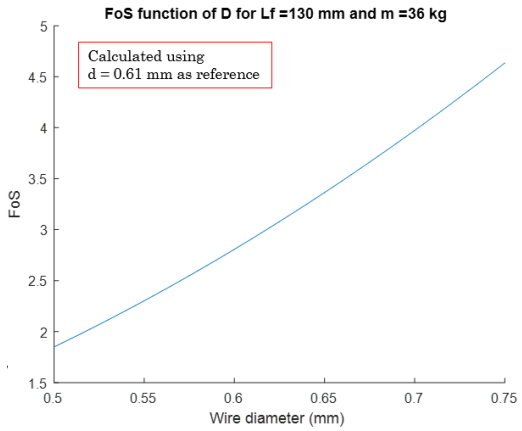

Figure 48: Estimated evolution of the FoS with the diameter of the wire for l=130mm and m=36kg

WIRE CLAMPS

Regarding the wire clamps, the ones used in this suspension are adapted from clamps from the Faraday Isolator Upper Wire Assembly. The function of this assembly is to keep the wire fixed and to ease the attachment to the blade and the first stage, and Figure 49 presents the basis of this system.

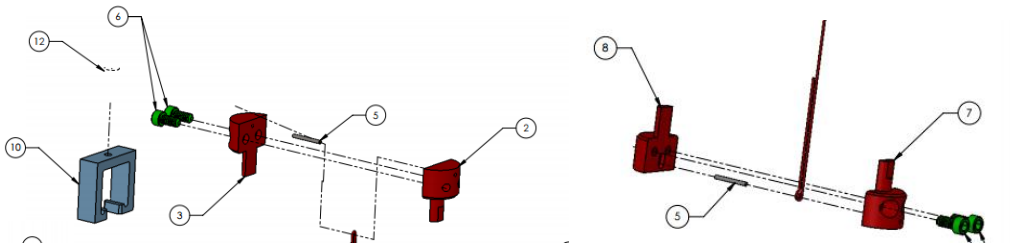

Figure 49: Wire clamp system overview

Nevertheless, the attachment method to the optical bench is slightly different. Initially it was considered to reuse the same clamping method, but it resulted in an important loss of wire length. As a consequence, a new attachment method, based on the use of an intermediate piece bolted to the first stage to block the wire's lower clamp, was designed. Figure 50 shows this piece, which is conceived with enough play in the whole to allow the position correction if the suspended stage moves when released.

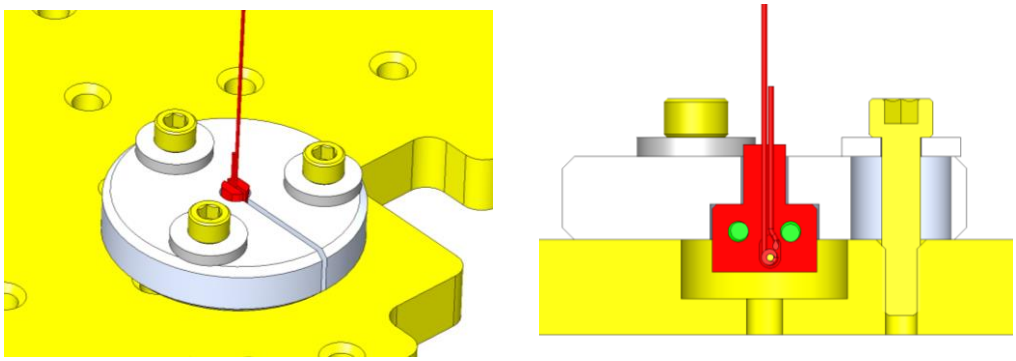

Figure 50 VOPO Wire Base Clamp

BLADE PLATFORM

The blade's platform is a key element of the assembly as it is responsible for the tilt in the blade, and rises the blade to increase the wire's length and hence control the lateral frequency. So both the height and the angle of this platform must be designed after the blade's bent has been defined and the angle α is known. After the contact study detailed in the corresponding section, the angle α is expected to be 35.32°, and the length that has been defined for the wire is 130mm. Thus, the shape of the platform has to be done to respect this two conditions. As shown in Figure 51, this part has to be highly machined, as it has many secondary functions other that holding the blades. This is why the material that has been designated for this part is the aluminum 6061-T6. Additionally, as it has not shown plasticity issues in the FEA.

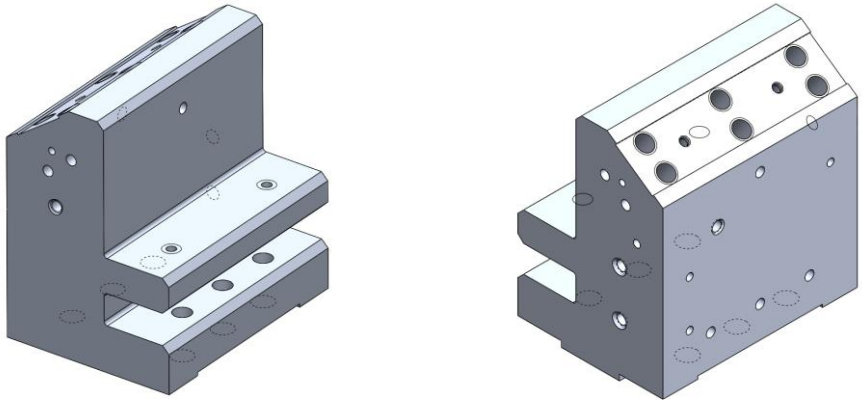

Figure 51: VOPO Blade Platform

As pointed out before, holding the blade is not the only purpose of the post. This post, as it is attached to the stage 0, is also used as motion limiter and attach point of the locker system. These two systems are detailed in (Subassemblies, Motion Limiters) and (Subassemblies, Lockers) respectively. All of this makes this post, along with the injection bench, the most important element of the suspension.

Finally, another important element of the blade assembly is the blade clamping system, whose objective is to guarantee a good contact between the blade and the post. The design is adapted from the OMC's upper blade and it is designed to maintain contact in the edges of the clamp as shown in Figure 52. This clamping system has been determined after a thorough contact analysis, described in further sections and that has shown that with six 17-4 PH SSTL screws and Nitronic 60 Emhart helicoils, the pretension that can be applied is so that the contact is almost equivalent to a perfect fixed attachment. Moreover, the clamps are both designed in stainless steel to guarantee a high friction coefficient with the blade, which is produced in 440C SSTL.

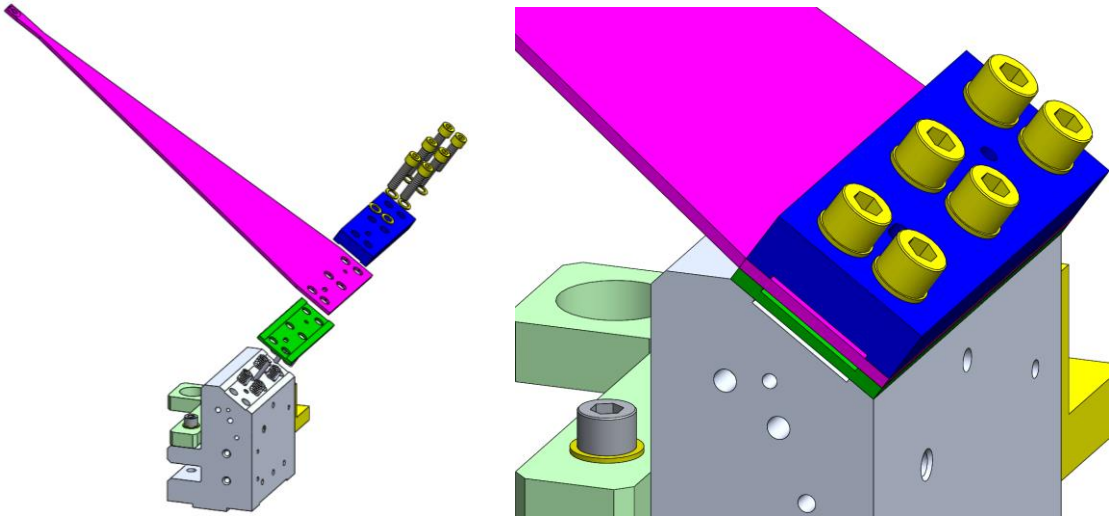

Figure 52: VOPO Blade clamping system overview

Finally, this figure also shows that Dowel pins are going to be employed during the assembly procedure to set the position of all the elements.

BLADE GUARD

In order to guarantee the safety three blade guards will be mounted on each blade to avoid the violent movement of the blade returning to its unbent shape if, for example, the wires break accidentally. Due to the lack of empty areas, and differently from other designs used in aLIGO, the blade guard is not composed by two risers and a long crossbar, but just by a single riser and a U shape crossbar, as presented in Figure 53. This element is also intended to be an indispensable contributor during the assembly procedure –refer to (E1500446-v) for details – as it is also going to be used to hold the blade in the bent position. The detailed drawing of the elements conforming this assembly may be found in Appendix, Drawings.

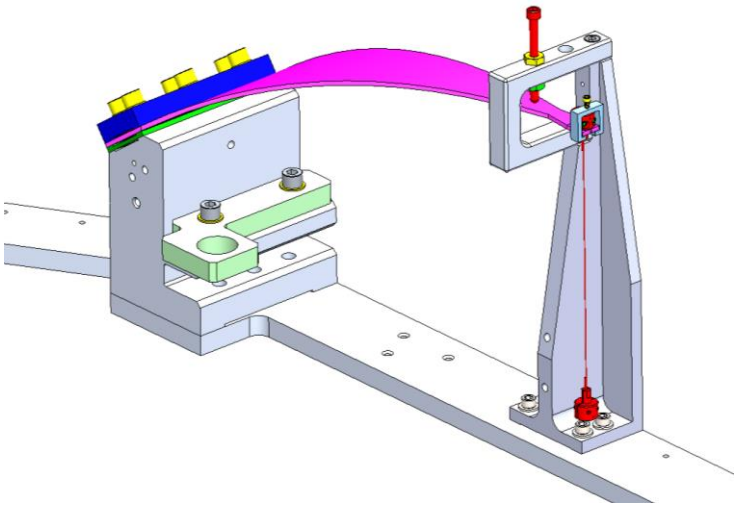

Figure 53: Blade guard assembly

The resonance frequency of the blade guard assembly has been carefully controlled during the design in order to avoid couplings with the main structure that will result in a weak performance. Figure 54 shows the result of the FE analyses run using both SW simulation and ANSYS. The first resonance frequency has a value of 513.47Hz, largely above the minimum requirement of 150-200Hz.

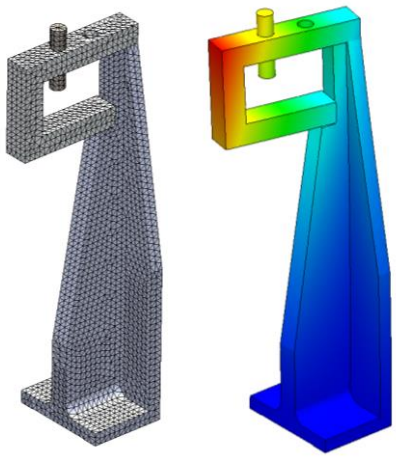

Figure 54: FEA of the simplified Blade Guard assembly. f = 513.47Hz

There is one last calculation to perform to validate that the element is well designed at it is study the resistance of the bolts. Particularly, the aim of this verification is to ensure that, in the case of a violent movement of the blade, the guard will operate as expected and it is not going to split up.

After a brief analysis of the force path in case of an impact of the blade, it has been stated that the critical bolt is the one placed vertically at the top of the assembly. The reason it that, even if the horizontal bolt -which seems to be weaker as it may be facing shear stress in addition to the normal one- breaks, the assembly will not fail unless the top bolt does. Of course, a combined failure of the four bolts in the base will also result in a global failure, but the top bolt will fail before. Consequently, the calculation has been performed considering that the horizontal screws has failed and that all the charge is going through the top one. Notwithstanding, it is delicate to preview the exact force that the blade guard will face if the blade is detached so the followed approach is to calculate the static case and check which is de Factor of Safety.

Thus, considering that the minimum diameter of the bolt is 0.136" and that it will face a 12kg weight load, the stress can be calculated as it follows:

$$\sigma = \frac{F}{A} = \frac{120}{\frac{\pi}{4}(0.136 * 0.0254)^2} = 12.8\ MPa$$

(Stainless Steel Fasteners) states that the Yield Strength for an 18-8 SSTL bolt is approximately 30ksi, which in equivalent to 206.8MPa. Therefore, the FoS of this bolt is:

$$FoS = \frac{\sigma_Y}{\sigma} = \frac{206.8}{12.8} = 16.16\ (6.19\%)$$

In the light of this result, and knowing that this is a pessimistic calculation as it is made supposing that one of the screws has already failed, the system is expected to be able to hold the violent impact of the blade's detachment.

Additionally, the blade guard will also be used as attachment point for the transport system. That is the reason why there is a hole in the U shaped crossbar, as it will allow the operators to secure the crane. So, a specific FEA has been developed to check is the interaction between the guard and the base plate is enough to ensure the transport. This FEA is detailed in (E1500446-v)

INJECTION BENCH

The VOPO Injection Bench, which is the table where all the optics will be screwed, has been designed taking into account the available space in the HAM6 chamber and the required area for the optics positioning. For that reason its shape is not a perfect hexagon but an approximately 2ft wide heptagon, as Figure 55 illustrates. The basic drivers during the design have been to keep the useful surface as big as possible and try to maximize the first resonance frequency of the assembly. After several preliminary designs, it has been proved that the best option to fulfill both requirements and try not to increase the mass it to use a 0.4" thickness for the whole platform and then increase the stiffness of the bench with a shaped contour in the bottom face so that it will not interfere with the optics positioning.

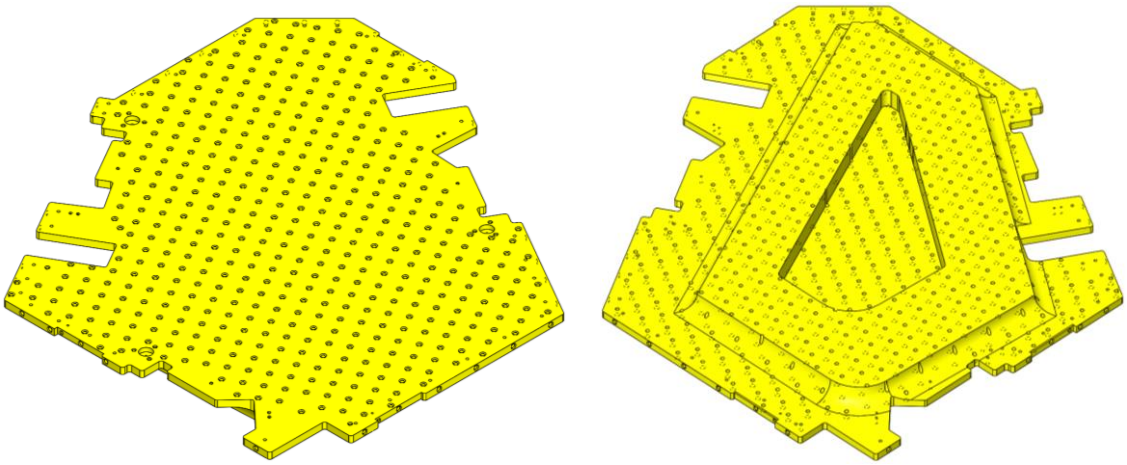

Figure 55: VOPO Injection Bench

The bench is an 18.4kg solid aluminum 6061 part with the underneath contour being defined after an optimization using SW Simulation Design Study. Even if the most relevant FEA is the one performed to all the suspended stage, a study of the bench has revealed that its first resonance frequency is 303.4Hz, as shown in Figure 56. The details of the optimization process are itemized in sections below.

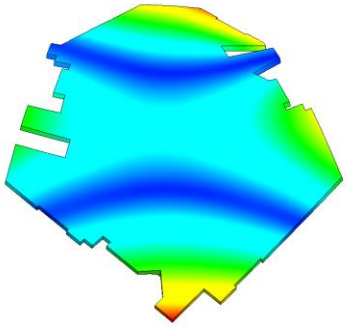

Figure 56: First mode of the FEA of the Injection Bench. f=303.42Hz

MOTION LIMITERS

The AOSEM actuators are extremely sensitive to shocks so, in order to keep them in working conditions, a motion limiter system has to be designed. In previous aLIGO suspensions, this system was also used as a locking systems using a huge number of screws placed around the bench, as presented in Figure 57 -refer to D1201441-, so that they could be in contact with the suspended mass to lock it or at an established distance from it in order to work as motion limiter. However, this system has shown difficulties in the assembly -it is not uncommon to forget to unscrew one of these bolts- and therefore for the new instrument it has been determined that a new concept, easier to use, had to be studied.

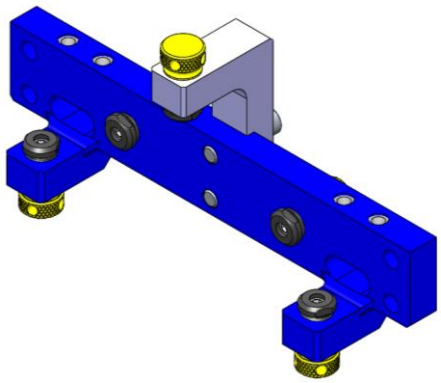

Figure 57: OMC EQ-Stops (D1201441)

Thus, the motion limiters have been designed to be immovable and guarantee a maximum translation of the first stage of 0.76mm (0.03"). This number has been chosen after the revision of the documentation of previous suspensions and to ensure that the AOSEM's cannot get any shock damage. Buoyancy effects have not been considered in this design of the motion limiters, but a proper calculation will be performed to assure the right election of the in air positioning. In order to limit the motion of the bench, the blade platform has been designed to also act as vertical stop, using two extensions as contact surfaces in the case of a bench vertical displacement, as illustrated in Figure 58. It has been considered that having those surfaces fixed is not a problem as the vertical position of the bench can be adapted by using the dummy masses.

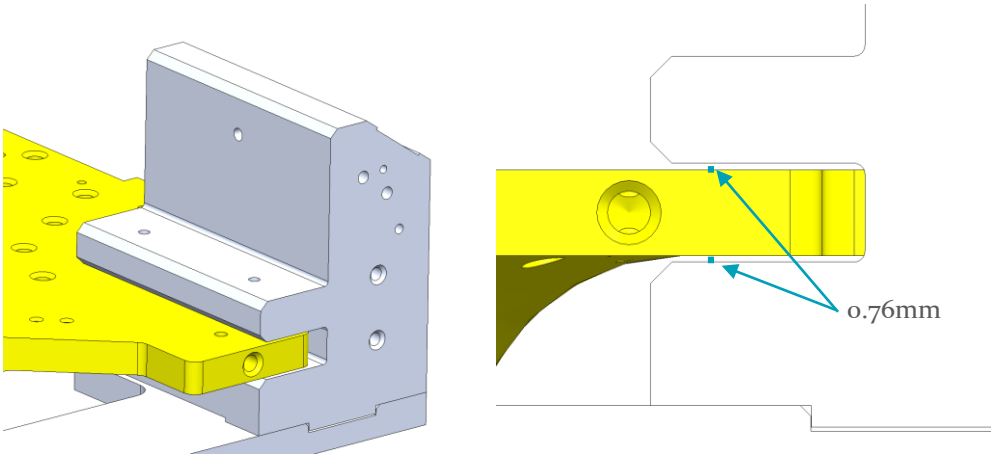

Figure 58: VOPO vertical motion limiter system

On the other side, a pin-hole system is in charge of guaranteeing that the horizontal translation does not exceed 0.76mm from the equilibrium position. As presented in Figure 59, a pin is fixed to the suspended stage while the tapped piece is fixed to the base plate by being bolted to the blade's platform. The tolerance between this two pieces has been carefully controlled in order to guarantee the maximum motion level. Also, as it might be a small difference between the expected equilibrium position and the real one, the stop hole can be slightly moved thanks to high play holes. The idea is that once the suspended mass is balanced and an the right height, the horizontal stop hole can be adjusted to be concentric to the pin. Again, both pieces are made of Aluminum 6061 (T6).

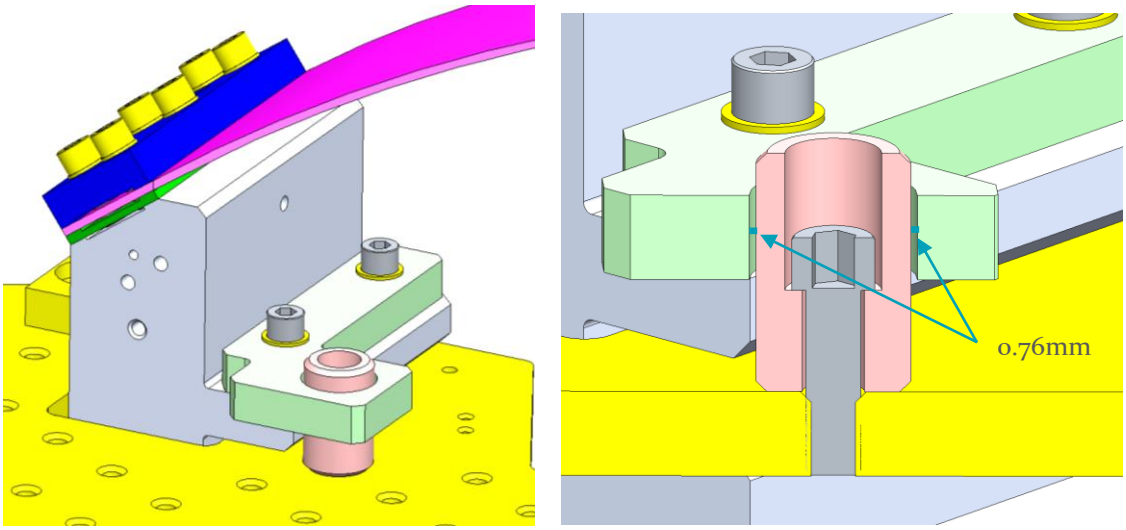

Figure 59: VOPO horizontal motion limiter system

The three motion limiters systems are positioned, as the blade platforms, forming a triangle, which guarantees that the maximum motion of any point of the suspension will not largely exceed the limit of ±0.76mm. In addition, one of the expected advantages of that limiter system is to be handy to operate and to avoid redundancies.

LOCKER

The capability of locking the motion of the suspended mass is also an important feature that the suspension needs to have. This locker will be used during several phases of the suspension's life, but it is crucial during the assembly and the transport. The first locker system that was designed the usage of an intermediate piece to increase the tolerance of the motion limiter was considerate, as presented in Figure 60.

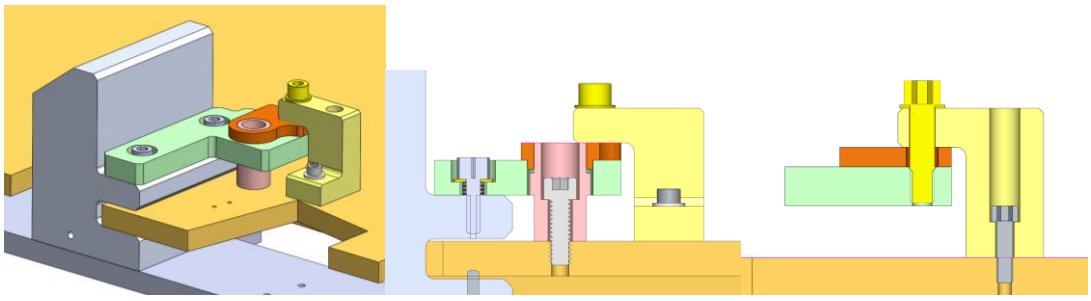

Figure 60: Early locker design overview

However, the weak point of this design was that one of the components (orange) was not part of the suspension during all the cycle of life and it had to be stored somewhere out of the chamber, with the risk of lost that this fact brings with it. Therefore, a much simpler locking system was developed using the post of the blade as attachment point. As illustrated in Figure 61, the locker can the easily raised and screwed in a position where its distance to the bench is larger than 0.2", whereas the motion limiters are set at 0.03".

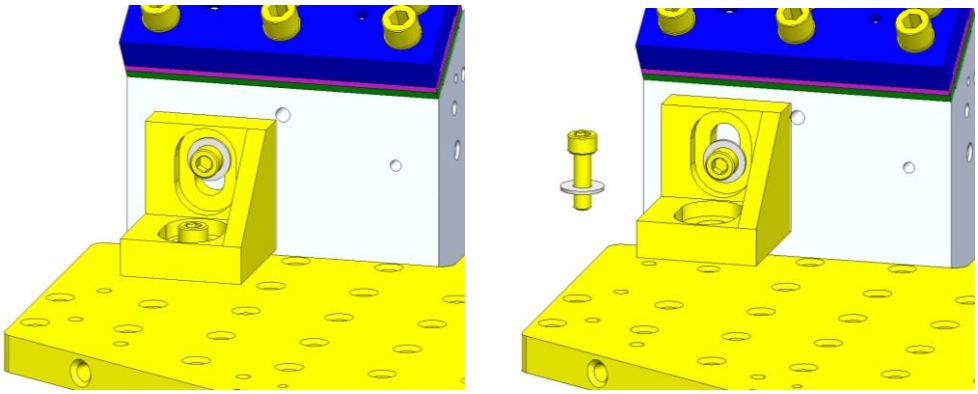

Figure 61: VOPO locker in the locked (left) and unlocked (right) positions

Moreover, this locker has taken into account the fact that the equilibrium position of the bench may differ from the predictions and this is why the slots have a high play, as presented in drawings.

CONTACT STUDY OF THE VOPO BLADES

As mentioned before, one of the purposes of this project is to detail the steps performed in the study of the bolted contact between the blade and the base of the VOPO suspension. This study has been developed after the experience acquired in the BSC-ISI assembly, where an extra compliance was detected in the blades, being the gap between the blade and its mount one of the main contributors (Matichard & al., Advanced LIGO two-stage twelve-axis vibration isolation andpositioning platform. Part 1: Design and production overviewF, 2015). It is important to keep in mind that one of the critical elements of the design of the blade is the capability to predict its deformed shape.

CONTACT STUDY RESULTS

The procedure to perform a contact study is detailed in the next section. However, it is interesting to show the results that this study, highly recommended for future suspensions, has illustrated. The more relevant contact studies are presented in Table 9.

PLATFORM ANGLE	LOAD (kg)	FORCE DIRECTION	PROGRAM	BLADE / ASSY	# BOLTS	BOLTS PRELOAD	ELEMENT SIZE	ELEMENT SIZE BLADE	HORIZONTAL	VERTICAL	ANGLE ALPHA	ANGLE HORIZONTAL	MAX STRESS (MPa)	FoS
0	12	N	SW	BLADE THE	-	-	-	0.075	-	-	33.16	0	547.87	3.285
54.14	12	V	SW	BLADE	-	-	-	0.075	-	-	34.98	0.880	567.15	3.174
54.77	12	V	SW	ASSY	6	5900	0.2	0.075	10.3424	3.2256	35.31	-0.080	566.789	3.176
54.76	12	V	SW	ASSY	6	5900	0.2	0.075	10.3418	3.2275	35.31	-0.070	567.154	3.174
54.68	12	V	A	ASSY	6	5900	0.2	0.075	10.4437	3.2520	35.32	0.003	570.71	3.154
54.68	12	V	A	ASSY	6	5900	0.2	0.075	10.4437	3.2520	35.31	0.009	570.71	3.154

Table 9: Main results of the contact studies (cases with low angle horizontal)

The *platform angle* in the angle at which the blade is inclined before being charged, the *load* is the charge per blade, *program* is SolidWorks (SW) or ANSYS (A), *horizontal* and *vertical* are the horizontal and vertical distances, in inches, between the base of the blade and the center of the hole in its tip, *angle horizontal* is the angle between in tip in the horizontal plane when deformed and *Max Stress* and *FoS* are, respectively, Maximum stress in the blade and Factor of Safety. This shows that the first row corresponds to the first analysis described in previous sections, this angle is 0 as the blade has been charged from an initial horizontal position. The second row is the study of the single blade but in an initial inclination, see Figure 62, and the rest of them are contact studies of the assembly as described in the next section.

This is one of the fundamental results of this study and the main contributor to the reduction of the FoS between the real situation and the theoretical study. In previous sections, using both Bernoulli theory and an initial FEA, the blade is charged vertically starting from a horizontal position. In this situation, the blade is undercharged if it is compared to the real situation where the load is indeed vertical –it is due to the gravity- but the initial position of the blade is not horizontal, as illustrated in Figure 62.

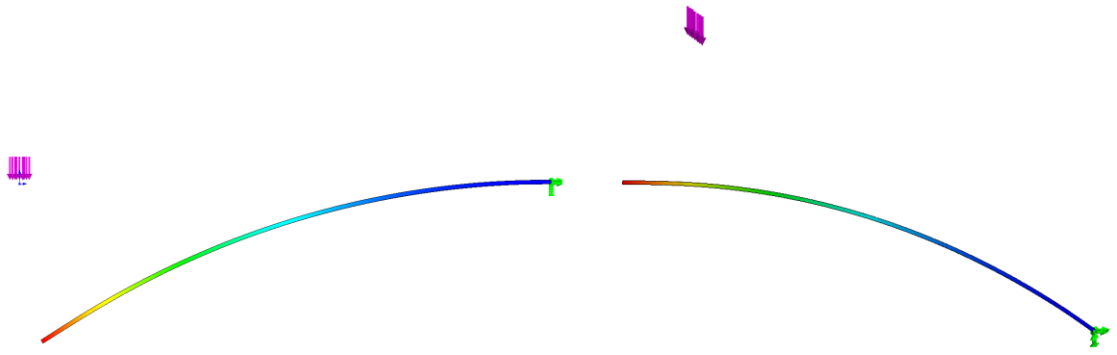

Figure 62: Comparison between the horizontal (left) and the inclined (right) FEA, both with vertical load

Due to this unrealistic study, which has the benefit of being easily performed, the FoS has been overestimated, approximately, a 3-4% by using the nonrealistic FEA study. Nevertheless, the expected FoS after this calculation is still over 3 so it has not been considerate necessary to redesign the blade. An excel sheet with all the information of all the studies can be found in (E1500446-v) and shows that this FoS decreases if the contact is not well designed.

Another important information is that, according to this results, the angle of the blade's post varies depending on the method, as illustrated in Figure 63. This figure shows the extra compliance effect due to the imperfect contact of the blade. This results also show that, again, the first analysis with the horizontal blade is not particularly good estimate of the real behavior of the assembly. On the other hand, the plot shows a difference between the single blade study and the assembly inferior that 1°, which means that the contact can be considered acceptable. Actually, in the first iterations of the process, when only 4 bolts where used, the difference between the angle for the study of the single blade and the assembly was higher, up to 3°. In the view of this results, the whole clamping system was redesigned and more clamps were added in order to improve the attachment. However, this difference is not a problem per se, but the unawareness of it.

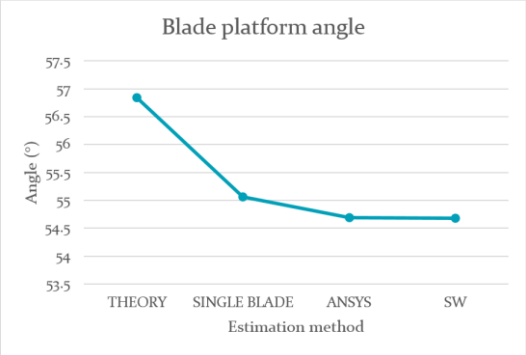

Figure 63: Predicted Blade Platform angle

It is also important to notice where does this difference come from at this is illustrated in Figure 64 and Figure 65. These figures are extracted from the FEA and show that the measured extra deflection comes from the bad contact in the clamp, where instead of having a full surface contact, the blade and the clamp have a line contact. Even if almost imperceptible, this detail may cause assembly problems and misalignments during the assembly of the suspension.

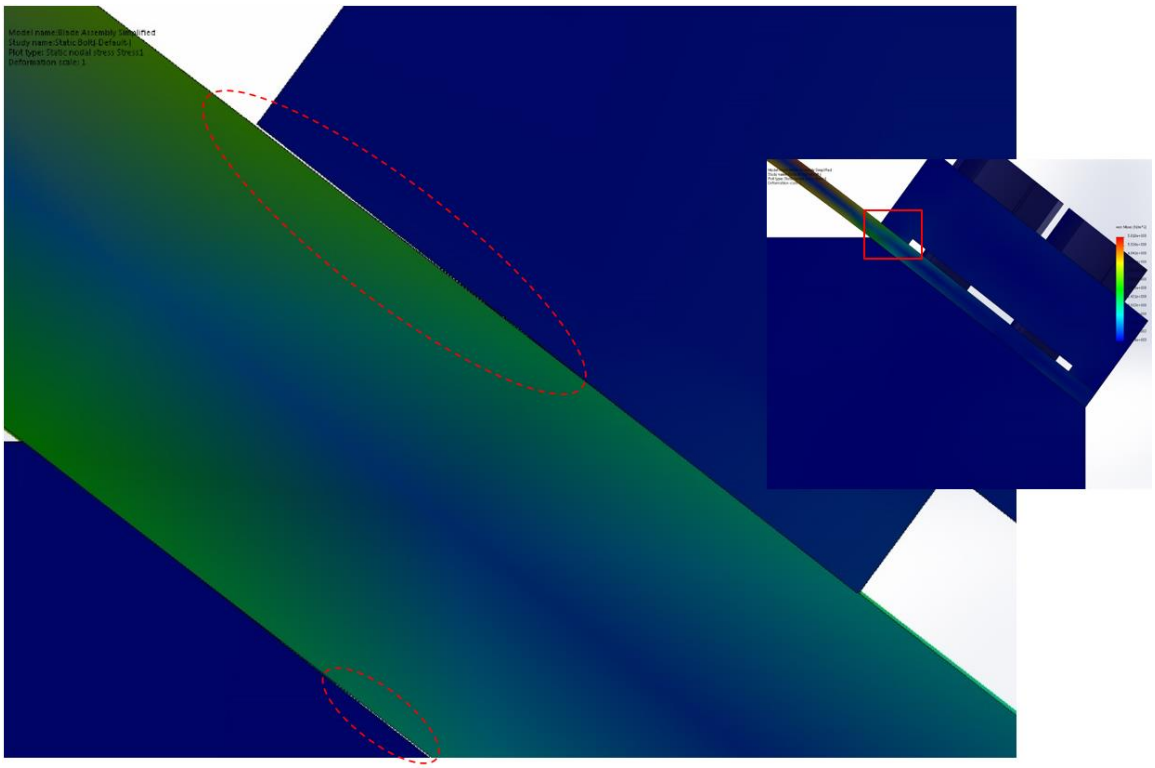

Figure 64: Detail with of the contact between blade and clap (SW Simulation), where the gap is shown

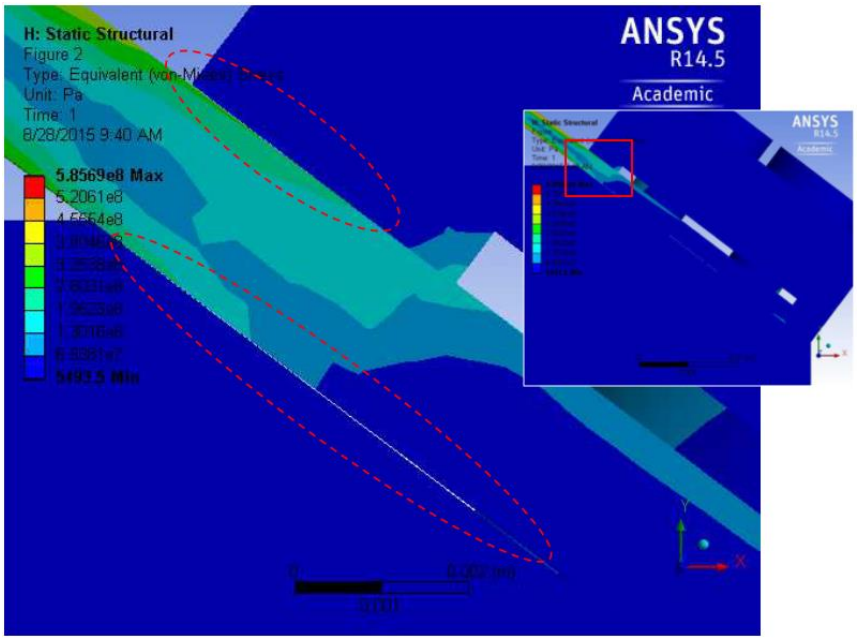

Figure 65: Detail with of the contact between blade and clap (ANSYS), where the gap is shown

On the other hand, the main result that is expected from this contact analysis is the data labeled as *horizontal* and *vertical* in the previous table. This parameters are highly dependent on the contact, as shown in Figure 66.

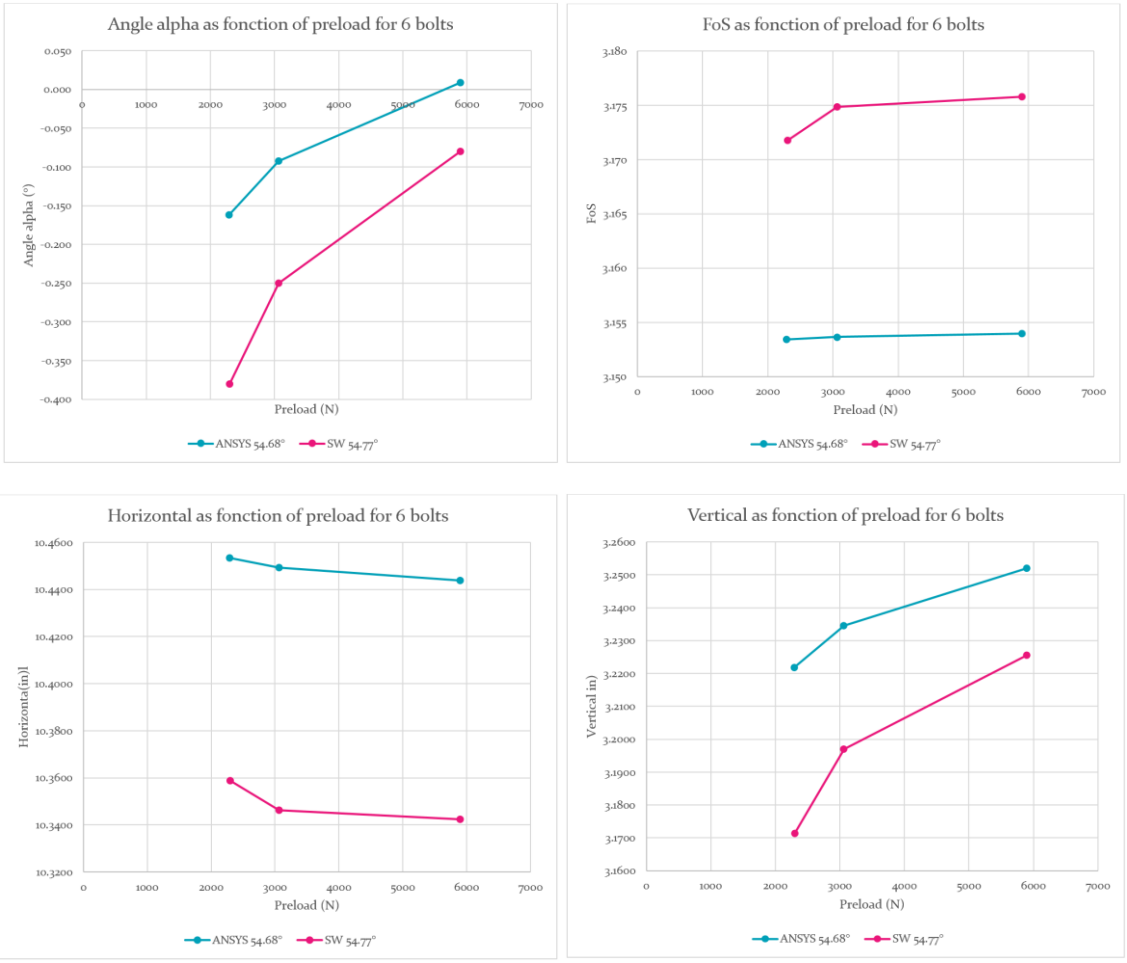

Figure 66: Variation of angle alpha, FoS, Horizontal and Vertical parameters for different preloads

All the presented data is extracted of the comparison for the same number of bolts and the same charge. The information that should be extracted from this plots is not the comparison between the two cases neither the absolute parameter of each case, but the relative evolution of them. Actually, the behavior could had been easily predicted as the general results is that a lower preload results into an increase of the tip deflection, which then reduces the FoS as more stress appears. Additionally, if the position of the base is fixed, it is clear that more deflection will mean more less vertical distance and more horizontal, as shown in Figure 66.

Finally, the values that have been considered for the design of the blade platform are shown hereafter:

$$Platform\ angle: 54.68°$$

$$Horizontal: 10.4437\ in$$

$$Vertical: 3.2520\ in$$

INJECTION BENCH DESIGN

As described before, the design of the injection bench is an iterative process in order to obtain the best performances. First off, it is important to define which are the constraints and requirements of this design. Given the methodology described in this document, by the time the bench has to be conceived the optical layout is already defined and as well is its position. Thus, the total area of the injection bench is not going to be one of the parameters of the design, but the thickness and the shape of the stiffener are. The stiffener is the flange underneath the bench that enhances the stiffness of it and it is illustrated in Figure 24.

Regarding the constraints, the first one that has to be considered is the physical constraint given by the height of the suspension. For the VOPO, as presented in Figure 16, the top of the bench has to be at 1.5" from the bottom of it, which gives a maximum total height of 1.4" for the overall bench (0.1" is margin enough as it is three times more than the maximum vertical movement allowed by the motion limiters. The other condition is that the stiffener cannot be in the edge of the bench as it will interact with the base plate. Another constraint is that the distance between the bench and the base has to be enough to allow the use of 0.4" high dog clamps. Finally, the weight of the suspension is also constraint to a maximum of 18kg.

On the other side, the conditions for this bench are basically related with its stiffness, and more precisely with the first frequency of the suspended assembly. This is why, the conception of the bench must not be done independently but in relation with all the elements that are going to be suspended. Additionally, as the suspended stage has to be balanced, the design of the bench has to take into account the optical layout to simplify the balancing.

In this optimization process is important to have a simplified model of the assembly. For the VOPO suspension, the details of each model are detailed in (E1500446-v), and the model utilized in the FEA is presented in Figure 67. Note that the configuration that needs to be optimized is the one involving the major number of optics, i.e. O3.

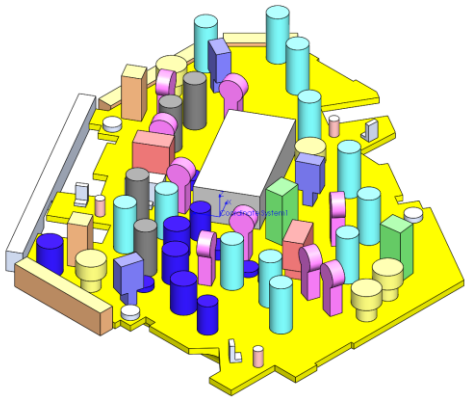

Figure 67: Simplified model of the suspended stage for FEA

With all this elements the iterative process consists in define the position of the balancing masses so that the center of gravity is in the desired position and run the optimization of the injection bench stiffener. This optimization gives an optimal solution that should then be applied, what will therefore change the position of the center of gravity. Thus, the masses have to be positioned again to have a balanced stage and that implies that the optimal solution might have changed. Figure 22 presents the schematics of this process.

Usually in a couple of iterations the solution should be found. Of course, the solution can be as refined as possible, but we need to accept that at some point the frequency is not going to change drastically from one iteration to the next one.

On the other hand, it is a good practice to run the optimization solver with a constraint in mass higher than the real and leave a certain amount of this mass, 500g for example, to the final manual tuning. This manual tuning is more intended to do the final balancing. The idea is that if it is know that the center of gravity of the optics is clearly displaced in the +X direction, we may want to consider having the center of gravity of the bench as far as possible in the -X direction in order to have a "naturally balanced stage". Obviously, the stage does not have to be balanced without the dummy mass on it (even if that situation would simplify the process), but it is preferable to avoid a highly decentered assembly to allow some freedom in the positioning of the dummy mass.

OPTIMIZATION OF THE BENCH

The optimization process itself uses the SW Simulation design study to define a set of variables in our model that will then be tested sequentially in the pursuit of the optimal solution. As the number of cases per optimization is limiter, the right selection and range of the parameters is important to save computing time. In Figure 68 the parameters that are going to be considered in the process are presented. The distances are with respect to the base plate and a minimum of 0.5" has been set.

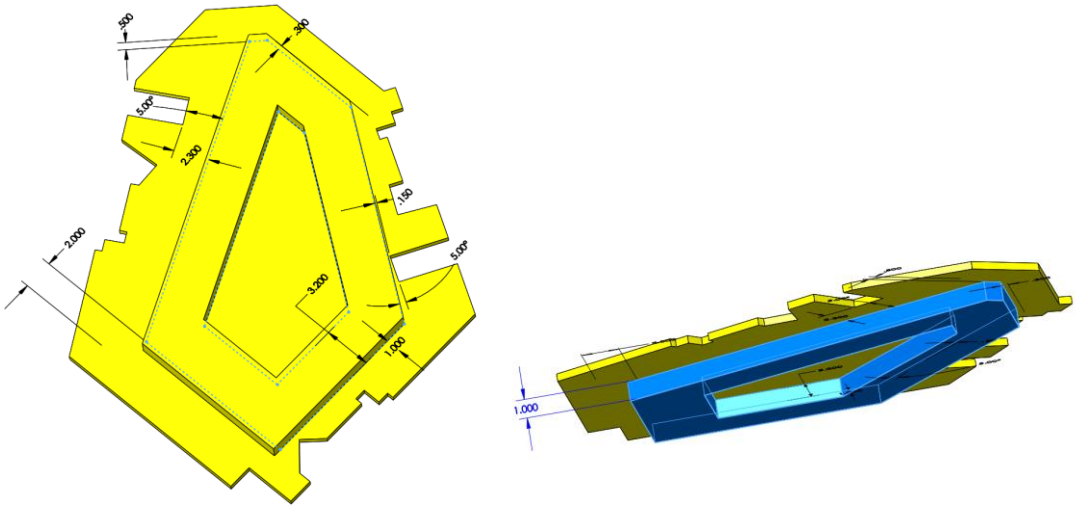

Figure 68: Parameters considered in the optimization

Actually, the above presented figures also show the optimal results of each one of the parameters. On the top of that, the shape has been slightly modified in the search of a compromise between the frequency and the good balancing. Table 10 is an example of the parameters introduced in one of the first optimization iterations.

Design Study Setup

Design Variables

Name	Type	Value	Units
A	Range with Step	Min:1 Max:3 Step:1	in
B	Range with Step	Min:1 Max:3 Step:1	in
C	Range with Step	Min:0.5 Max:2.5 Step:1	in
D	Range with Step	Min:0.5 Max:2.5 Step:1	in
G	Range with Step	Min:0.5 Max:2.5 Step:1	in
I	Range with Step	Min:0.5 Max:2.5 Step:1	in
W	Range with Step	Min:2.4 Max:4.8 Step:0.8	in

Constraints

Sensor name	Condition	Bounds	Units	Study name
Mass	Is lower than	Max:18	kg	-

Goals

Name	Goal	Properties	Weight	Study name
Frequency	Maximize	Frequency 7	10	Frequency Injection Assembly

Table 10: Example of the parameters introduced in one of the early optimization iterations

For the VOPO cavity, the presented final design of the injection bench has a weight of 18.37 kg, as shown in Table 2. Regarding its performances, the first resonance frequency of the assembly is around 250 Hz, as shown in Figure 69.

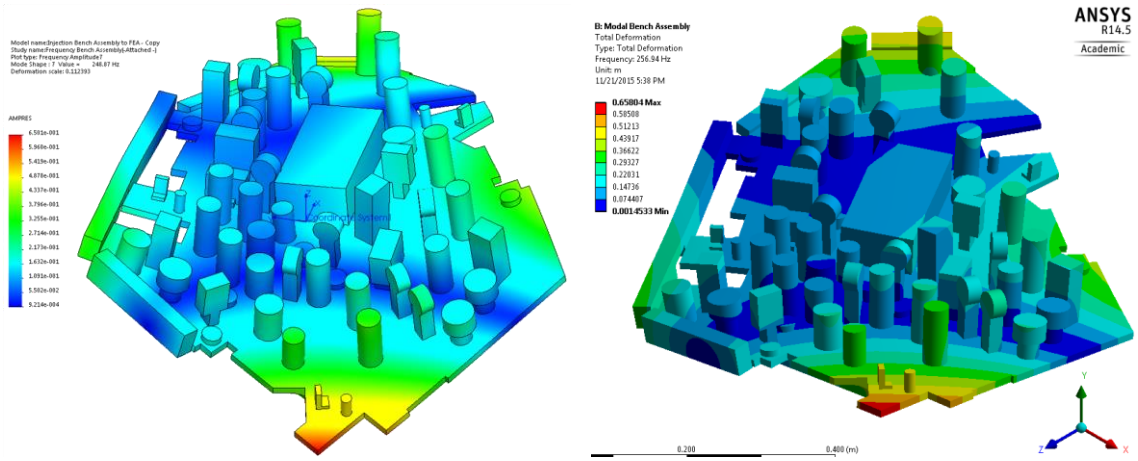

Figure 69: FEA modal analysis of the assembly. SW f = 248.74Hz (left); ANSYS f = 256.94Hz (right)

Again, the last FEA has been run using both SW and ANSYS, even if during the optimization just the first of them has been used, and the results are similar, with an error inferior to 5%. In addition, ANSYS has the option of presenting the strain plots in a modal analysis. This may be useful when trying to do the final adjustments as the strain is an indicator of the areas that need to be reinforced.

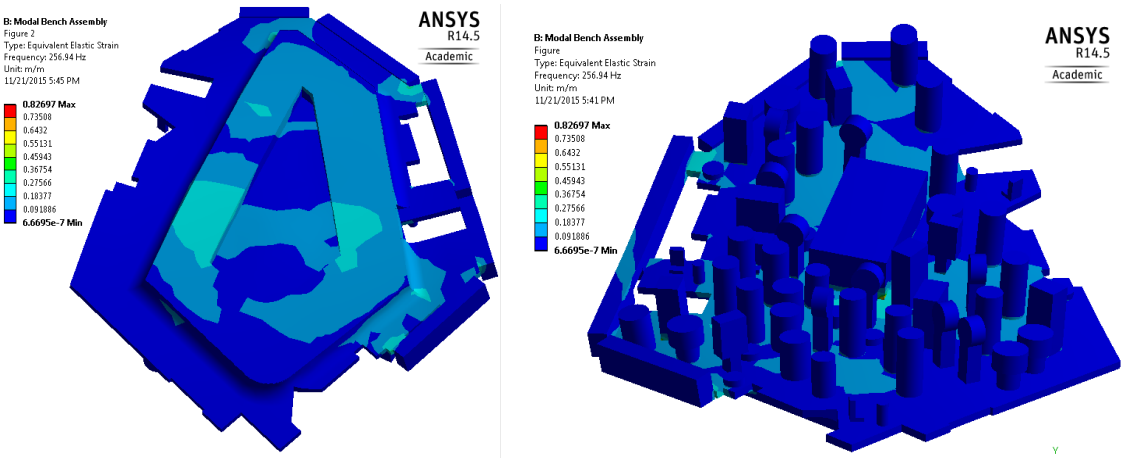

Figure 70: Strain in the modal FEA using ANSYS

VOPO SUSPENSION MECHANICAL DATA

The information below is the mechanical information of the VOPO suspension for both O2 and O3 configurations. This is the result of the study described above and that is used in further sections.

O2

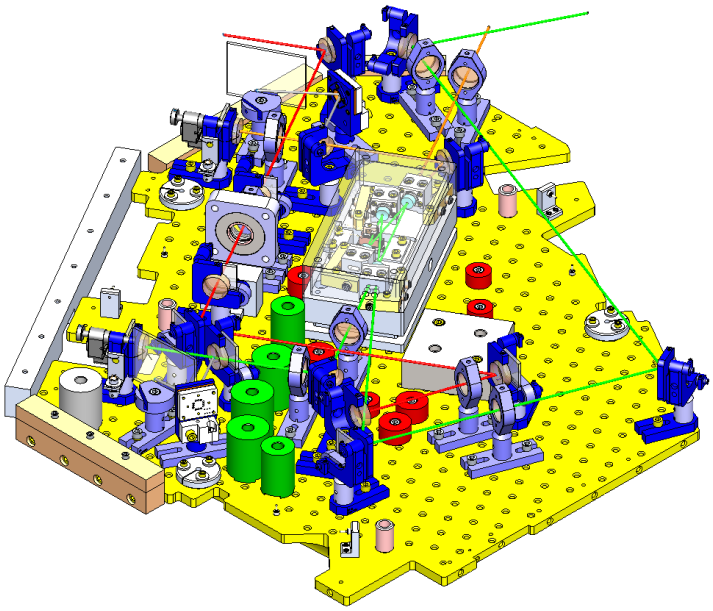

Mass properties of D1500302 aLIGO VOPO Suspended Optical Layout
Configuration: O2
Coordinate system: Coordinate System2

Mass = 35.993 kilograms

Volume = 0.011 cubic meters

Surface area = 2.263 square meters

Center of mass: (meters)
X = 0.000
Y = 0.000
Z = 0.005

Principal axes of inertia and principal moments of inertia: (kilograms * square meters)
Taken at the center of mass.

Ix = (-0.979, -0.202, -0.002)	Px = 0.638
Iy = (0.202, -0.979, -0.014)	Py = 1.397
Iz = (0.001, -0.014, 1.000)	Pz = 1.984

Moments of inertia: (kilograms * square meters)
Taken at the center of mass and aligned with the output coordinate system.

Lxx = 0.669	Lxy = 0.150	Lxz = 0.001
Lyx = 0.150	Lyy = 1.366	Lyz = 0.008
Lzx = 0.001	Lzy = 0.008	Lzz = 1.984

Moments of inertia: (kilograms * square meters)
Taken at the output coordinate system.

Ixx = 0.670	Ixy = 0.150	Ixz = 0.001
Iyx = 0.150	Iyy = 1.367	Iyz = 0.008
Izx = 0.001	Izy = 0.008	Izz = 1.984

Figure 71: Mechanical information of O2 configuration extracted from SW model

O3

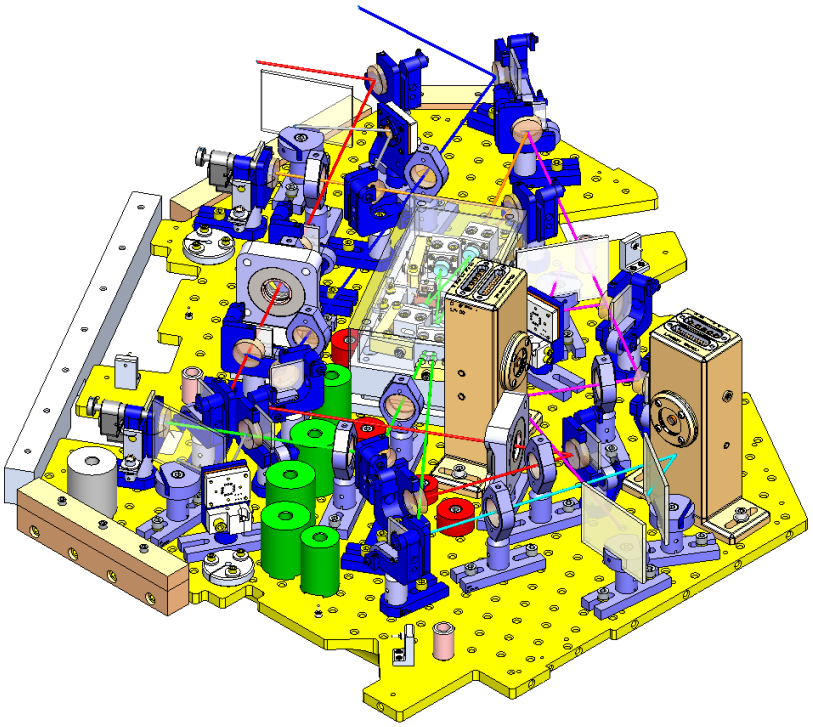

Mass properties of D1500302 aLIGO VOPO Suspended Optical Layout
Configuration: O3
Coordinate system: Coordinate System3

Mass = 35.999 kilograms

Volume = 0.012 cubic meters

Surface area = 2.729 square meters

Center of mass: (meters)
X = 0.000
Y = 0.000
Z = 0.007

Principal axes of inertia and principal moments of inertia: (kilograms * square meters)
Taken at the center of mass.

Ix = (-0.908, -0.419, 0.000)	Px = 0.660
Iy = (0.419, -0.908, 0.002)	Py = 1.428
Iz = (-0.001, 0.002, 1.000)	Pz = 2.022

Moments of inertia: (kilograms * square meters)
Taken at the center of mass and aligned with the output coordinate system.

Lxx = 0.795	Lxy = 0.292	Lxz = 0.000
Lyx = 0.292	Lyy = 1.293	Lyz = -0.001
Lzx = 0.000	Lzy = -0.001	Lzz = 2.022

Moments of inertia: (kilograms * square meters)
Taken at the output coordinate system.

Ixx = 0.796	Ixy = 0.292	Ixz = 0.000
Iyx = 0.292	Iyy = 1.295	Iyz = -0.001
Izx = 0.000	Izy = -0.001	Izz = 2.022

Figure 72: Mechanical information of O3 configuration extracted from SW model

GLOBAL FREQUENCIES OF THE ASSEMBLY

In the design of the suspension both the lateral and the vertical frequency have been carefully selected in order to attain the desired level of performance. However, the roll, yaw and pitch frequencies have also to be checked. Indeed, all the frequencies have been considerate separately, but it may be a coupling between them. This is usually a step that does not compromise the whole design but that may lead to some changes, especially in the wire and the wire clamp design. Figure 73 states the reference system for the VOPO suspension, being the X axis parallel to the beam in the cavity.

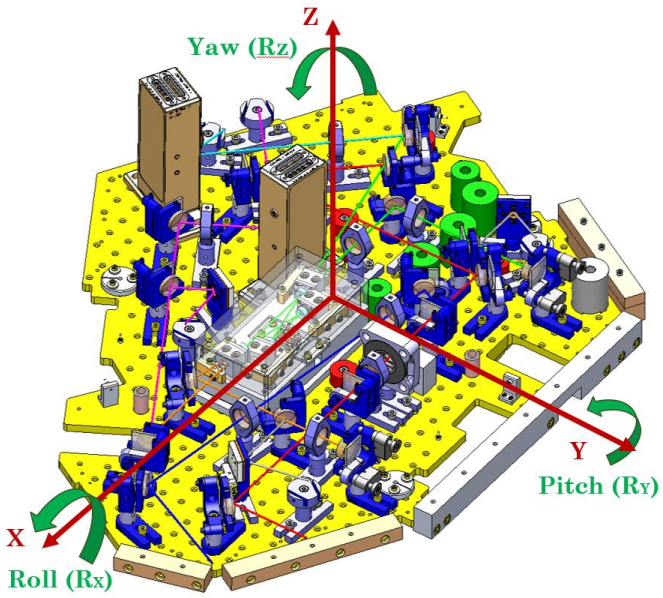

Figure 73: Definition of the coordinate system used for VOPO suspension

With the aim of defining all the frequencies, the modal problem will be written in its matrix form and the resonance frequencies are then obtained as the eigenvalues of the matrix, as presented below.

$$M\ddot{U} + KU = 0$$

$$\ddot{U} + [M^{-1}K]U = 0$$

$$\omega^2 = eigenvalue(M^{-1}K)$$

$$f = \frac{2}{2\pi}\sqrt{eigenvalue(M^{-1}K)}$$

This is a classical modal analysis problem and the difficulty of this one is to find the value of the matrix M and K. Particularly, the difficulty is to find the matrix K, as the matrix M is almost given by SW.

$$\mathbf{M}=\begin{bmatrix} m_u & 0 & 0 & 0 & 0 & 0 \\ 0 & m_u & 0 & 0 & 0 & 0 \\ 0 & 0 & m_u & 0 & 0 & 0 \\ 0 & 0 & 0 & J_{xx} & 0 & 0 \\ 0 & 0 & 0 & 0 & J_{yy} & 0 \\ 0 & 0 & 0 & 0 & 0 & J_{zz} \end{bmatrix} \qquad \mathbf{U}=\begin{Bmatrix} x \\ y \\ z \\ rx \\ ry \\ rz \end{Bmatrix}$$

Figure 74: Mass [M] and displacement [U] matrix definitions

$$\mathbf{K}=\begin{bmatrix} 3k_{xx} & 0 & 0 & 0 & 3k_{xx}h & 0 \\ 0 & 3k_{yy} & 0 & 3k_{yy}h & 0 & 0 \\ 0 & 0 & 3k_{zz} & 0 & 0 & 0 \\ 0 & 3k_{yy}h & 0 & \frac{3}{2}k_{zz}r_s^2+3k_{yy}h^2-m_u gh-m_s gh_s & 0 & 0 \\ 3k_{xx}h & 0 & 0 & 0 & \frac{3}{2}k_{zz}r_s^2+3k_{xx}h^2-m_u gh-m_s gh_s & 0 \\ 0 & 0 & 0 & 0 & 0 & \frac{3}{\sqrt{2}}\sqrt{k_{xx}^2+k_{yy}^2}r_s^2+3\frac{GJ_f}{l_f} \end{bmatrix}$$

Figure 75: Stiffness [K] matrix defined for the coordinate system defined below and with 3 springs

Fortunately, the fact that the blades are forming an equilateral triangle simplifies the writing of the stiffness matrix K. However, in order to do so, the definition of the axis X and Y have been slightly changed, as illustrated in Figure 76, where the specific moments of inertia are also presented.

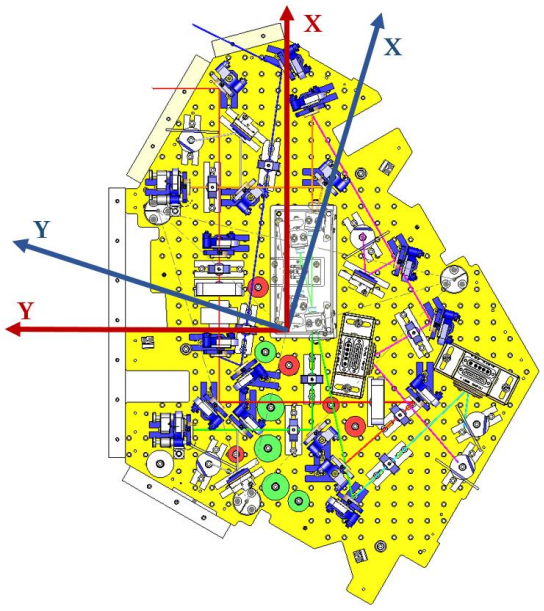

Moments of inertia: (kilograms * square meters)
Taken at the center of mass and aligned with the output coordinate system.

Lxx = 0.795	Lxy = 0.292	Lxz = 0.000
Lyx = 0.292	Lyy = 1.293	Lyz = -0.001
Lzx = 0.000	Lzy = -0.001	Lzz = 2.022

Figure 76: Difference between the coordinate system defined in [K] (blue) and the previously defined

All the values of Kxx, Kyy and Kzz are known and extracted from the previous section and hf is the offset between the CoG of the suspended stage and the flexure ZMP. This concept is illustrated in Figure 77. Additionally, r_s is the radius at between the wire and the center of gravity.

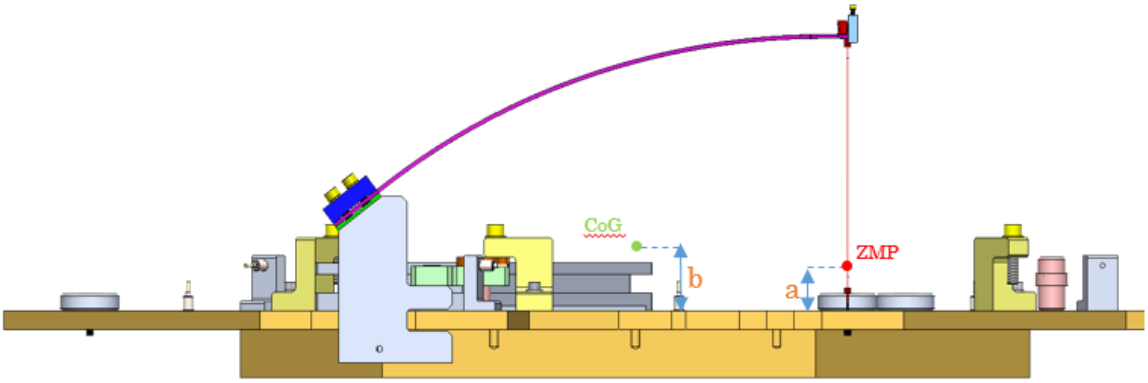

Figure 77: Parameter hf is defined as b-a

This calculation has been implemented in *GlobalFrequencies.m* (E1500446-v) and the results are presented below, where a coupling between certain modes can be perceived but its influence on the value of the resonance frequency is low.

```
Natural_frequencies =

    1.4175         0         0         0         0         0
         0    1.6222         0         0         0         0
         0         0    1.4190         0         0         0
         0         0         0    2.0666         0         0
         0         0         0         0    1.6277         0
         0         0         0         0         0    1.6114


Mode_shapes =

   -0.8585    0.0215         0         0         0         0
         0         0    0.9667   -0.0059         0         0
         0         0         0         0    1.0000         0
         0         0   -0.2561   -1.0000         0         0
    0.5129    0.9998         0         0         0         0
         0         0         0         0         0    1.0000


Response_variables =

X
Y
Z
RX
RY
RZ
```

Figure 78: Results of GlobalFrequencies.m

Additionally, this calculates the response of the system to an external excitation. At this point, the code is being revised but the first results show the response presented below. Of course, this response is considering the passive isolation and all this modes will have to be carefully damped thanks to the AOSEMs.

CONCLUSIONS

The first result of this project is the final design of the VOPO suspension that is now going to be manufactured and subsequently tested. However, these project has also been the opportunity of testing and developing new methodologies that had not been applied in LIGO before.

First off, the VOPO suspension itself it is a new kind of suspension because, even if it keeps the spring and wire isolation system, it is much lighter and easy to manufacture. Actually, proofing that a suspension that does not use a high welded structure is feasible for aLIGO is one of the contributions of this project. These huge structures carried problems in low frequency band and also in the manufacturing process, as the weldment had to be specially performed to be UHV compatible. Thus, these new kind of suspension, which in addition can be better adapted to the available area, is expected to be less costly and faster to procure.

On the other side, with the election of the 440C for the blades, the possibility of using less expensive materials, again easier to procure, has been tested. Additionally, an important work has been made in the prediction of the deformation of the bent blades. This study is particularly useful when the blade is machined flat and the results, which will have to be compared with the prototype, show that such study is possible and proves the cause of the extra compliance found in previous designs. If confirmed as a good prediction, the procedure described in this project could be used in almost all the upcoming suspensions and abandon the use of curved blades, whose monetary and time cost is huge compared with the flat ones.

Moreover, the process of optimization of the blade has been successfully performed using SW Simulation Design Study. This tool, incorporated in the last versions of the program and never been used before in aLIGO, seems to be of great help in the design of this kind of suspensions. On the top of that, several comparisons between SW and ANSYS have been performed during the project in order to "validate" the use of the second one. The results show that the difference is usually below 3%.

Finally, there are two main task that have to be performed in the upcoming months. The first one is to design the active control system using the AOSEM in order to guarantee the damping of the rigid modes of the suspension. The second one is, clearly, to assembly and test the suspension in order to confirm that the performances are as expected and otherwise come back to the design. This second task is the one that will confirm if, indeed, all the stated before about the possibility of this new kind of suspension is or not correct.

ACKNOWLEDGEMENT

Firstly, I would like to express my sincere gratitude to my advisor Dr. F. Matichard for the continuous support of my project, for his patience, motivation, and immense knowledge. His guidance helped me in all the time of research and writing of this thesis.

Besides my advisor, I would like to thank the rest of the people in LIGO MIT working in the VOPO project: Dr. J. Miller, Dr. L. Barsotti and Dr. P. Fritschel. And Prof. M. Evans, for their insightful comments and encouragement, but also for the hard question which incented me to widen my research from various perspectives and for their optics classes. My sincere thanks also goes to Dr. Zucker and Dr. Mason for their help during this project.

I would like also to thank SUPAERO for giving the opportunity of doing this project and in particular to Dr. G. Michon that has been my home institution advisor.

I thank my fellow labmates at LIGO MIT for the stimulating discussions and for all the fun and movies we have had in the last months.

Last but not the least, I would like to thank my family: my parents and to my brothers for supporting me during these months.

BIBLIOGRAPHY

Directory of Fastener Manufacturers. (n.d.). Stainless Steel Fasteners.

E. Oberg, F. J. (2008). *Machinery's Handbook.* New York: Industrial Press.

Fernandez, A., Matichard, F., Miller, J., & Barsotti, L. (E1500446-v). *VOPO Suspension.*

Greenhalgh, J. (LIGO-T030285-01-K). *Investigation of blade spring design parameters.*

Lewis, J. (LIGO-E1100187 -v4). *Advanced LIGO Music Wire Specification for California Fine Wire Company.*

Matichard, F., & al. (2015). Advanced LIGO two-stage twelve-axis vibration isolation andpositioning platform. Part 1: Design and production overviewF. *Precision Engineering 40*, 273-286.

Matichard, F., & al. (2015). Advanced LIGO two-stage twelve-axis vibration isolation andpositioning platform. Part 2: Experimental investigation and tests results. *Precision Engineering 40*, 287-297.

Miller, J. (2015). *aLIGO VOPO Optical Layout.* D1500302.

Miller, J., Barsotti, L., Matichard, F., Evans, M., & Fritschel, P. (2015). *VOPO - Preliminary optical design.*

Saulson, P. R. (1998). *Fundamentals of Interferometric Gravitational Wave Detectors* .

Steplewski, S. (LIGO-T1200468). *AOSEM/BOSEM Calibration.*

The LIGO Scientific Collaboration. (2015). Advanced LIGO. *IOP Science*.

Waller, M. (LIGO-T1400539-v2). *LIGO SURF Summary: Risk Reduction for Advanced LIGO.*

APPENDIX

CONTACT STUDY OF THE VOPO BLADES

Prior to the FE analysis of the whole assembly it is important to make an analysis of the blade in order to know approximately what is the expected angle between the base and the tip once the blade is deformed. This preliminary study, where a fixture condition is imposed in the base of the blade, gave an angular deflection (angle α) of 33.16° (see Figure 79). Consequently, this value was used to design the Base in order to have the Blade's tip parallel to the optical bench.

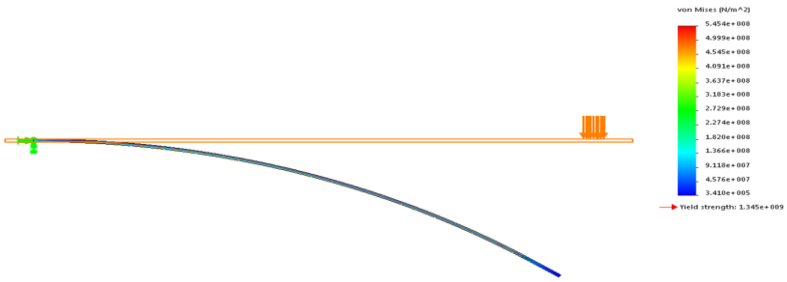

Figure 79: Bent Blade from Blade study

The next step is to validate this deformation performing a FE analysis of the whole assembly and check whether the blade's tip is horizontal or not after the load is applied. With that purpose a simplified CAD model of the assembly has been developed (Figure 80).

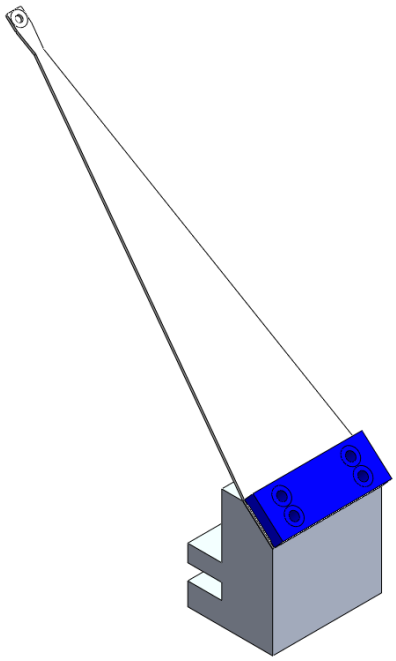

Figure 80: Simplified assembly used for contact study

Another important point to treat before the FE analysis is to define the pre-load that will be applied in the screws (x4) and the friction coefficient between the surfaces. Considering that all the interactions will be between Aluminum (Base and Clamp) and Steel (Blade and Screws) the friction coefficient used in all the study is 0.61, which is the coefficient between this two materials in clean conditions. Once this is defined, the

pre-load of the screws has been calculated using *ClampsDesign.m* (E1500446-v). Using ¼-20 screws the results of the calculation are:

$$Axial\ Load\ per\ Screw = 1984.5\ N$$

$$Torque = 9.2871\ Nm$$

Also, the calculation shows that in order to have a factor of safety of 3 the number of screws needed is 2 per row (i.e. 4 screws). Once all the previous properties have been defined, the contact analysis can be performed.

USING SW SIMULATION

We have decided to perform the analysis using both SW Simulation and ANSYS. In this section we are going to focus on the SolidWorks FE analysis Add-In called Simulation (ancient COSMOS). An important part of the study using SW for bolted assemblies is that it is not needed to create a specific part for the screw (Figure 3). Once we have the assembly fully defined and with all the parts in the right position we have to go to the Simulation window and apply for a New Study (Figure 81).

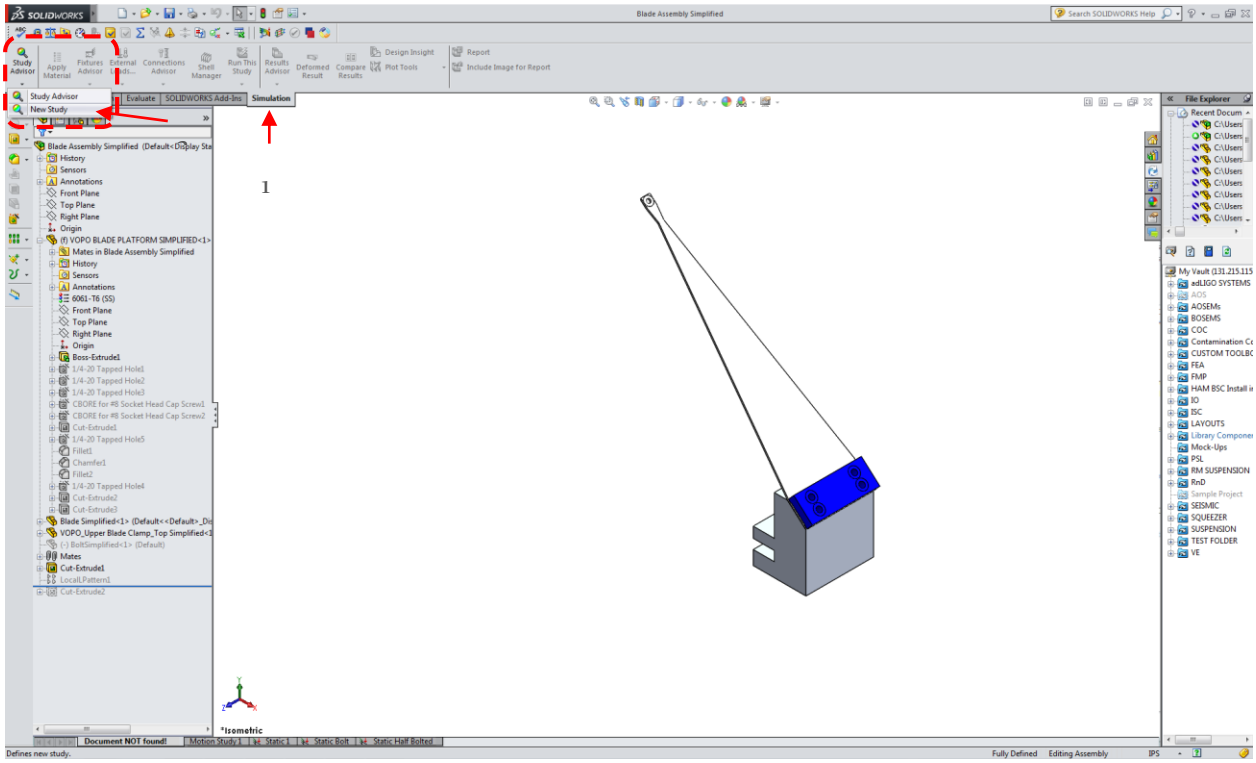

Figure 81: Simulation tab

In that case we want to perform a static analysis so we select the "Static" study tab and give a name to the study (Figure 82)

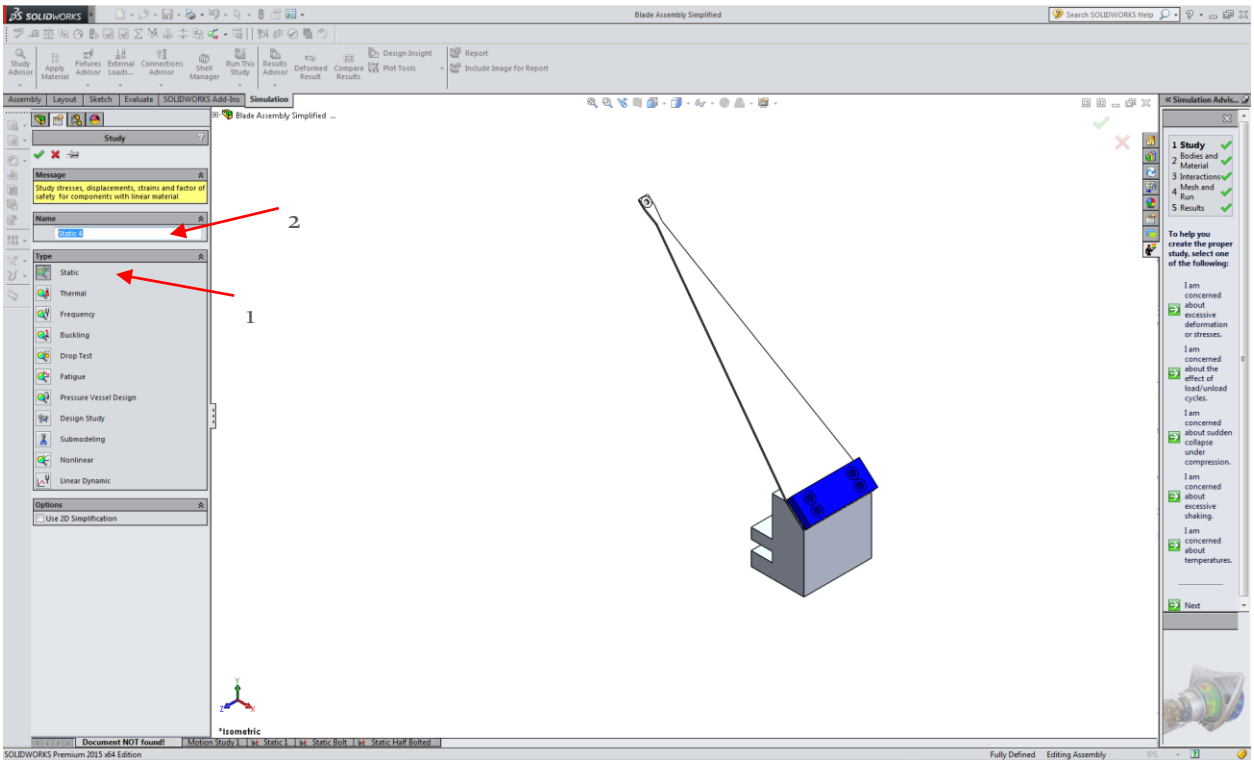

Figure 82: Select Static Study (1) and give a name (2)

Once in the Static Study the first think to do is to define the material of each part of the assembly. Usually we already have defined the material of each part individually before the assembly but it is important to check that they are well defined in the Study. For that purpose select individually each part in the scroll menu (Figure 83) and click on Apply/Edit Material. Remember that if the material is not in the default library of SW you will have to define a new material prior to the study.

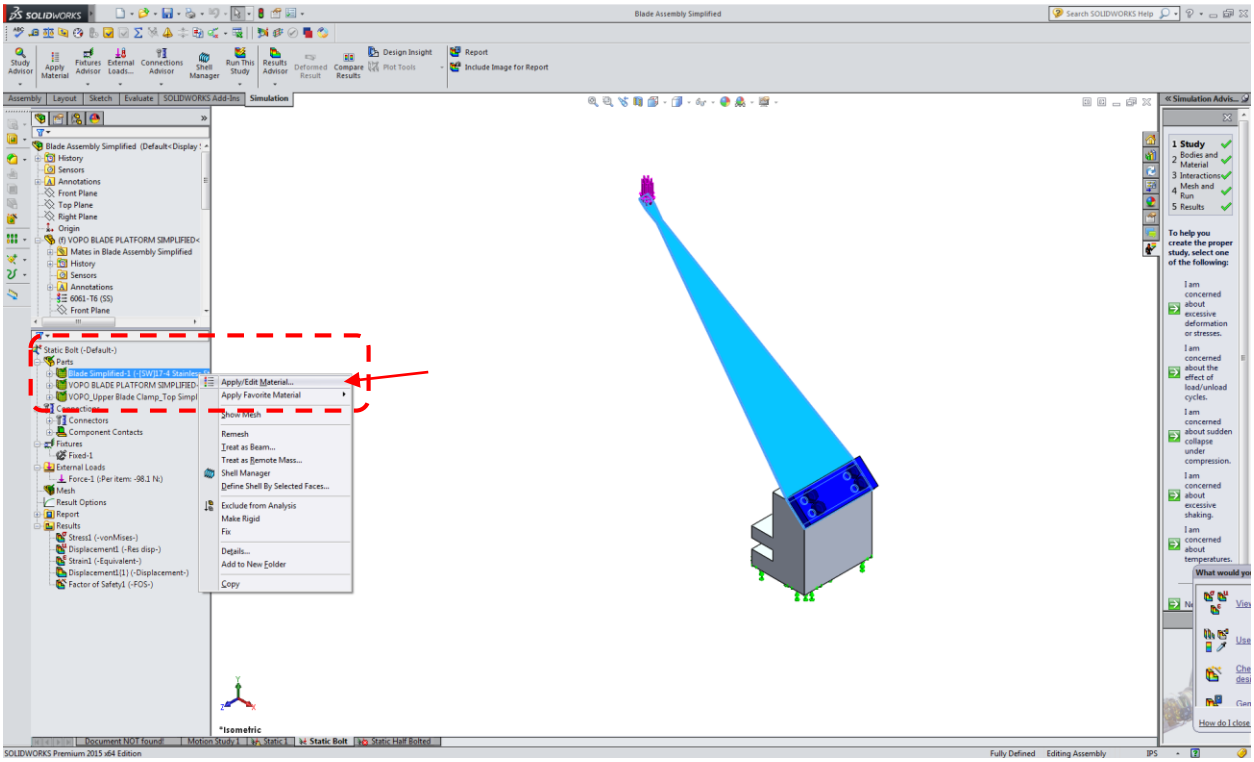

Figure 83: Apply material

The next step is to define the contact between the surfaces. The default set in SW is to create a Global Contact for all the interaction between parts. This default contact is set as "Bonded", so it is not what we want in this study. However, as in our study all the contacts are between Aluminum and steel, we can just re-define this global contact (Figure 84). And set it as "No Penetration", with a friction coefficient of 0.61 (Figure 85).

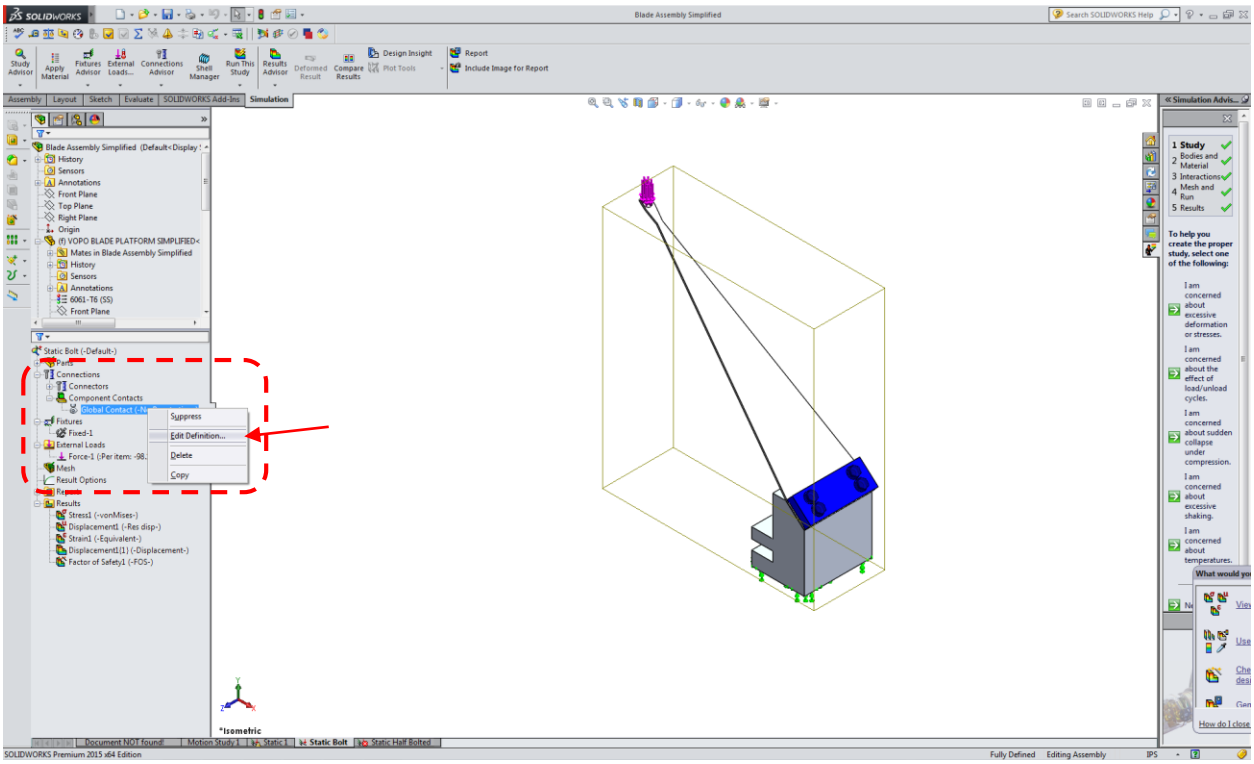

Figure 84: Define the global contact of the assembly

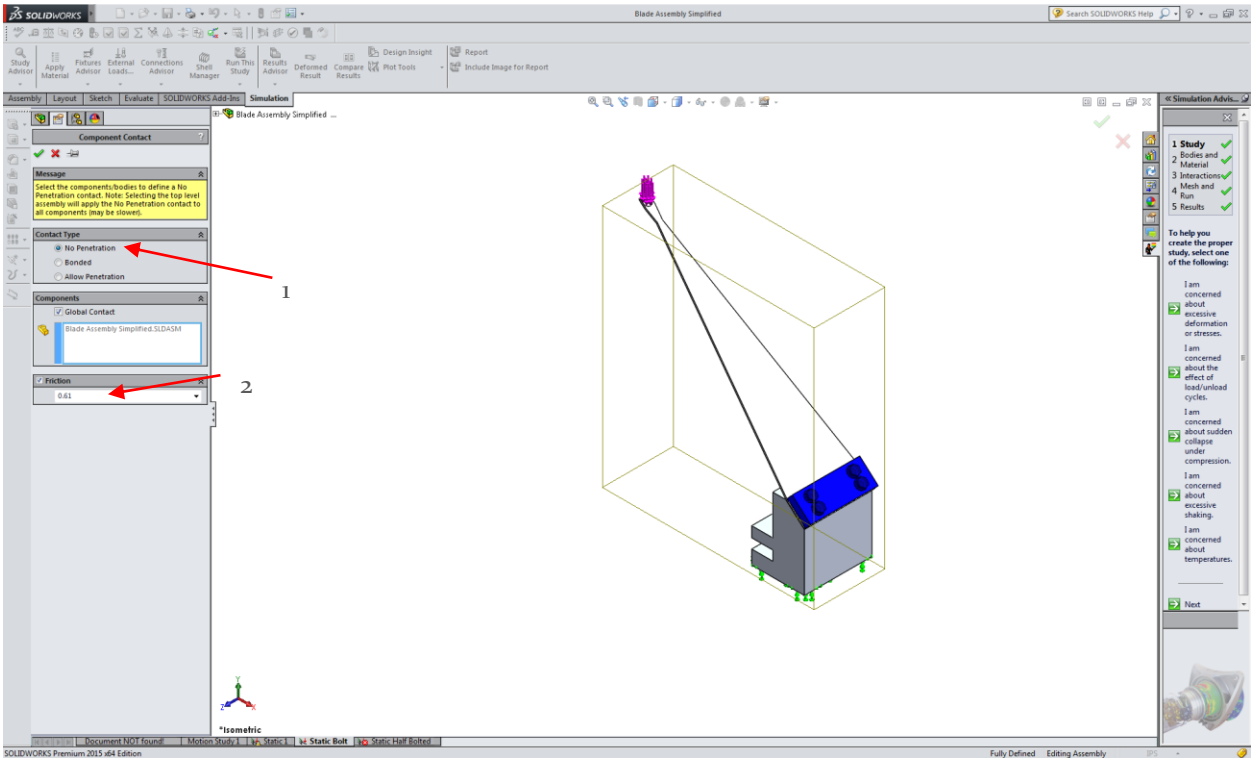

Figure 85: Global contact definition. Contact Type (1) and Friction Coefficient (2)

However, not in other studies it may happen that not all the contacts are between the same materials so different contacts have to be defined. In that case, delete the global contact and apply for Component Contact (Figure 86), selecting in each case the interacting parts and choosing in each case the right coefficient.

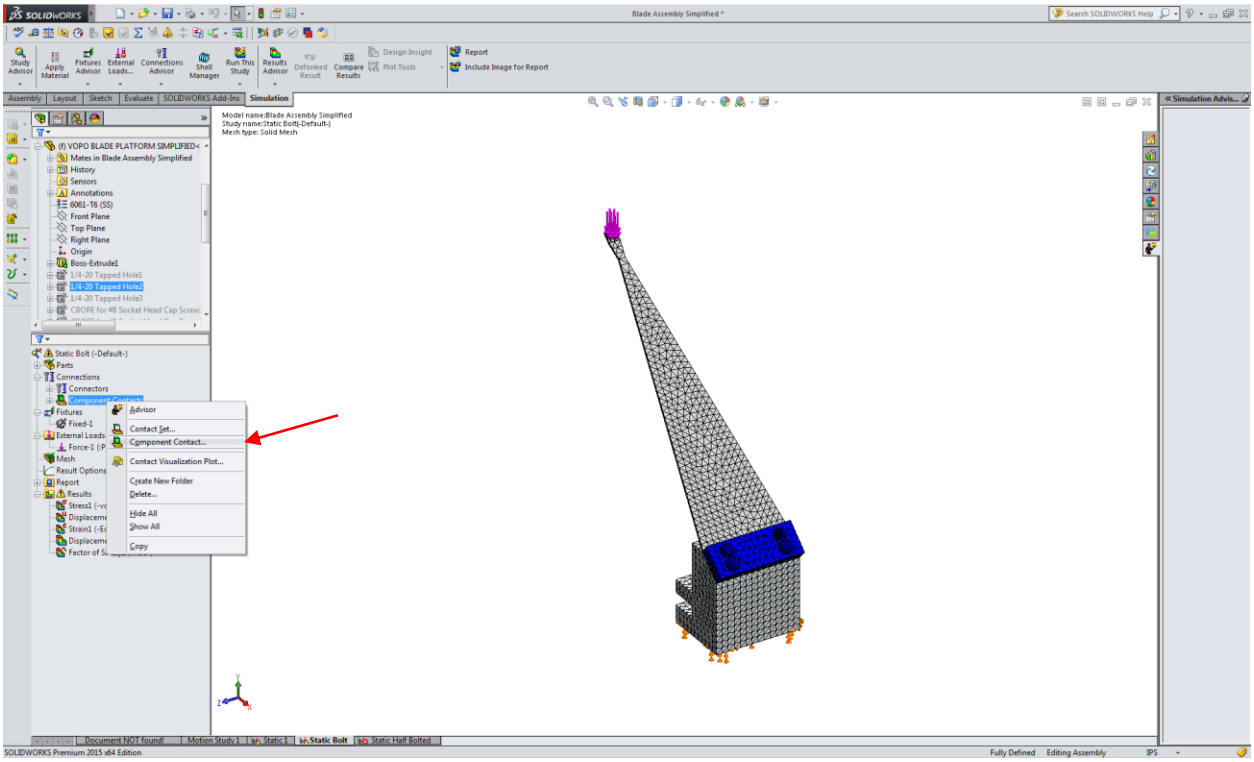

Figure 86: Define different components between parts

After the contact definition, the bolted junction has to be defined. The way bolts are defined in SW Simulation is going to the "Connections Advisor" tab and click on Bolt (Figure 87). A new "Bolt" menu will appear where we can select the type of bolt that we want to define. In that case a threaded screw has been defined (Figure 88).

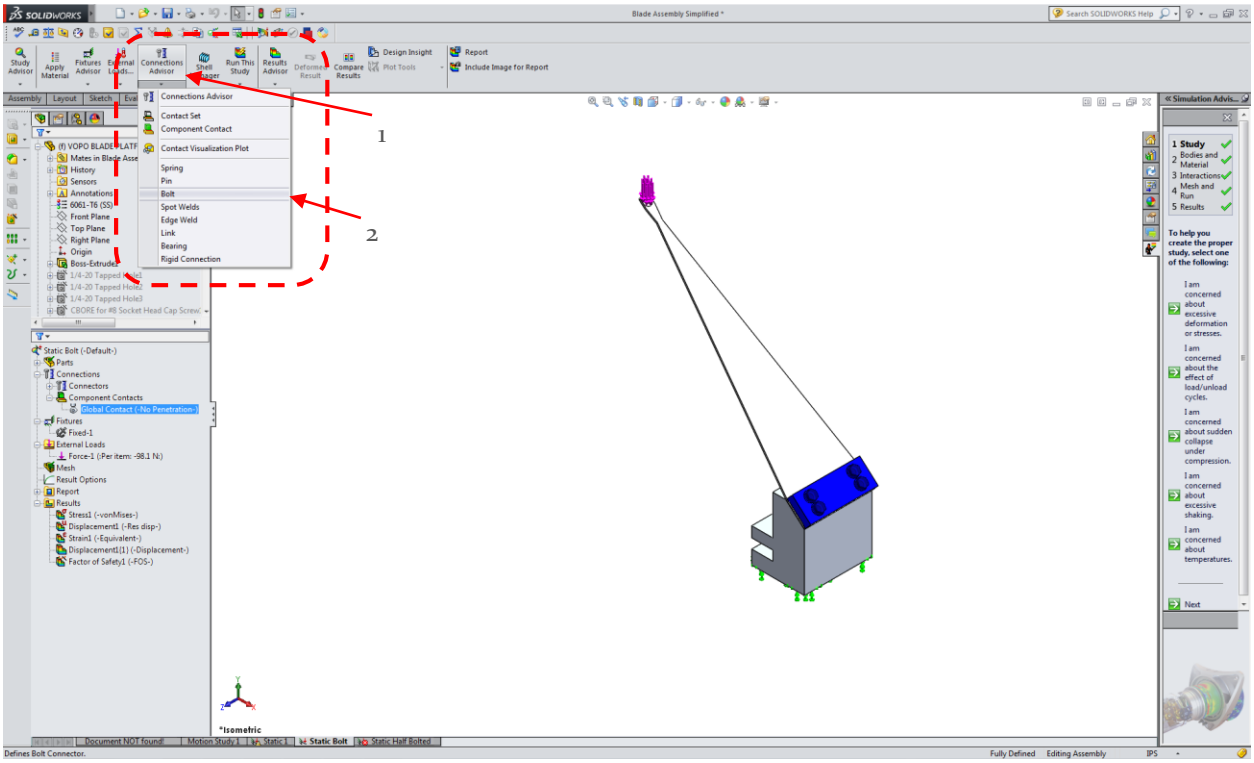

Figure 87: Apply for a bolted contact

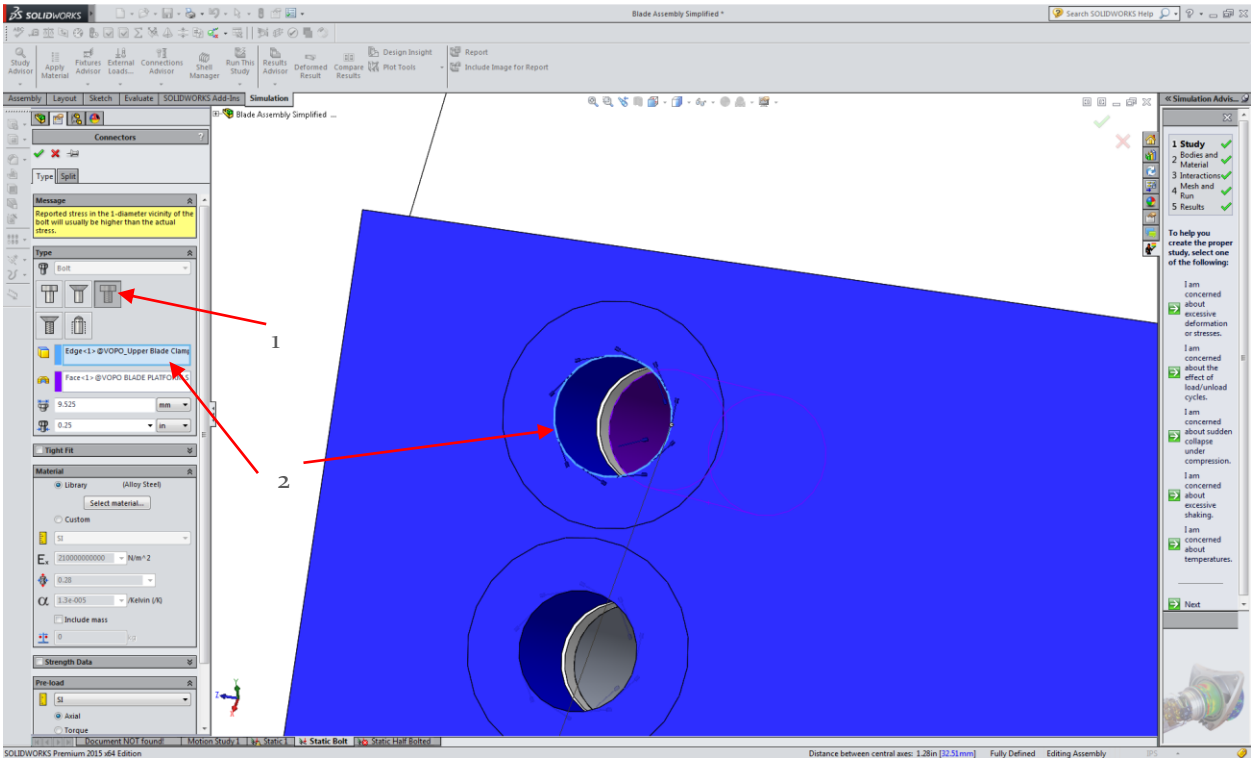

Figure 88: Define bolted contact. Define threated screw (1) and Circular Edge of the Bolt Head Hole (2)

In the Threated Bolt menu SW will ask to define the Circular Edge of the Bolt Head Hole (Figure 89). As shown in the picture we select the Edge of the Trapped Hole in the Clamp (that is ¼ inch diameter). Actually this diameter is the one that defines by default the diameter of the screw. However, if the hole made is larger than the desired diameter (i.e. the hole is loose), we can manually set the bolt's diameter. Next thing to be done is to define the Threaded Surface as can be seen in Figure 12.

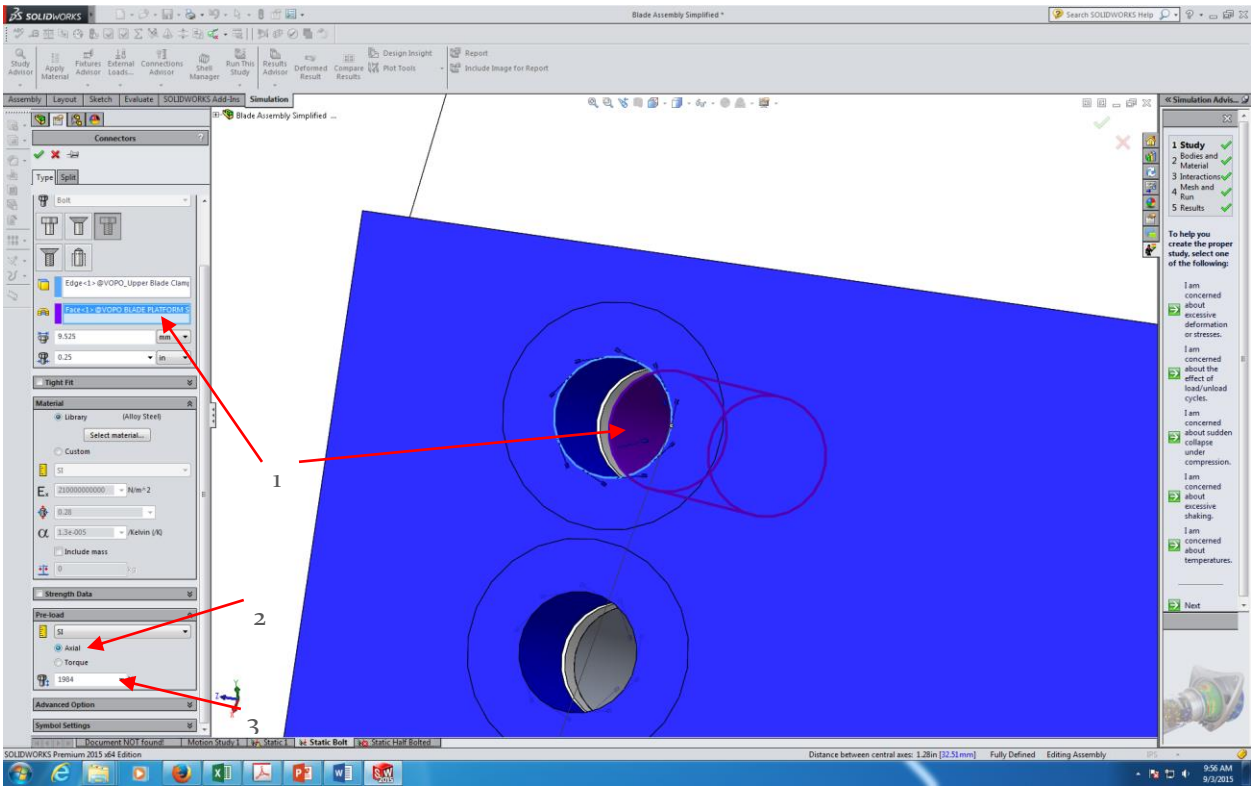

Figure 89: Define the bolted contact. Select the threated surface (1) and the Axial Load (2 & 3)

Finally we need to define the Pre-load of the Bolts. For that purpose we use the values calculated using *ClampsDesign.m* and define the axial load as 1948N (Figure 90). Once this is defined we click on the green tick and the bolted junction is fully defined.

Next step is to define the forces and the boundary conditions of the assembly. First thing we are going to do is to fix the bottom of the Blade Base. To do it so we click ok the Fixture Advisor tab and select fixed geometry in the scroll menu (Figure 91).

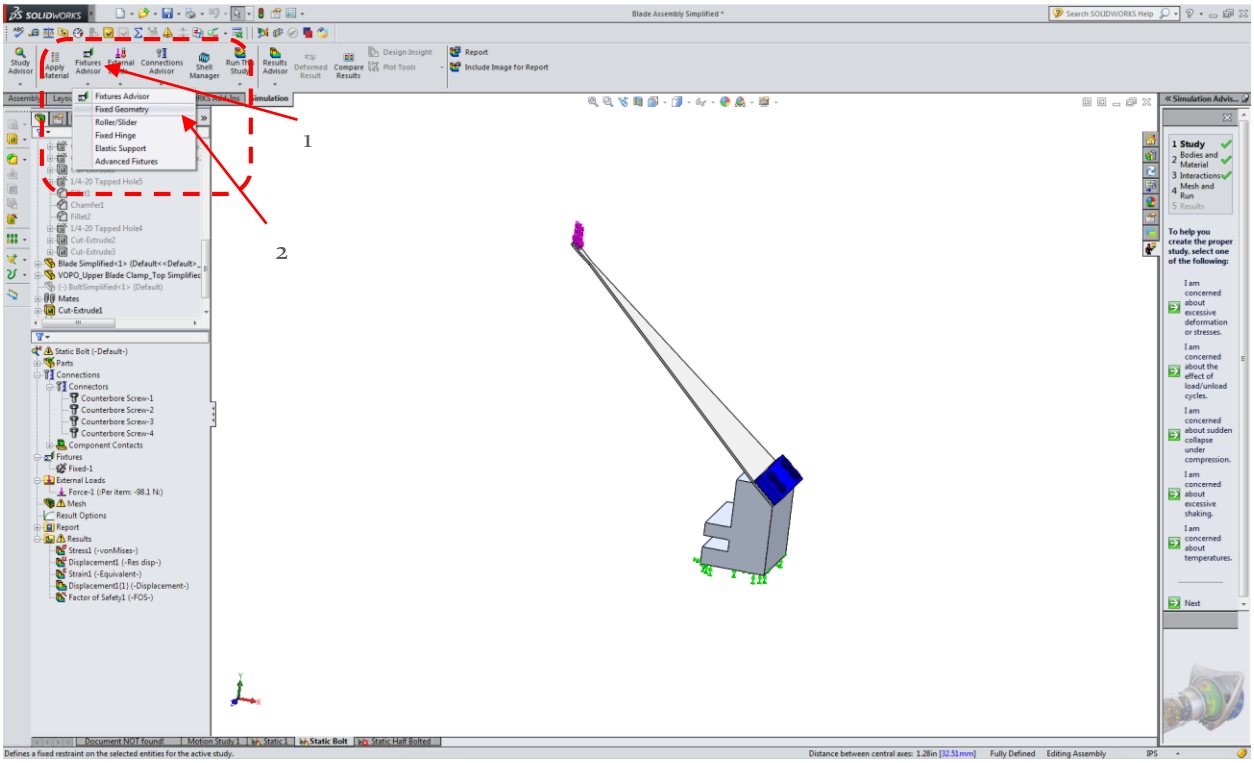

Figure 90: Apply for a Fixture

Then we just select the surface we want to fix and click on the green tick (Figure 91).

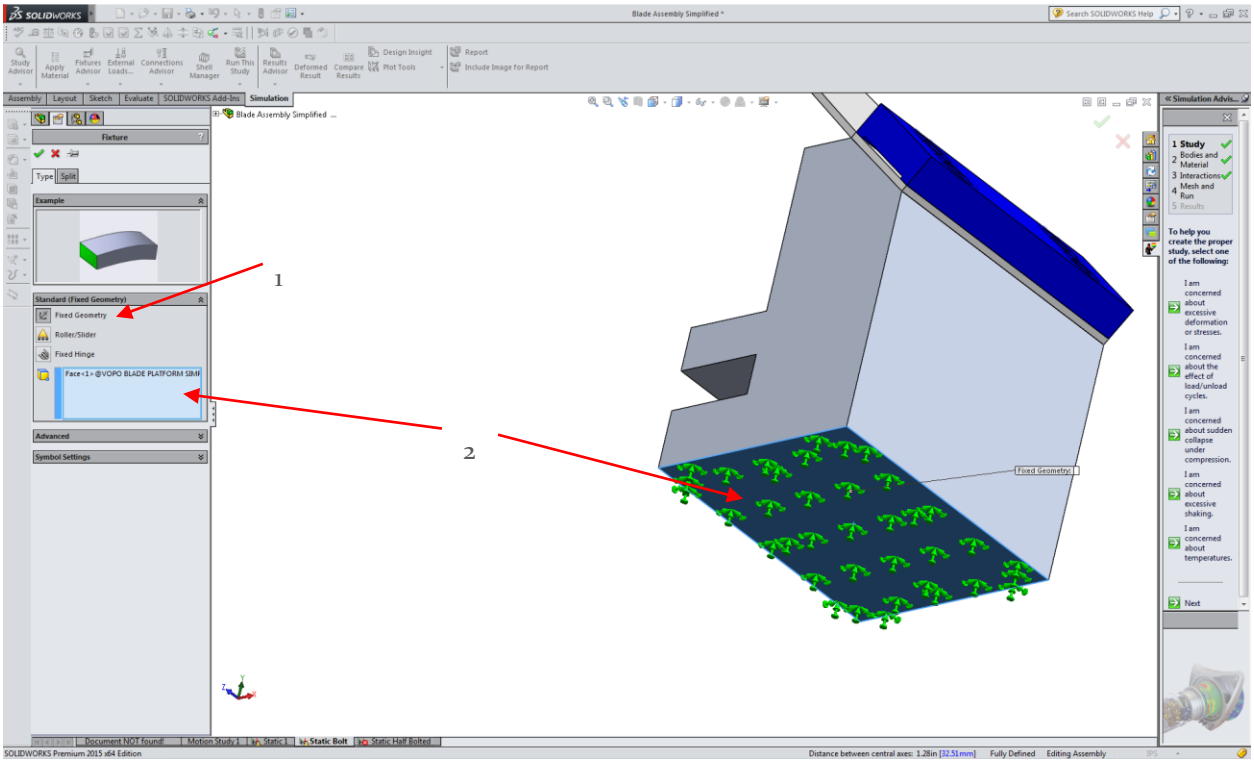

Figure 91: Fixed Geometry definition

Finally we need to apply for a Force in the "External Load" tab (Figure 92) and select the surface were we want to apply this load (Figure 93). In this case a split line has been created in the upper surface of the blade in order to apply the load in all the area were the upper wire clamp will be.

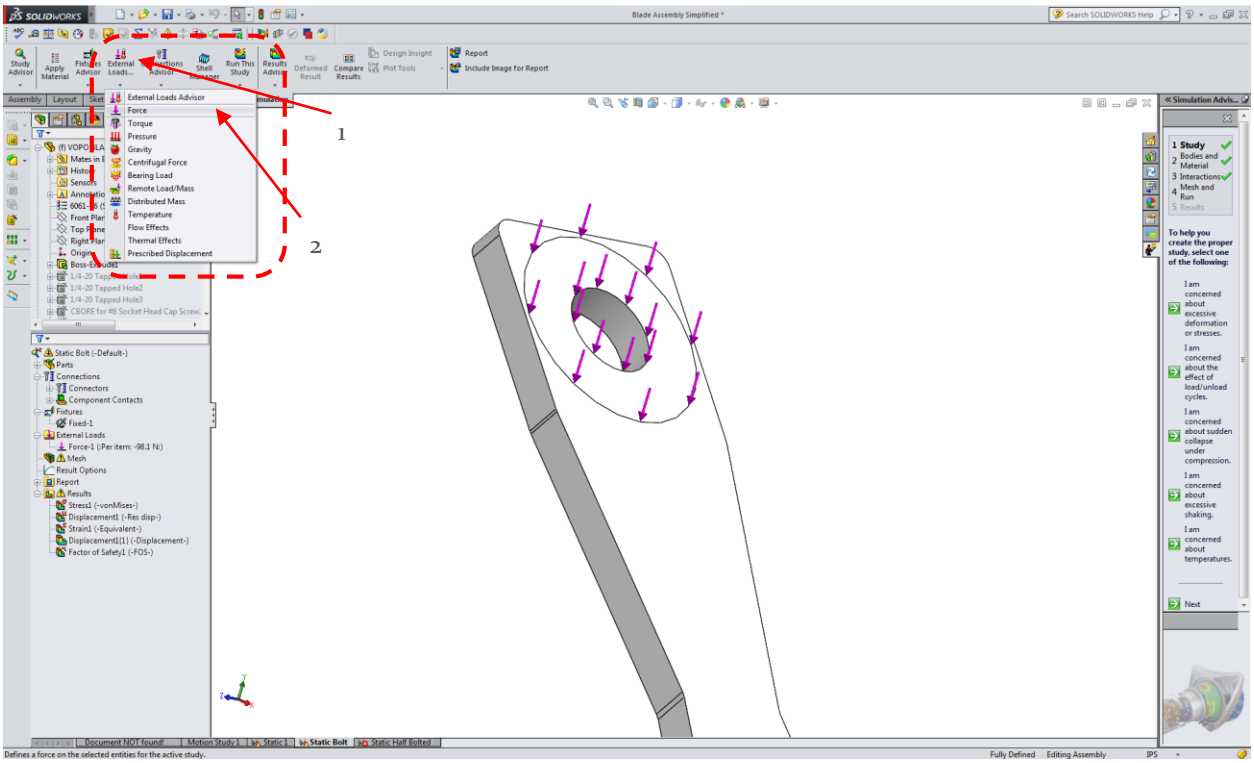

Figure 92: Apply for a Force

In that case we want the load (117.72 N) to be always in g direction so we need to define a "Selected direction" instead of choosing the default option of a force "Normal" to de surface, as shown in Figure 93.

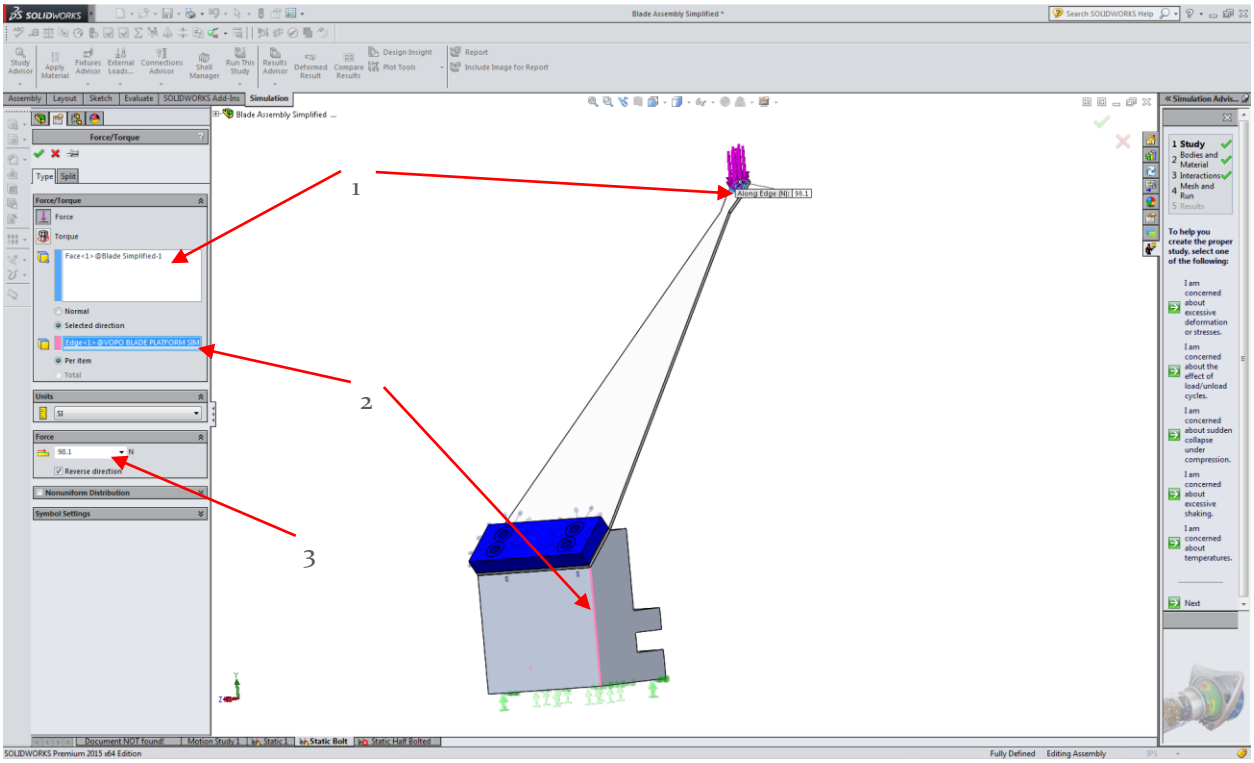

Figure 93: Define Force parameters. Application Surface (1), Direction (2) and Value (3)

The last two steps are to mesh the assembly and to run the study. For the mesh we can apply for the automatic mesh, where a homogeneous level of refinement is defined (and can bet set as Fine as we want), as shown in Figure 94. However, in that case is better to manually control the mesh in the different bodies as they do not need the same refinement. Another possibility to improve the calculation time is to use the symmetry of the assembly and to analyze only half of it, applying for the roller/Slider fixture in the symmetry plane.

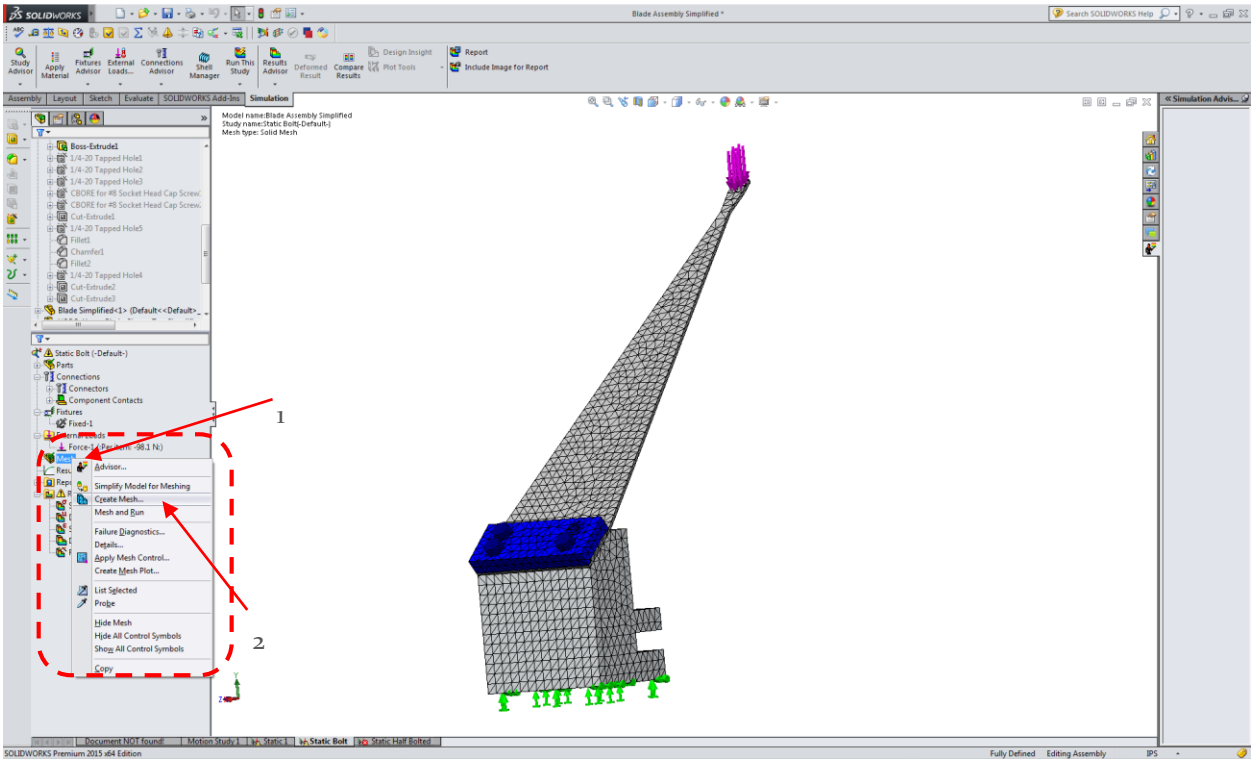

Figure 94: Create Mesh (Automatic Mesh)

Once the mesh is done the only remaining thing is to RUN the study (Figure 95).

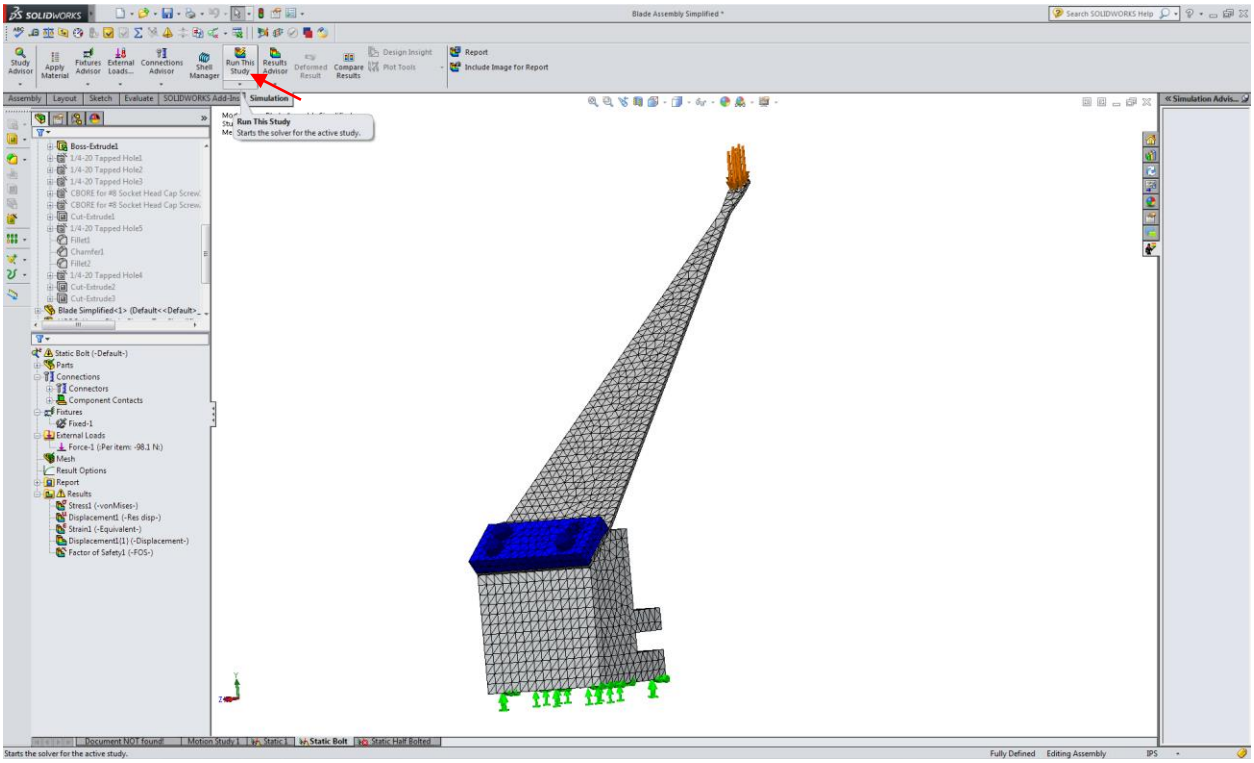

Figure 95: Run Study

USING ANSYS

The analysis with ANSYS is a little bit different from SW Simulation. There are many different ways to simulate the bolted assembly with ANSYS, using line bodies for example. However, we have decided to create specific bodies to simulate de screws. This bodies are basic SW cylindrical parts without any thread detail and a head (Figure 96).

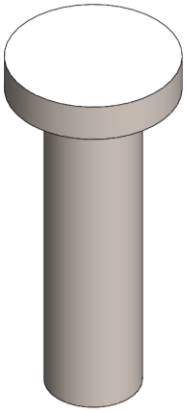

Figure 96: Bolt Model

Once we create that body we insert it in the assembly and we can proceed by opening the ANSYS Workbench and applying for a new Static Structural study. The second step will be then to define the materials we want to use in the study accessing to the "Engineering Data" (Figure 97).

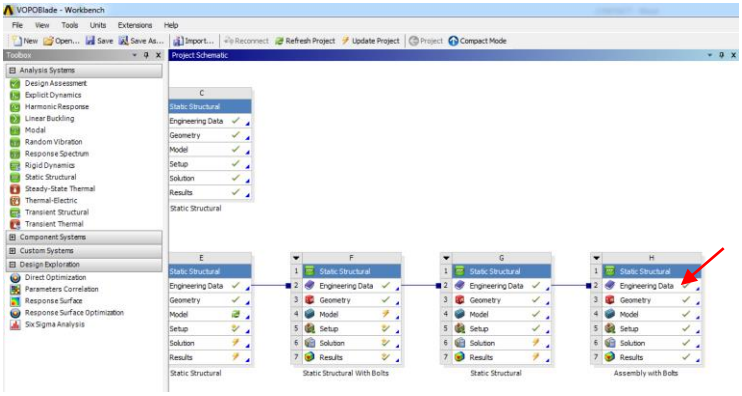

Figure 97: Access the Engineering Data edition

Like in SW, if the materials we are using in our assembly are not in the default library we will need to define them as shown in Figure 97. Otherwise, we can apply for the library material and select as much materials as we need for the assembly. It is important to know that when we will import the SW geometry we do not import the materials so they need to be redefined in ANSYS.

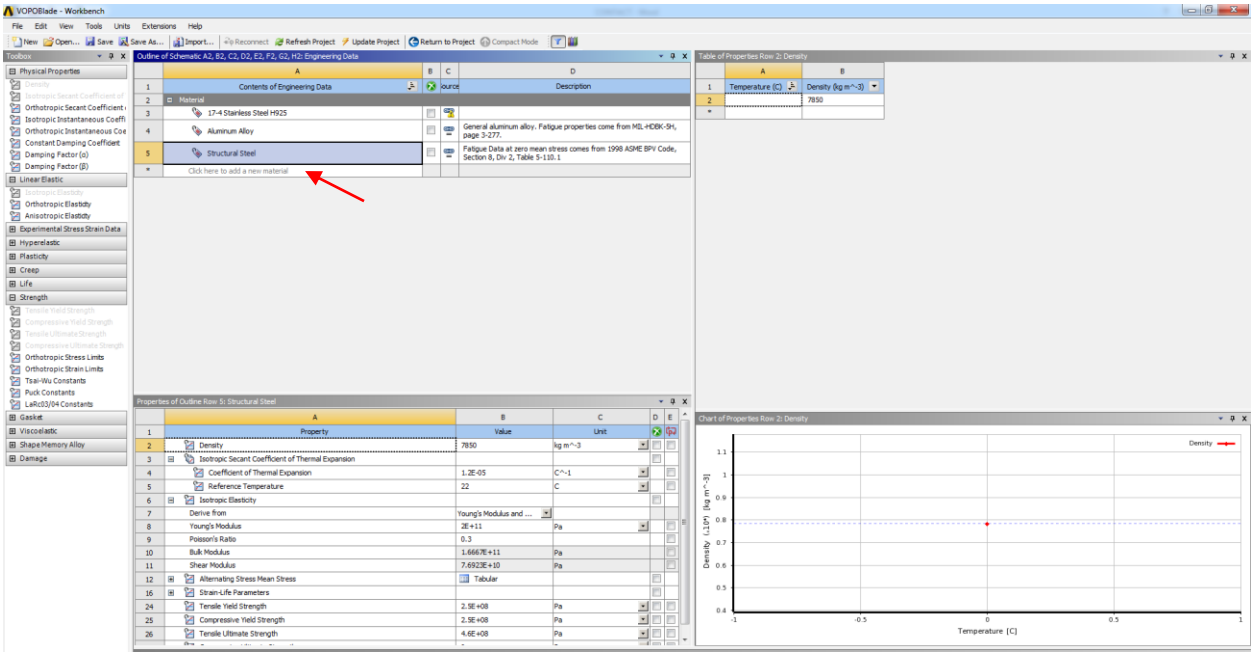

Figure 98: Material Selection and Edition menu. Apply for new Material (1)

Next step of the study is to import the geometry from SW. The way to do that is to right click on the Geometry tap and select "Import Geometry" in the scroll document and select the assembly document (Figure 98). If there is anything we need to change from the SW geometry we should then double click on the geometry tab. However, in our case there is nothing we want to change from the CAD design so we proceed with the model edition (Figure 99).

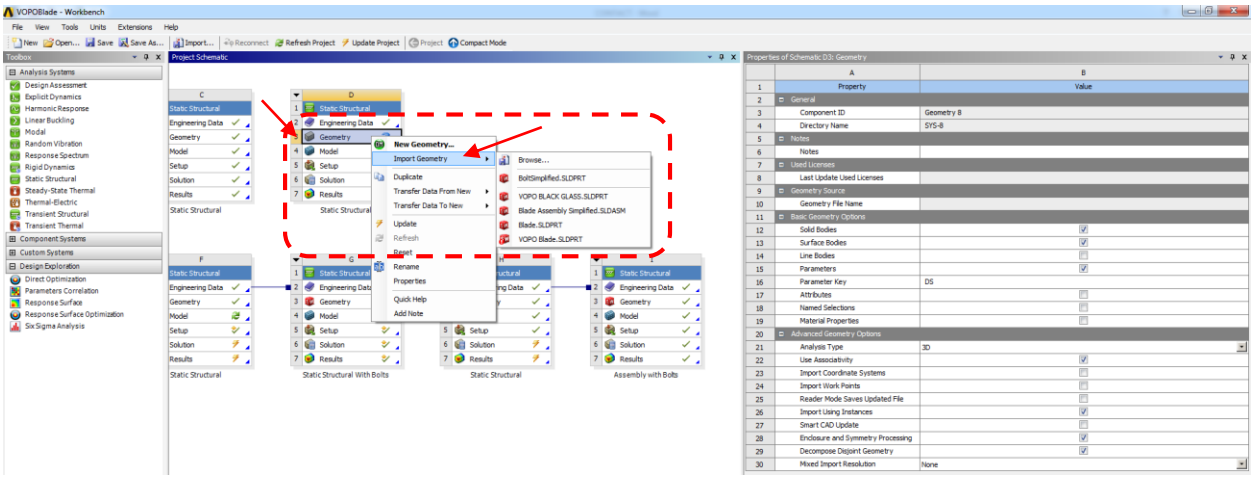

Figure 99: Import Geometry from CAD design

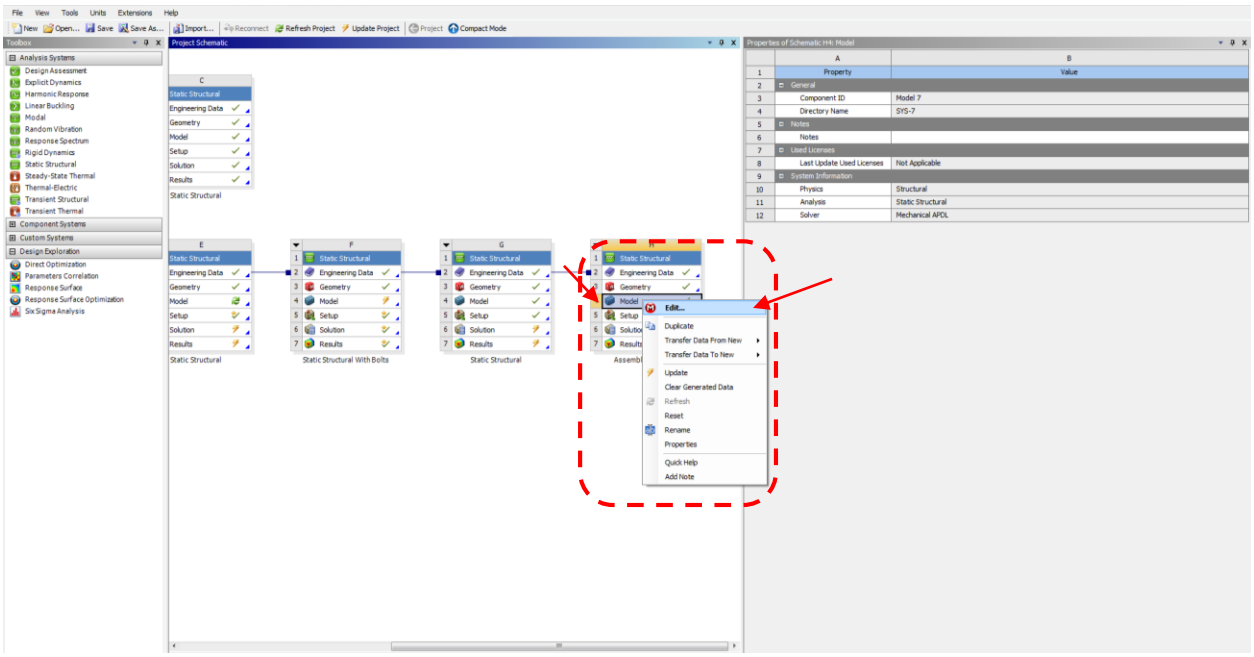

Figure 100: Open the Model edition

Once you da that a new window will open with the Model Edition (Figure 100). We will be working in this window until the end of the study so we do not need to come back to the Project window.

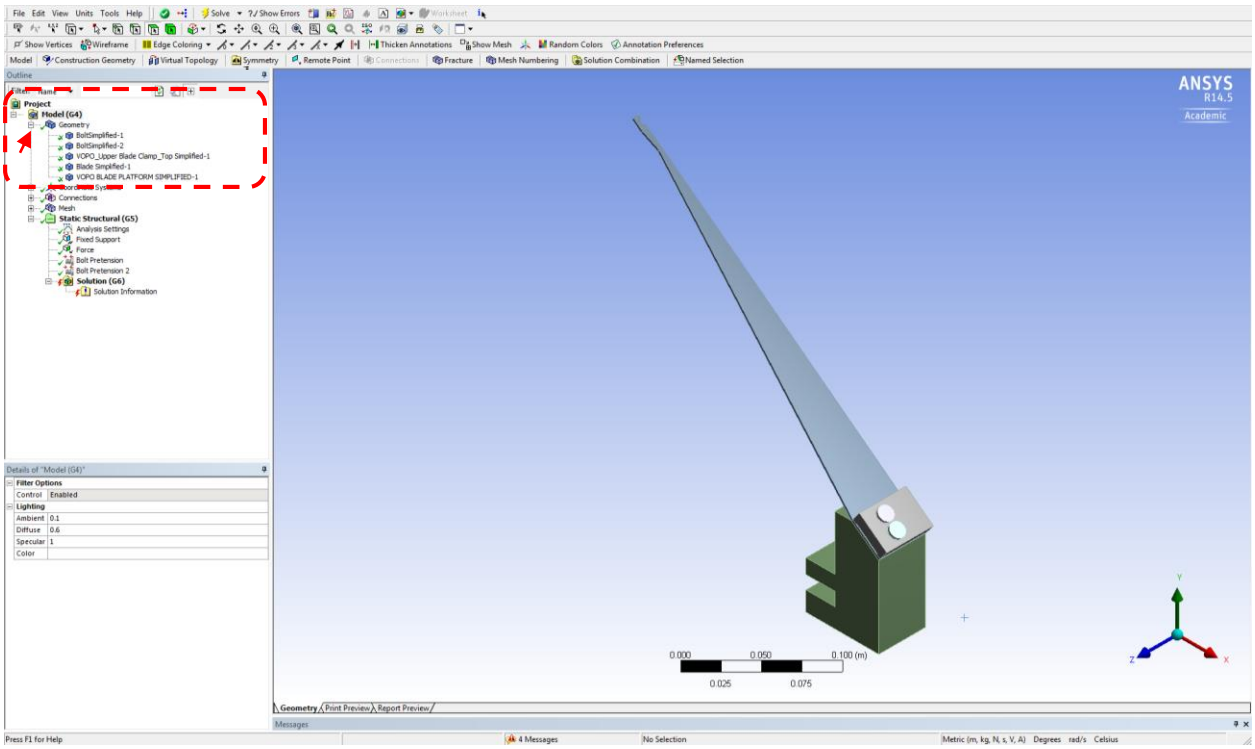

Figure 101: Model Edition View and access to the Model parts

The view that should appear in the Model Edition window is similar to the one shown in Figure 101, with the assembly geometry already imported. In that case we have used half the geometry to perform the study as it

is a good way to reduce the calculation or to increase the refinement of the important areas of the assembly. If we deploy the Geometry tab (Figure 101) we should see all the different parts that form the assembly. In this study there are five components (Blade, Clamp, Base and 2 screws). The next step, an important one, is to define the material of all this parts. To do that we need to individually apply for material to each part (Figure 102). Usually the default material is Structural Steel, but we can change that in the Engineering Data manager. When we try to change the material the list of material that appear directly is the same that we defined when we worked on the Engineering Data, this is why it is important to define the materials prior to that step. However, if we have forgotten to define the material we can always click on "Define New Material" and we will be redirected to the Engineering Data manager.

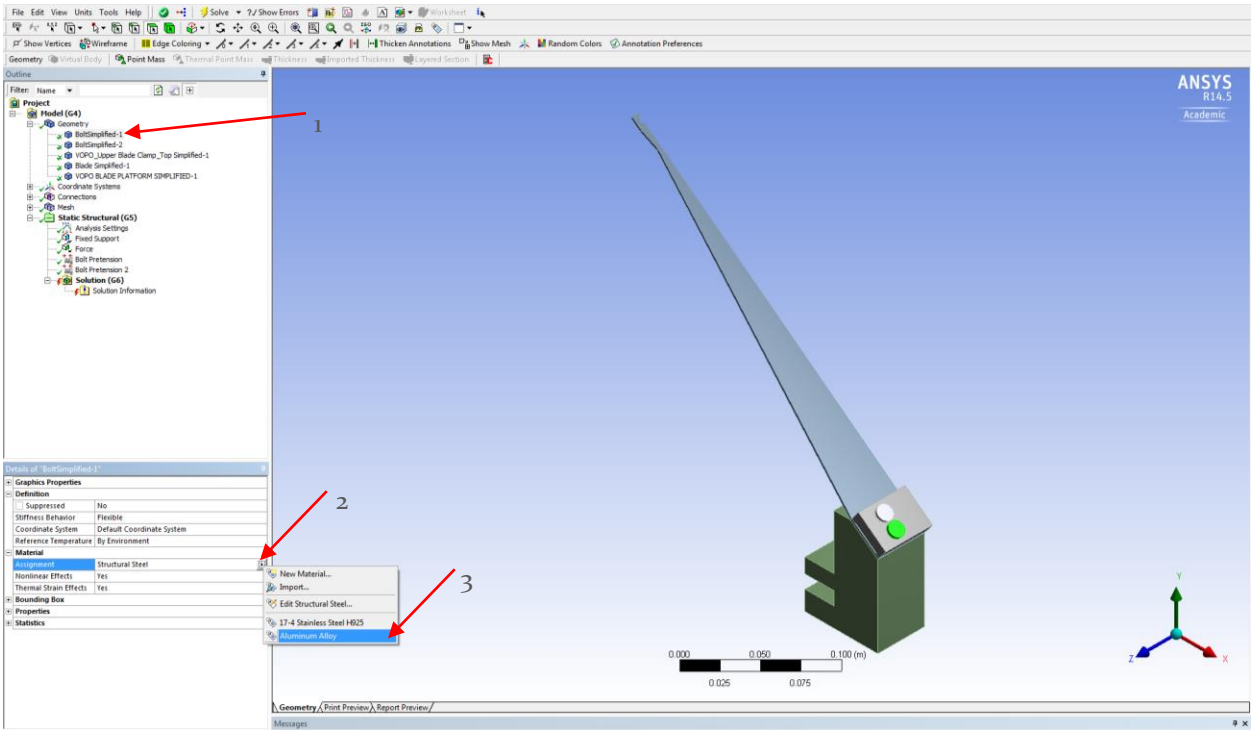

Figure 102: Material definition. Select part (1), open Material options (2) and select the material (3)

After applying the material for all the parts, the connections between them have to be defined. As with SW, ANSYS has already defined a default connection between the parts that is "Bonded". We need to redefine those connections as we will not simulate the real behavior of the bolted contact otherwise. To do so we just click on each connection definition and we change the parameters in the connection menu (Figure 103). To make it easier we can apply for the Body views, where we will be able to see which bodies are concerned by each definition.

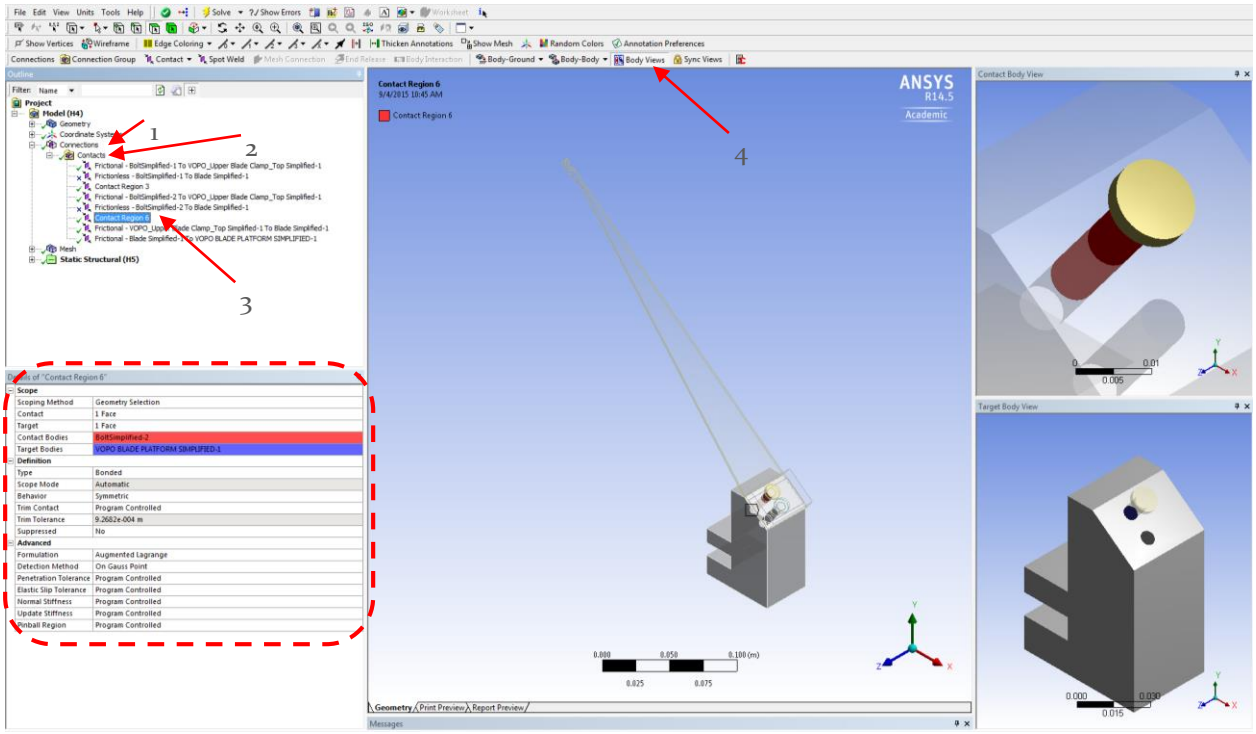

Figure 103: Contact Definition. Show Contact Menu (1, 2 & 3) and apply for multiple views (4)

First off, we define the contact Blade-Clamp and Blade-Base, which is a Frictional contact with a 0.61 (Figure 104). We usually apply for a Symmetric behavior of the friction contact but it is possible that the solver automatically changes that as the coefficient is bigger than 0.2. On the other side, the recommendation is to change the advanced settings to those shown in Figure 104 instead of the "Automatic" default value. However, it should also work with this default values.

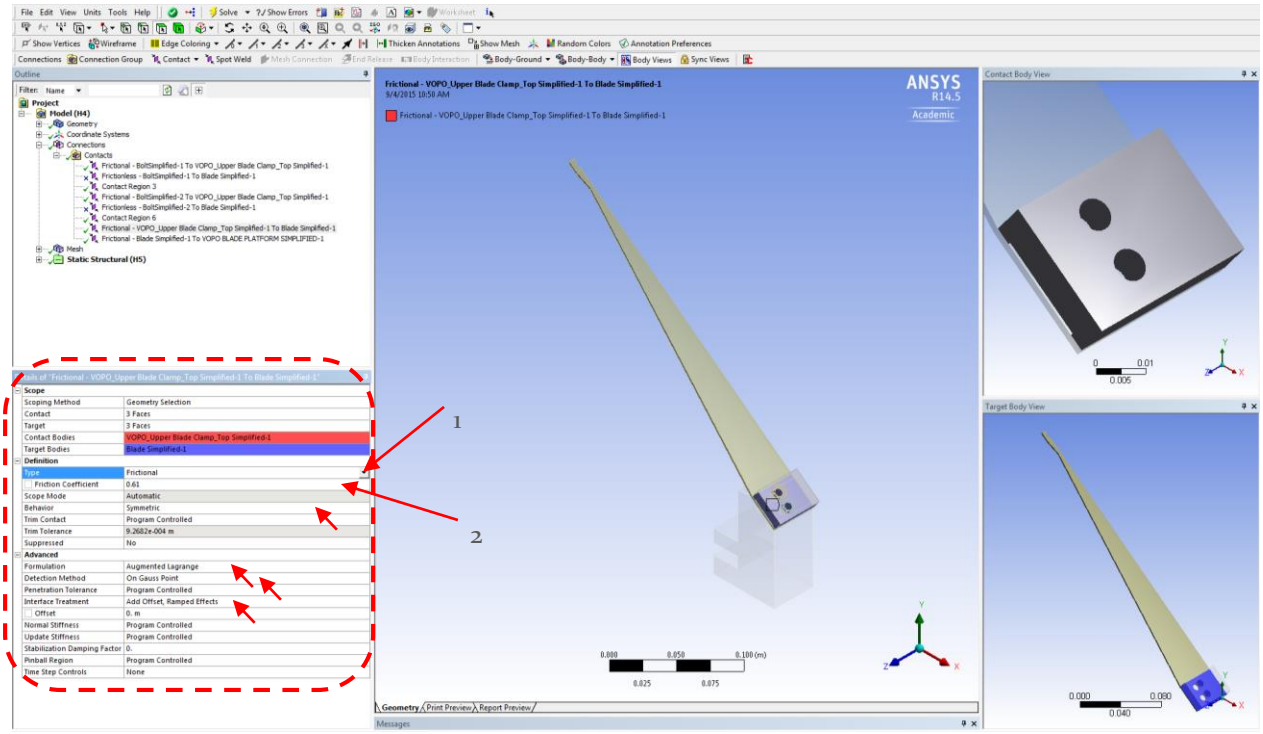

Figure 104: Frictional Contact Definition

Secondly, we need to define the bolted contact. To do that we will use three different contacts. The first one is to define a bolted contact between the bolt and all the parts that have a threated hole (Figure 105). In our case this contact has to be defined between both bolts and the Base.

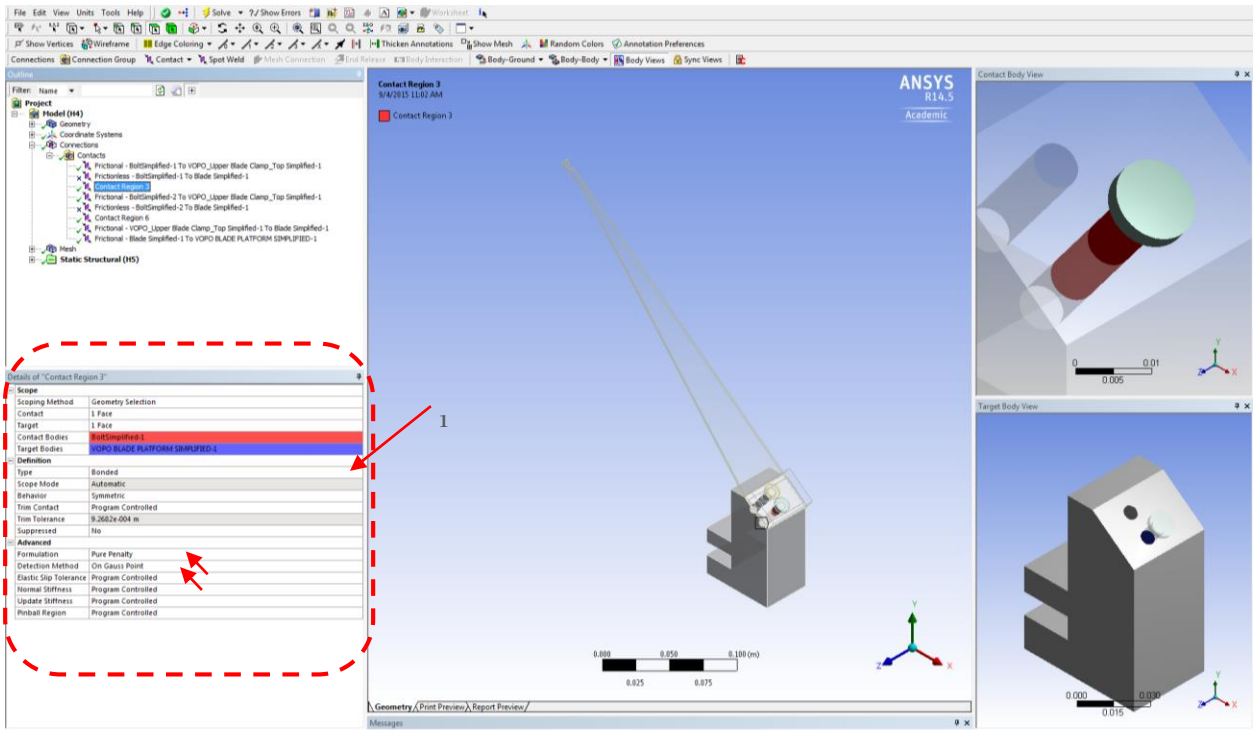

Figure 105: Bonded Contact Definition

Then we need to define the contact between the head of the bolt and the body that is in contact with it. In our case this body is the clamp so we have to define this contact as Frictional, with a friction coefficient (0.61 in that case as it is between clean steel and aluminum) and with the advanced settings as shown in Figure 106.

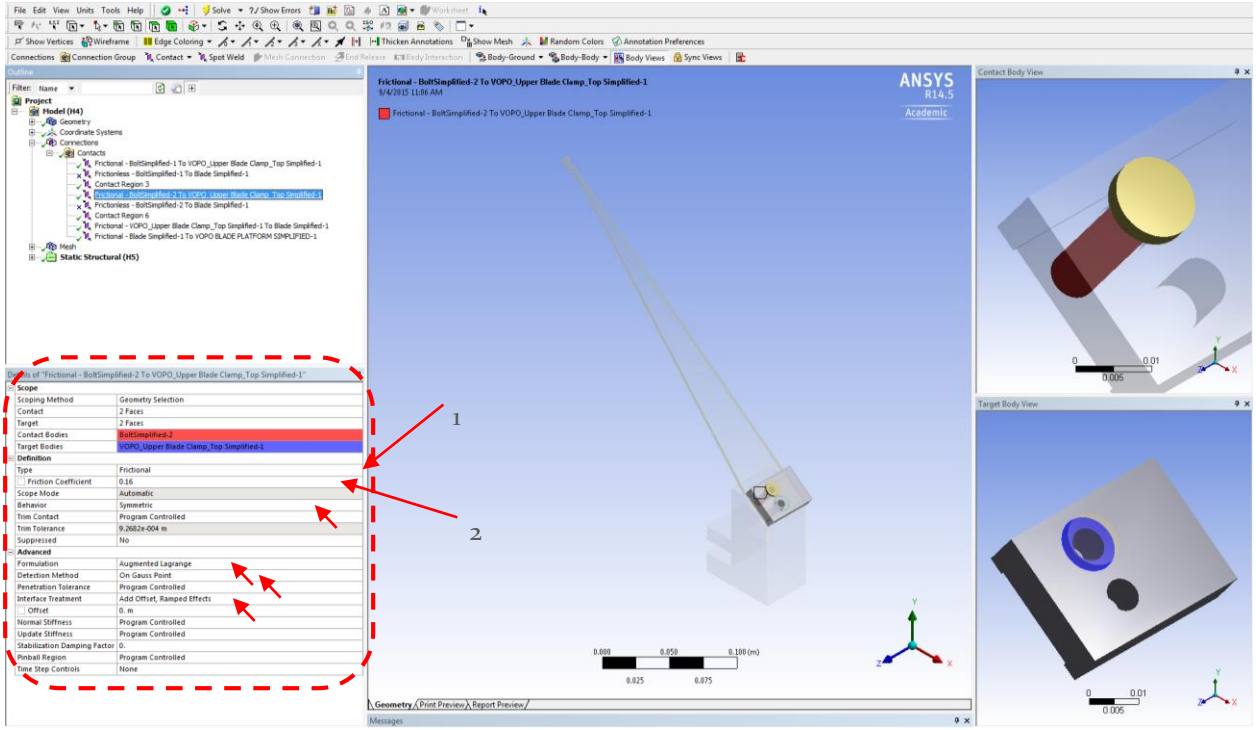

Figure 106: Frictional Contact Definition for Bolt. Contact type (1) and 0.61 Frictional Coefficient (2)

However, at this point we can also define the contact between surfaces and not between bodies as there are two different contacts between the bolt and the clamp. The first one is between the head of the screw and the upper surface of the clamp (where we want a frictional contact) and then between the screw thread and the hole in the clamp. Actually in this second contact there is no real contact, as the hole is loose, but a Frictionless contact would probably be more accurate. Anyway, where we do need to define a frictionless contacts is between the bolt and the blade (Figure 107).

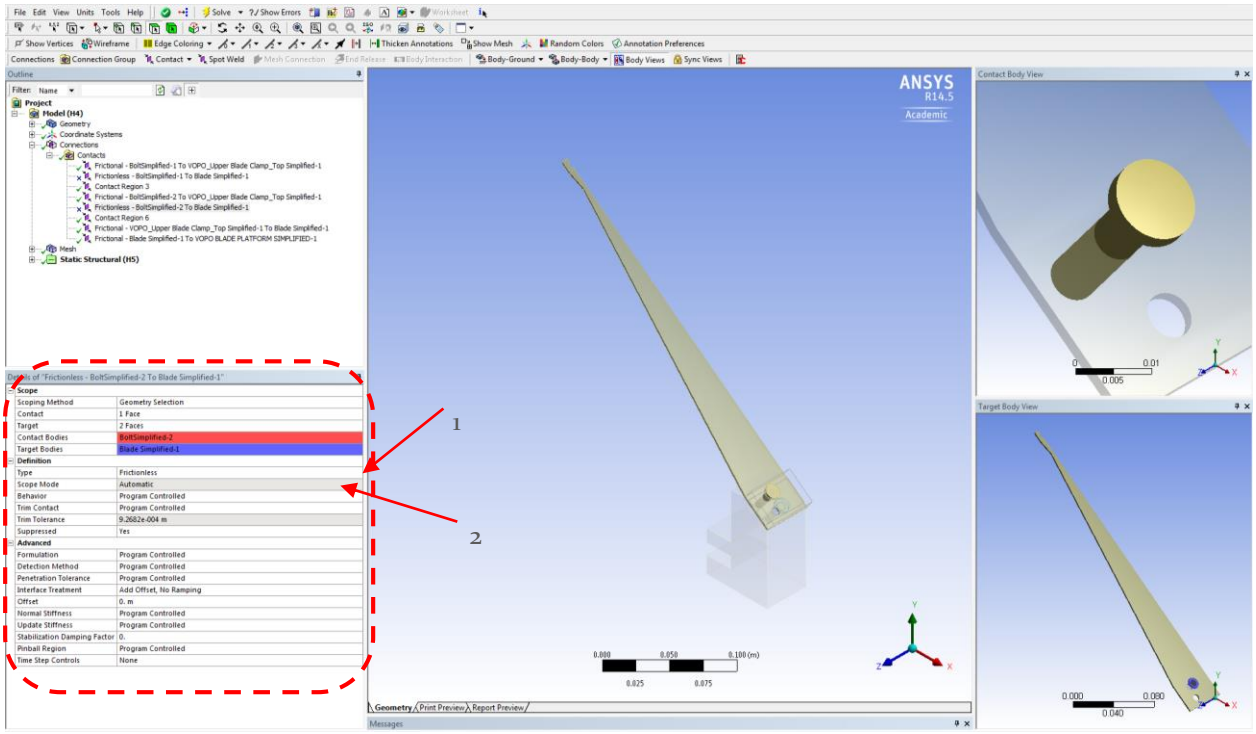

Figure 107: Frictionless contact definition

Next step is to create the mesh. The best option is to use the mesh control to define how fine we do want the mesh in each part of the assembly. However, another possibility is to apply for the automatic mesh (Figure 108) and then refine it in the contacts and the blade.

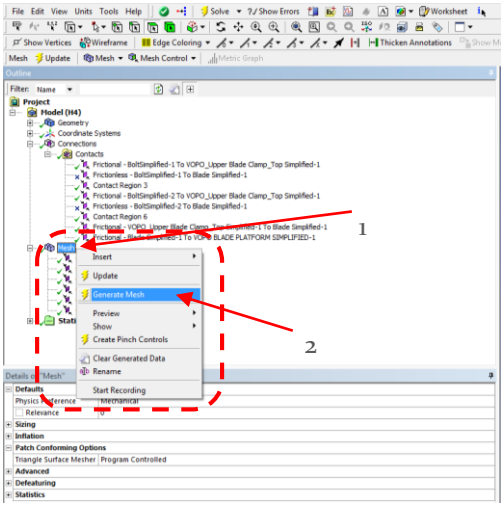

Figure 108: Applying mesh generation

ANSYS has the possibility of automatically refine the mesh in the contact between entities. To do it we need to apply for the Contact Sizing, where we will be asked to select the contact we want to refine and the element size (Figure 109).

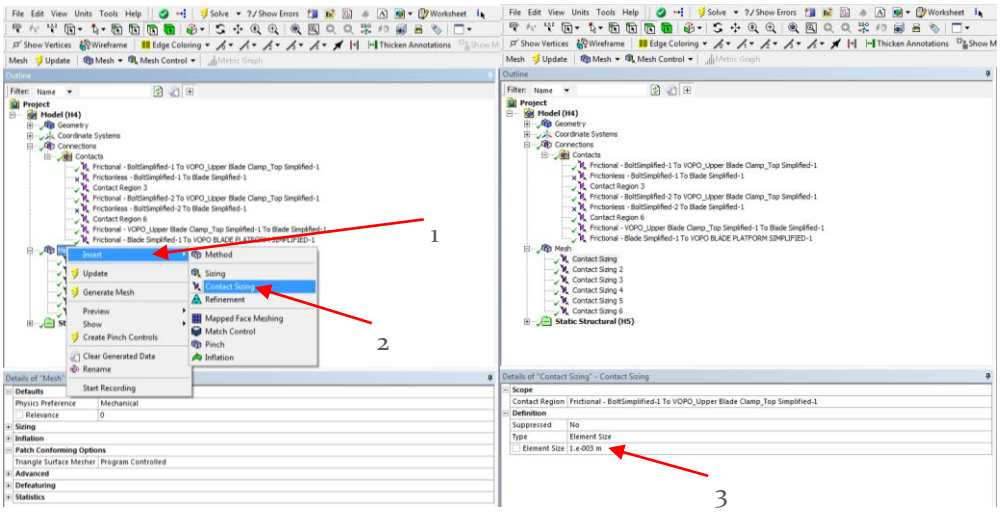

Figure 109: Apply for Contact Mesh Refinement

Finally, we can move onto the Static Structural tab. First thing we are going to do is to define the load (Figure 110), that has to have half the value of the global load because we are working with just half the model.

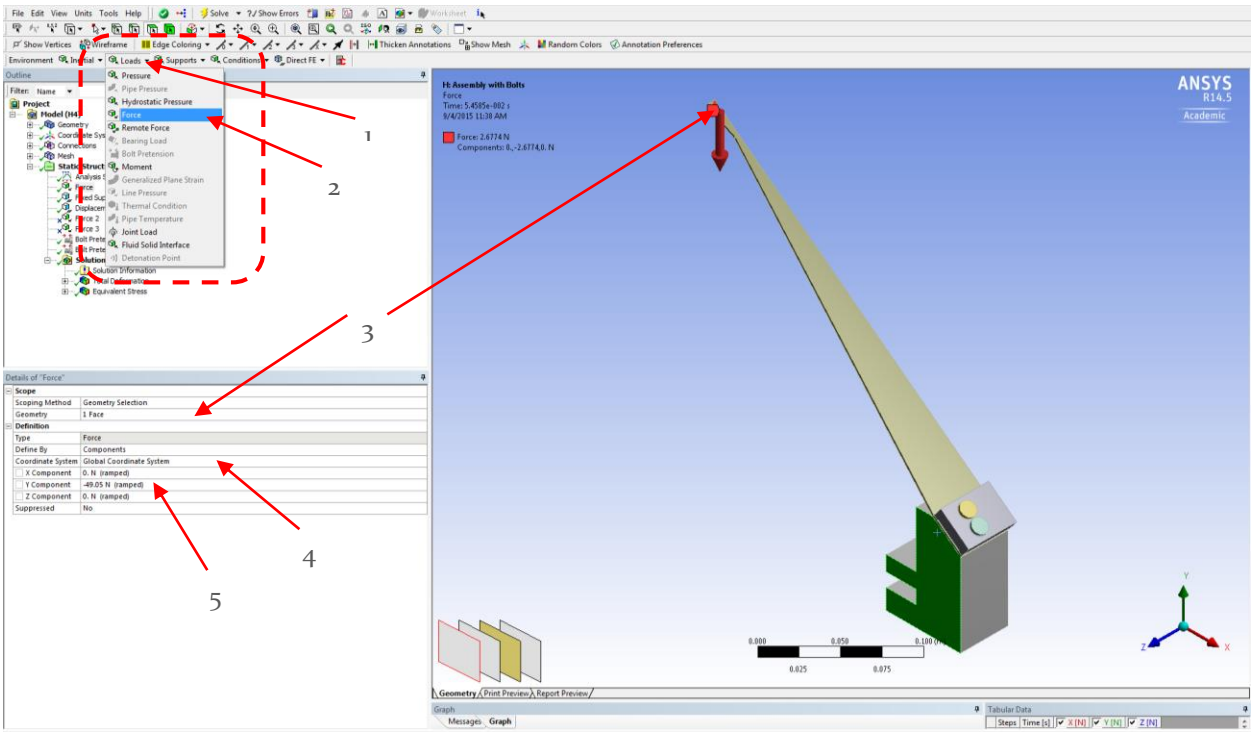

Figure 110: Force definition. Surface selection (3) and value definition (5)

Then we proceed with the definition of the supports. The first step is to define a Fixed Support (Figure 111) for the lower surface of the Base, which will be bolted to the Base Plate. Then, as we are working with half of the model, we need to block the movement of the symmetry plane (Figure 112).

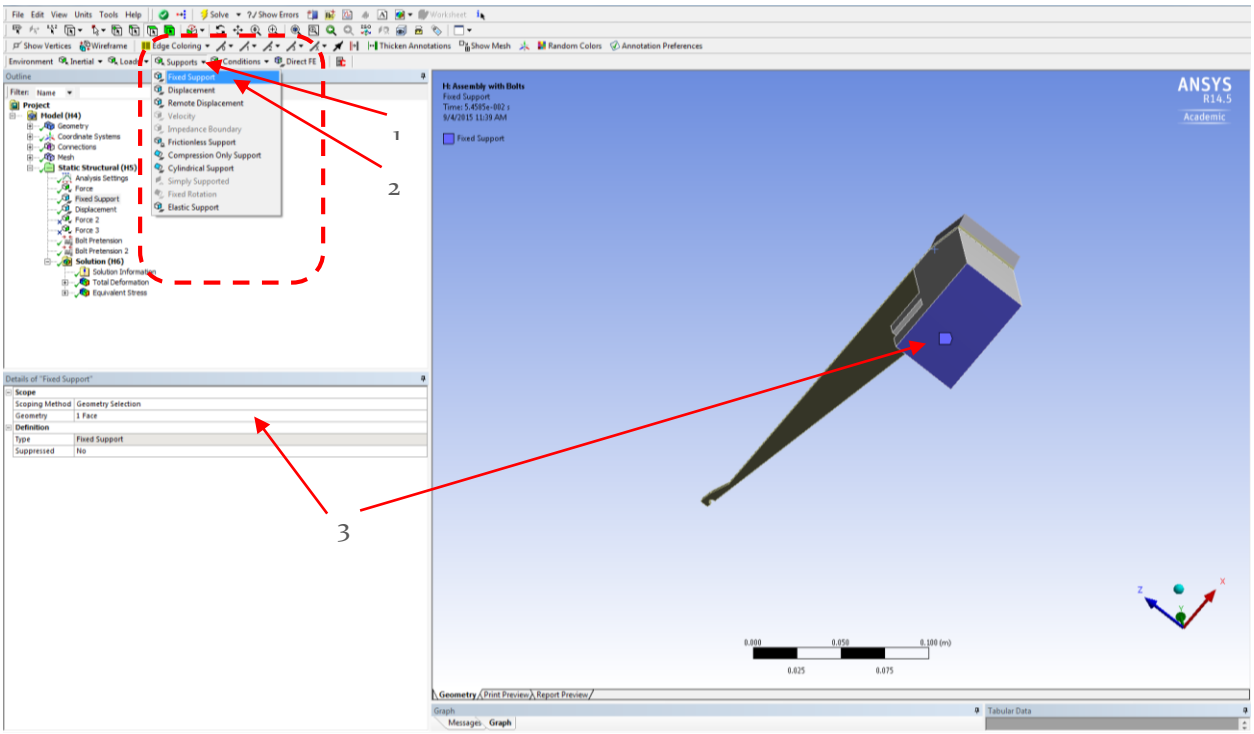

Figure 111: Fixed Geometry definition

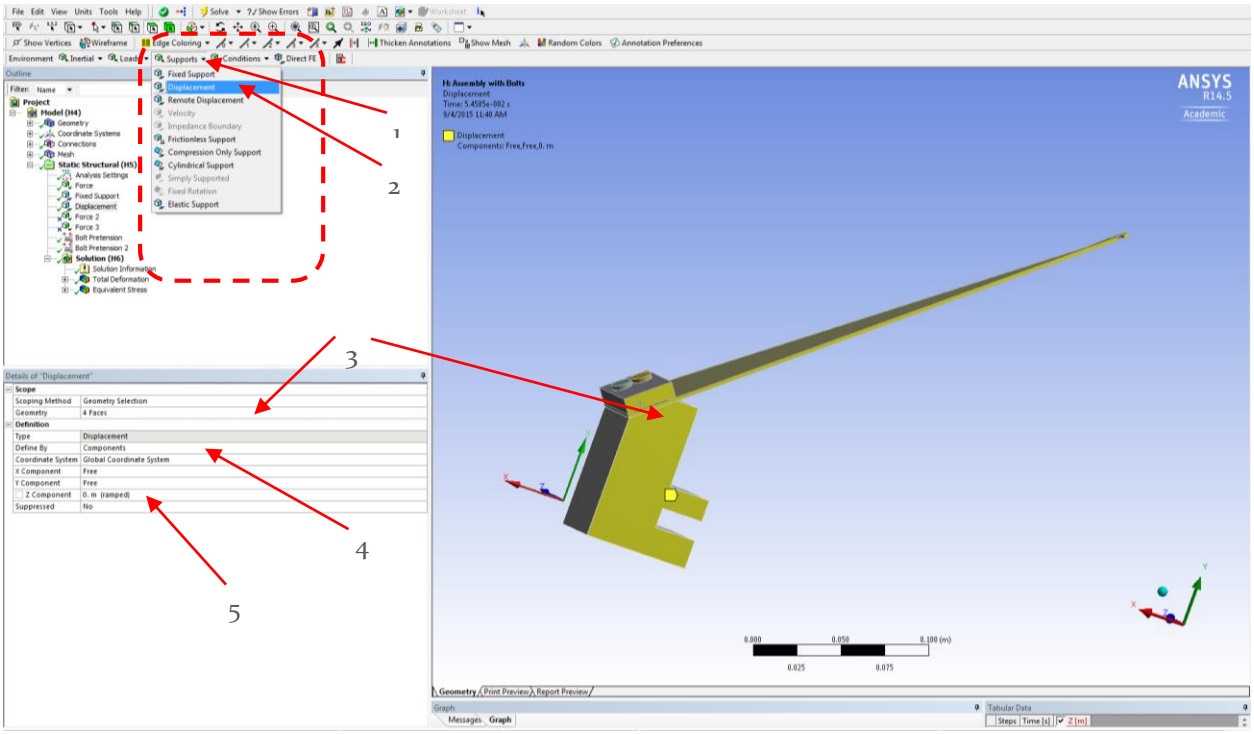

Figure 112: Block Displacement on symmetry plane

Last thing to do before running the solver is to define the preload of the screws. That can be made applying the "Bolt Pretension" in the Loads scroll menu (Figure 113). Then, in the Bolt Pretension menu we need to select the cylindrical surface of the screw and select the value (defined by load) of the pre-stress.

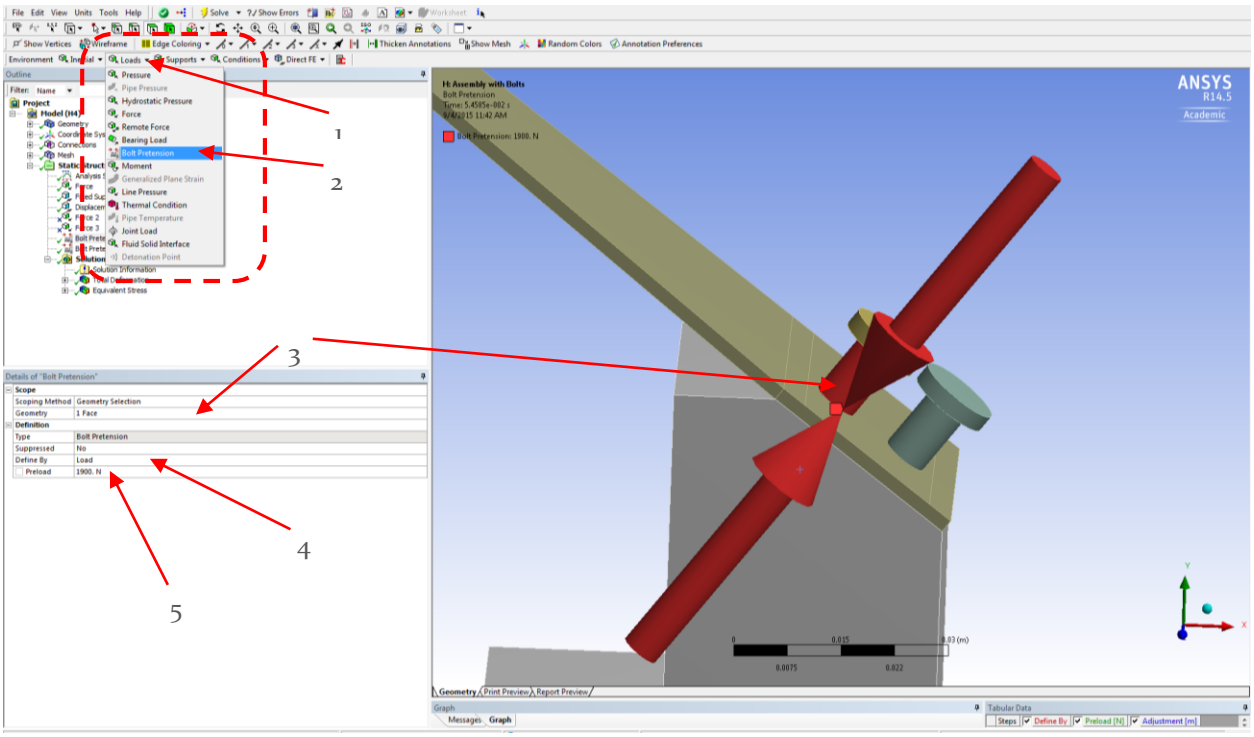

Figure 113: Bolt Pre-Load Definition

Finally, we just need to select the Solution Information we want (i.e. Deformation, Stress, Strain, etc.) and launch the solver.

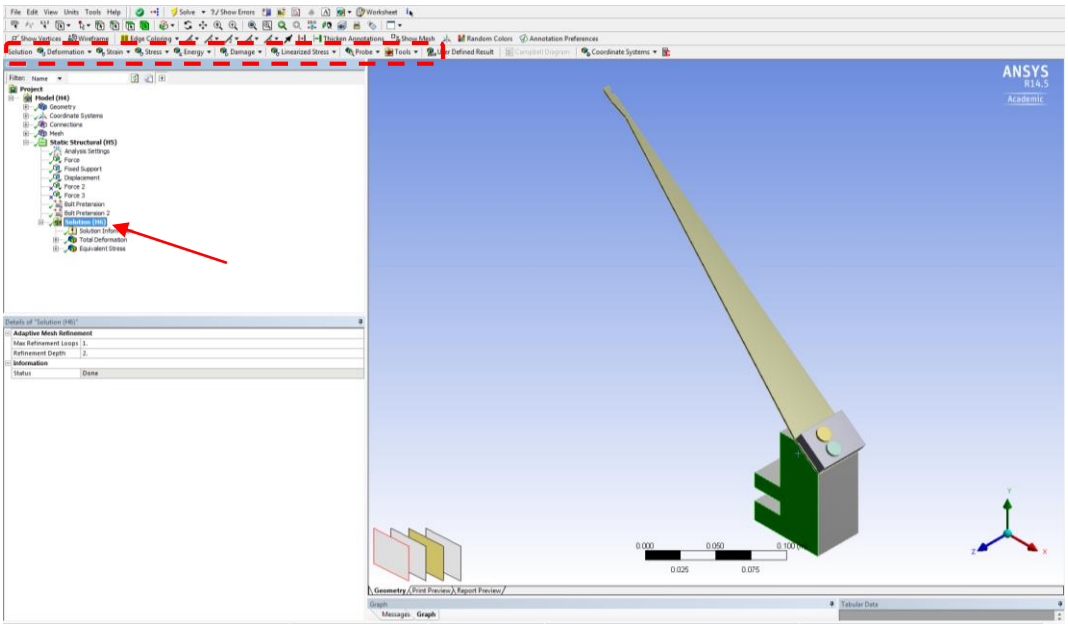

Figure 114: Apply for Solution Information

LARGE DISPLACEMENT SIMULATION ANALYSIS

Both ANSYS and SW Simulation have the option of "Large Displacement" simulation. The idea behind this option is that the static analysis uses a linearized model to find the solution. However, this linearization leads to a wrong solution when the deformation is large. In that case, the assumption of linearity is incorrect and we need to apply for the "Large Displacement" simulation in order to increase the accuracy of the solution. To run the Static study of the VOPO Blades we have used this option to find the right solution of the problem. We do not usually know the displacement before running the simulation (even if we usually can have an approximate idea) so both programs show alerts if it is the case where large displacements appear and the corresponding flag has not been activated.

In SW Simulation, once we have opened a new Static study, we just need to right click on the Static Simulation name (Figure 115), then apply for properties and finally activate the corresponding Flag.

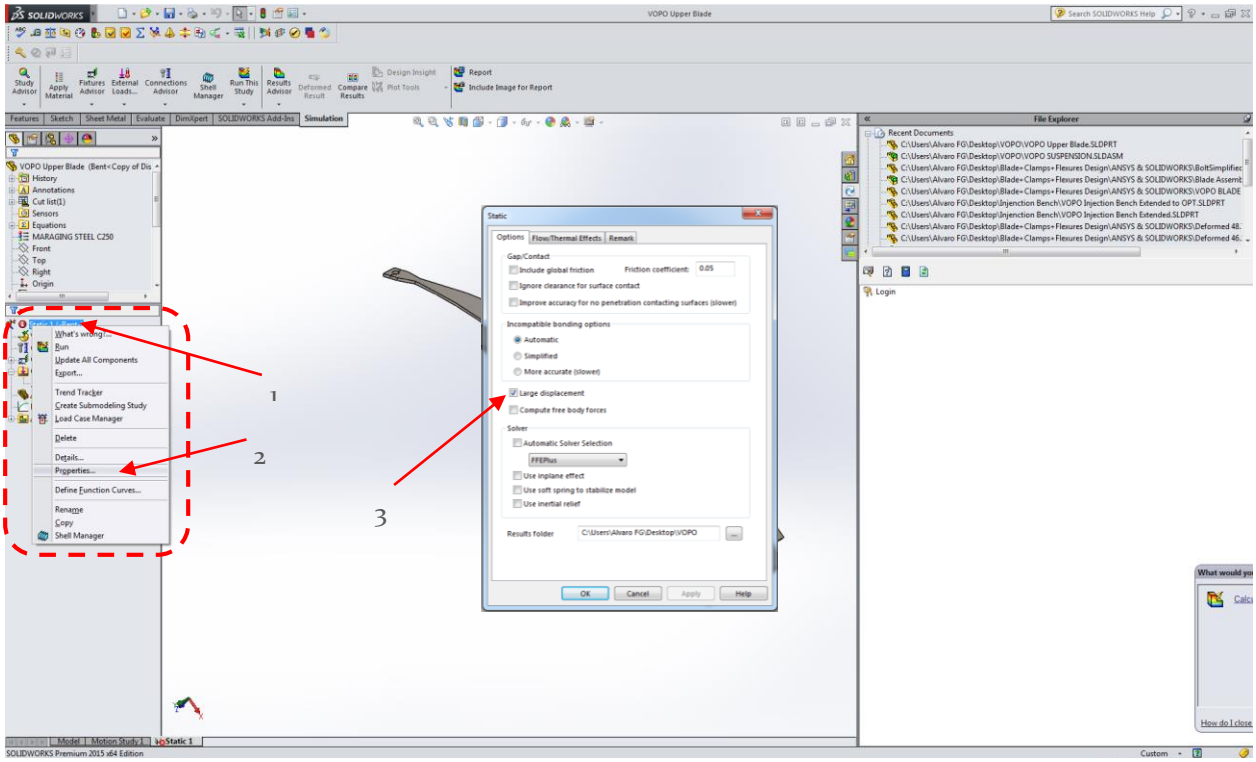

Figure 115: Large Displacement in SW Simulation

On the other side, if we are using ANSYS, we can select the Large Deformation mode once in the Model Manager. The way to do it is by clicking in analysis settings and activating the large deflection mode (switch off to on), as shown in Figure 116.

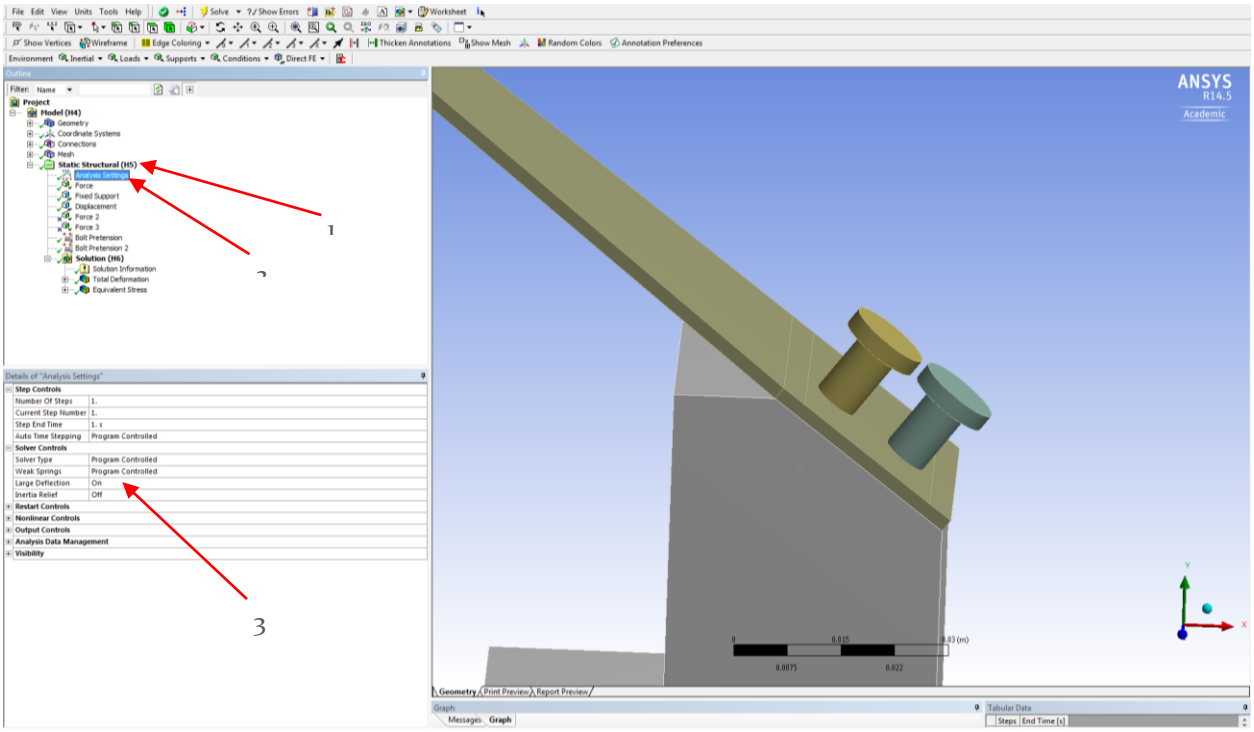

Figure 116: Large Deflection selection in ANSYS

It is important to notice that selection the large deformation mode will increase the calculation time as it uses an iterative process to get the final solution, but it is the only way to obtain an accurate solution of the problem. In Figure 117we can observe the difference between the same study with the Large deformation Flag selected or not.

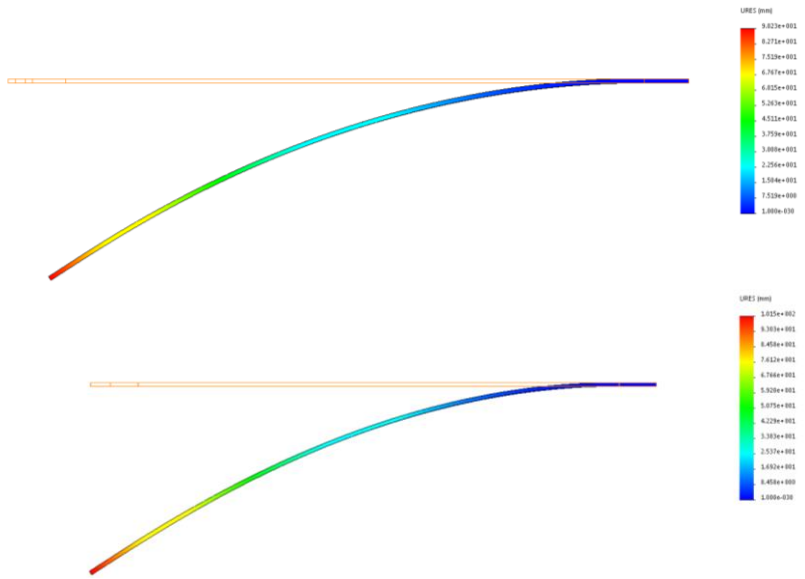

Figure 117: Comparison between Large (Upper) and Small (Lower) Displacement solution